Great Britain
Journals Press

IMAGE: OBSERVATORY WITH STAR
TRAILS ON MOUNTAINS FOR
CLEAR SKY

They were leaders in building the early foundation of modern programming and unveiled the structure of DNA Their work inspired environmental movements and led to the discovery of new genes They've gone to space and back taught us about the natural world dug up the earth and discovered the origins of our species They broke the sound barrier and gender barriers along the way The world of research wouldn't be the same without the pioneering efforts of famous research works made by these women Be inspired by these explorers and early adopters- the women in research who helped to shape our society We invite you to sit with their stories and enter new areas of understanding This list is by no means a complete record of women to whom we are indebted for their research work but here are of history's greatest research contributions made by...

Read complete here:
https://goo.gl/1vQ3lS

Women In Research

Computing in the cloud!

Cloud Computing is computing as a Service and not just as a Product Under Cloud Computing...

Read complete here:
https://goo.gl/VvHC72

Writing great research...

Prepare yourself before you start Before you start writing your paper or you start reading other...

Read complete here:
https://goo.gl/np73jP

Journal Content
In this Issue

Great Britain Journals Press

Editorial Board

Curated board members

Dr. Rocío Maceiras

Associate Professor for Integrated Science,
Defense University Center, Spain Ph.D., Chemical
Engineering, University of Vigo, SPAIN

Dr. Rolando Salgado Estrada

Assistant Professor,
Faculty of Engineering, Campus of Veracruz,
Civil Engineering Department, Ph D.,
Degree, University of Minho, Portugal

Dr. Abbas Moustafa

Department of Civil Engineering,
Associate Professor, Minia University, Egypt, Ph.D
Earthquake Engineering and Structural Safety,
Indian Institute of Science

Dr. Wael Salah

Faculty of Engineering,
Multimedia University Jalan Multimedia,
Cyberjaya, Selangor, Malaysia, Ph.D, Electrical and
Electronic Engineering, Power Electronics and Devices,
University Sians Malaysia

Prof. Baoping Cai

Associate Professor,
China University of Petroleum,
Ph.D Mechanical and Electronic Engineering,
China

Dr. Kao-Shing Hwang

Electrical Engineering Dept.,
Nationalsun-Yat-sen University Ph.D.,
Electrical Engineering and Computer Science,
Taiwan

Dr. Mu-Chun Su

Electronics Engineering,
National Chiao Tung University, Taiwan,
Ph.D. Degrees in Electrical Engineering,
University of Maryland, College Park

Nagy I. Elkalashy

Electrical Engineering Department,
Faculty of Engineering,
Minoufiya University, Egypt

Dr. Vitoantonio Bevilacqua

Department of Electrical and Information
Engineering Ph.D., Electrical Engineering
Polytechnic of Bari, Italy

Prof. Qingjun Liu

Professor, Zhejiang University, Ph.D.,
Biomedical Engineering,
Zhejiang University, China

Research papers and articles

A Novel Approach to Analyzing the Microstructures of Thermal Protection Systems Materials for Hypersonic Applications

Samantha Bernstein, Colin Yee, Steven Kim, Kaelyn Wagner, Wei Li & Joseph H. Koo

University of Texas

ABSTRACT

The purpose of this research is to outline a novel methodology for using microstructures to inform Thermal Protection Systems (TPS) materials research. This method involves the Micro-Computed Tomography (Micro-CT) scanning of materials, rendering, segmentation of each element class, and then quantitative analysis of the materials using their microstructures. The microstructures of TPS materials were characterized using the Lawrence Berkeley National Laboratory (LBNL)'s Beamline 8.3.2 at the Advanced Light Source (ALS). The Synchrotron-based Hard X-ray Micro-Tomography instrument allowed for non- destructive 3-Dimensional imaging of 72 different samples of TPS materials.

Understanding the behavior and composition of TPS materials before and after aerothermal testing is key to meeting the demands of new space exploration goals so materials were examined in both virgin and char states.

Keywords: microstructures, micro-computed tomography, thermal protection systems, ablative materials, deep learning, segmentation, machine learning.

Classification: LCC: QC951- QC999

Language: English

A Novel Approach to Analyzing the Microstructures of Thermal Protection Systems Materials for Hypersonic Applications

Samantha Bernstein[α], Colin Yee[σ], Steven Kim[ρ], Kaelyn Wagner[CƆ], Wei Li[¥] & Joseph H. Koo[§]

ABSTRACT

The purpose of this research is to outline a novel methodology for using microstructures to inform Thermal Protection Systems (TPS) materials research. This method involves the Micro-Computed Tomography (Micro-CT) scanning of materials, rendering, segmentation of each element class, and then quantitative analysis of the materials using their microstructures. The microstructures of TPS materials were characterized using the Lawrence Berkeley National Laboratory (LBNL)'s Beamline 8.3.2 at the Advanced Light Source (ALS). The Synchrotron-based Hard X-ray Micro-Tomography instrument allowed for non-destructive 3-Dimensional imaging of 72 different samples of TPS materials.

Understanding the behavior and composition of TPS materials before and after aerothermal testing is key to meeting the demands of new space exploration goals so materials were examined in both virgin and char states. Char materials were tested on an Oxy-Acetylene Test Bed (OTB). The Micro-CT scans were then rendered into 3D images, which were manipulated and examined for qualitative learnings about the materials. Deep learning segmentation was then used to separate and label each element within the samples. Finally, segmented samples were used to calculate various material parameters such as weight percent, volume percent, and thermal conductivity. These computed values are then compared to empirical information in order to validate this novel methodology. The applications of this methodology for improving the development and iteration of novel ablative materials will be discussed.

Keywords: microstructures, micro-computed tomography, thermal protection systems, ablative materials, deep learning, segmentation, machine learning.

Author α σ ρ CƆ ¥: The University of Texas at Austin; samantha.
§: KAI, LLC.

I. INTRODUCTION

TPS materials are used to protect vehicles from disintegration during atmospheric reentry due to aerodynamic heating [1]. Ablative materials used in TPS cool the reentry vehicle by sending the shock layer's heat away through gases that are produced during pyrolysis. The pyrolysis reaction results in a char layer within the material that further insulates the vehicle from the free stream heat [2, 3]. The development of modern ablative materials is heavily dependent on both laboratory ground testing and material modeling as actual flight testing for materials in development is rare and expensive. For this study, low-density flexible ablators (LDFAs) and medium-density ablators were examined.

X-ray micro-computed tomography (micro-CT) has been used in medical imaging for over 50 years. It has only recently been applied to the analysis and characterization of TPS materials [4, 5]. The LBNL/ALS synchrotron provides a much brighter X-ray source than standalone CT scan devices can generate. This allows for faster shutter speeds and significantly lower scan times.

The tight wavelength band and high quality of the synchrotron X-rays also permits a higher resolution and cleaner sensor readouts, making this method to be even more applicable to materials science. The method works by taking a series of 2D slices by rotating the material on one axis. These slices can then be compiled through tomographic reconstruction to create a 3D image [6]. Recent work into the analysis and reconstruction of highly porous materials has also contributed to the viability of using this methodology for low-density TPS materials [7].

The microstructures of TPS materials were characterized using the Lawrence Berkeley National Laboratory's (LBNL) Beamline 8.3.2 at the Advanced Light Source (ALS) [8, 9]. Experimental methods and challenges are described.

3D images were then rendered for each sample using the image analysis software ORS Dragonfly [10]. 2D and 3D images were examined for each sample and qualitative differences were examined. Semantic segmentation was then applied to label each voxel as an element class such as fiber or void (air) [11-13]. Once the segmentation was applied to the entire sample using machine learning, the microstructures were quantified. Parameters such as weight percentages, volume percentages, and density were calculated. Finally, NASA's Porous Microstructure Analysis (PuMA) software was used to calculate thermal conductivity of the virgin and char samples [14].

II. MATERIALS AND TESTING

2.1 Material Preparation

LDFAs used in this study include samples of graphite felt and quartz felt infiltrated with polysiloxane resin (UHTR) [15]. These novel Polymer Matrix Composite (PMC) ablative materials are being analyzed, tested, and developed for the next generation of re-entry mission requirements. The UHTR was infiltrated into the fiber preform (felt) and then the samples were cured and cut to size. The low-density VDG and WDF graphite felts were provided by Morgan

Advanced Materials. VDG is a high purity graphite felt that is heat treated to a minimum of 1,900°C and exhibits exceptionally low thermal conductivity. WDF is a high purity graphite felt that is heat treated to a minimum of 2,500°C and exhibits low thermal conductivity [16]. The low-density quartz felt was provided by Saint-Gobain. It is made from pure fused quartz fiber and contains more than 99.95% SiO_2 [17].

The solventless polysiloxane resin UHTR 6398-S is a colorless semi-solid resin system manufactured by Techneglas LLC (Perrysburg, OH) [18, 19]. It is formulated using pro- prietary polysiloxane chemistry tailored for composites in flame shielding applications. The viscosity of UHTR 6398-S is 35,000 cPs at 70°C and the density is 1.2 g/cc [20].

The medium-density materials used in this study include the glass/phenolic (G/Ph) material MXB-360. It is manufactured by Sioux Manufacturing, carbon/phenolic (C/Ph) material MX-4926N MC C/Ph manufactured by Solvay and carbon/polysiloxane (C/UHTR) material manufactured by the University of Texas at Austin (UT Austin) [15, 21].

2.2 Oxy-Acetylene Test Bed

For this project, pre-and post-test materials were investigated. Differences between the virgin and char states must be quantified to understand the materials' ablation behavior and qualities more fully. The segmentation of virgin and char materials is therefore explored in the results section. The char samples included in this study were tested at various heat fluxes and exposure times on the Oxy-Acetylene Test Bed (OTB) at UT Austin, pictured in Figure 1a [22-25]. The standoff distance between the torch tip and the sample surface determined the heat flux. This was calibrated using a water-cooled Gardon heat flux transducer to measure the cold-wall heat flux [26]. The results of this calibration are shown in Figure 1b.

(a)

(b)
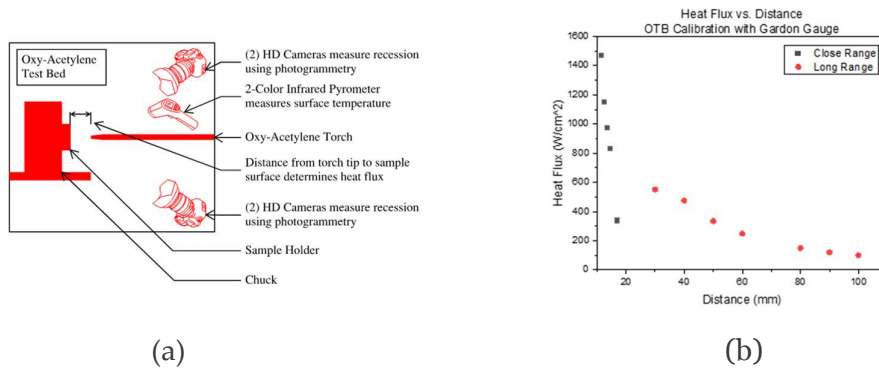
Figure 1: Oxy-Acetylene Test Bed (OTB) at the University of Texas at Austin: (a) Schematic Diagram of OTB; (b) OTB Calibration Curve, Heat Flux vs. Standoff Distance

III.   THE METHOD

3.1   Step 1: Synchrotron Micro-Computed Tomography

For this project, the microstructures of TPS materials were characterized using the LBNL's Beamline 8.3.2 at the ALS. The synchrotron-based hard X-ray micro-tomography instrument allowed for non-destructive 3-dimensional imaging of 72 different TPS mate- rials. The tomography voxels were used to reconstruct images using the rendering software Dragonfly [27, 28]. A resolution of 3.45 voxels per micron was achieved by balancing scan length and intensity. The Beamline 8.3.2 provided 500 mA of current to the instru- ment for imaging. The instrument was set to take 2,625 continuous tomographic images over the course of 511.4 seconds.

A schematic diagram and image of the synchrotron micro-CT instrument is shown in Figure 2a and Figure 2b, respectively.

(a)

(b)
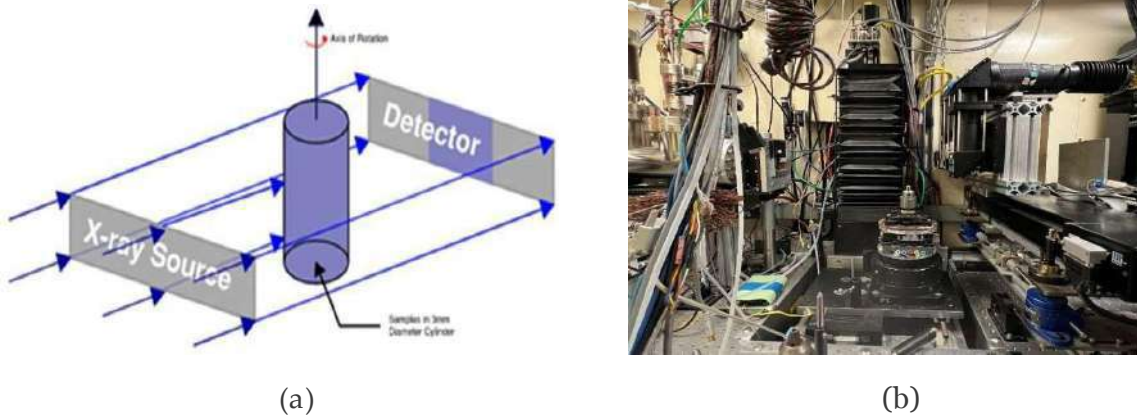
Figure 2: Synchrotron Hard X-Ray Micro-CT at the LBNL/ALS: (a) Schematic Diagram of Synchrotron Instrument; (b) Picture of Synchrotron Instrument

The synchrotron-based hard X-ray micro-tomography instrument allowed for non-destructive 3D imaging of 72 different samples of TPS materials over two visits in June and October of 2022. Small samples of each TPS material of interest were collected and inserted into small diameter plastic tubes with wooden spacers to separate materials, see Figure 3. A challenge associated with this method is the preservation of low-density samples' original density when put into the sample holder and avoiding crushing or altering the sample configuration.

(a)   (b)
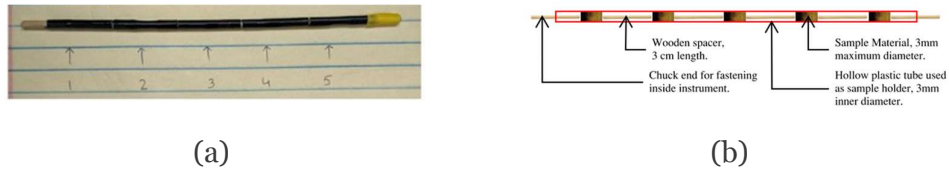
Figure 3: Sample Preparation of 72 TPS Material Samples for Micro-Tomographic Scanning at the LBNL/ALS: (a) Picture of Sample Holder; (b) Schematic Diagram of Sample Holder Setup

3.2 Step 2: Image Rendering and Qualitative Comparison

The synchrotron scan data was then loaded into ORS Dragonfly and rendered into 3D images. A selection of the more morphologically interesting samples are shown in Figure 4, Figure 5, and Figure 6. Colors were assigned for contrast and the void (air) was removed using the Otsu method in order to make the images more readable, see Figure 4c, Figure 5, and Figure 6. [29].

(a)   (b)   (c)
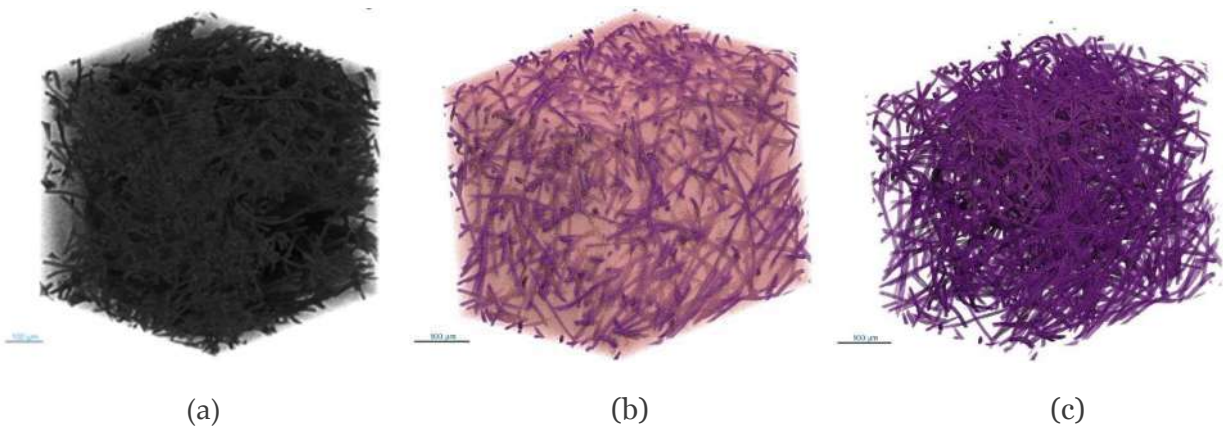
Figure 4: Synchrotron Scans Rendered in ORS Dragonfly: (a) High-Density Quartz Felt With UHTR; (b) High-Density Quartz Felt With UHTR; and (c) High-Density Quartz Felt With Void Digitally Re- Moved

Preforms are pictured below in Figure 5, and Figure 6. These are graphite and quartz felts prior to infiltration with resin. Differences in relative fiber size and shape are clearly visible. The density difference between the low-density and high-density quartz preforms in Figure 6 is also visible to the human eye.

(a)   (b)
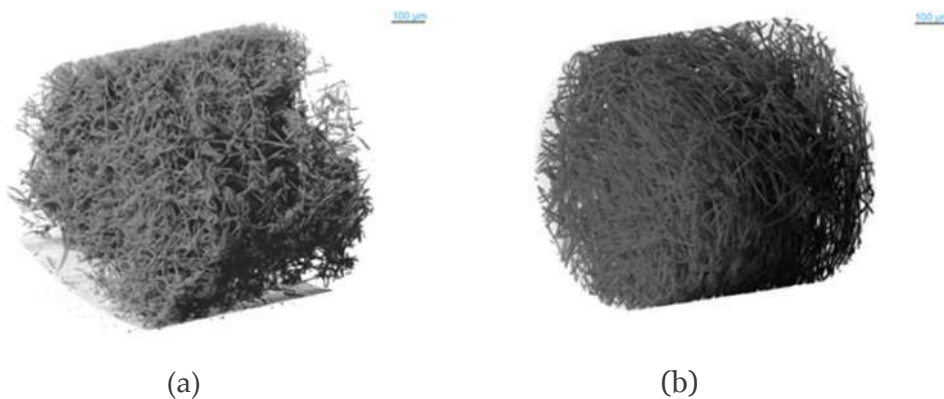
Figure 5: Synchrotron Scans Rendered in ORS Dragonfly: (a) VDG Graphite Felt; (b) WDF Graphite Felt

Figure 6: Synchrotron Scans Rendered in ORS Dragonfly: (a) Quartz Felt; (b) High-Density Quartz Felt

3.3 Step 3: Deep Learning Semantic Segmentation

Segmentation of each sample is key to further characterization and analysis. After comparison between gray scale and semantic segmentation methods, it was found that semantic segmentation was more accurate [11-13]. Rather than dealing with hand painting over 2,000 slices for the semantic segmentation, it was decided to use the machine learning capabilities of Dragonfly to segment the samples [10, 28]. The images were cropped to a size of 750 voxels or around 0.5 mm to lower computation time. They were cropped from 750 to 1500 pixels in the x, y, and z directions. Cropping the images also allowed for the selection of a representative area of the sample volume. 2.5D U-net deep learning models were used to segment all six samples [30]. The patch size was 128, the batch size was 32. The model ran for 50 epochs using a categorial cross entropy loss function and the Adadelta optimization algorithm [31, 32]. The model was built to segment the material into three classes: void, fiber, and resin. The void is shown below in green, the fiber in pink, and the resin in blue.

The TPS materials examined in this study are the LDFAs, with density around 0.3 g/cc. They are novel ablative materials created to replace earlier generations of heat shield materials. These novel Polymer Matrix Composite (PMC) ablative materials consist of a reinforcement of graphite or quartz fibers, and polymer matrix is made of polysiloxane resin. Segmentation of these materials consists of three elements: the void (air), the fiber, and the resin.

In this process, the ten training slices were hand painted so that each pixel was assigned to the classes: void, fibers, and resin. The void (green) was assigned using the lower Otsu, and any issues were then fixed by hand [29]. The rest of the pixels were assigned to the fiber class (pink) and then the UHTR resin was selected by hand and assigned to the resin class (blue). An example of one of the ten semantically segmented 2D slices is shown in Figure 7. A training set of seven slices and validation set of three slices were prepared for the semantic segmentation. The trained model was then applied to the remaining 740 slices. The isometric view before and after the deep learning model was applied is shown in Figure 8.

(c) (b)
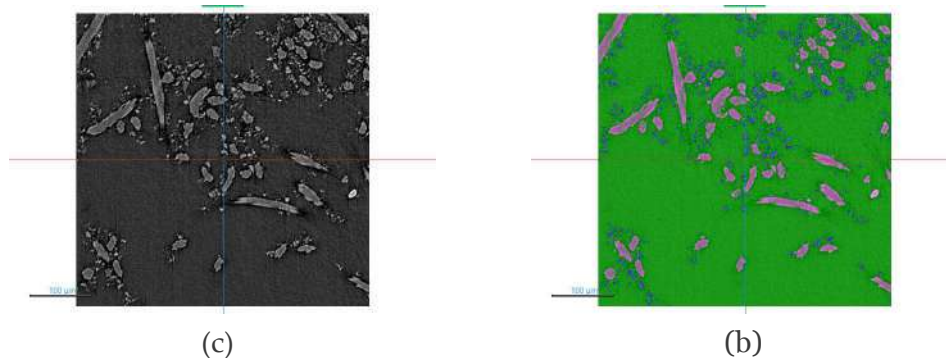
Figure 7: Synchrotron Scans Rendered in ORS Dragonfly, VDG Graphite/UHTR: (a) Original Render; (b) Semantic Segmentation Training Slice

A Novel Approach to Analyzing the Microstructures of Thermal Protection Systems Materials for Hypersonic Applications

London Journal of Engineering Research

<p align="center">(a)   (b)</p>
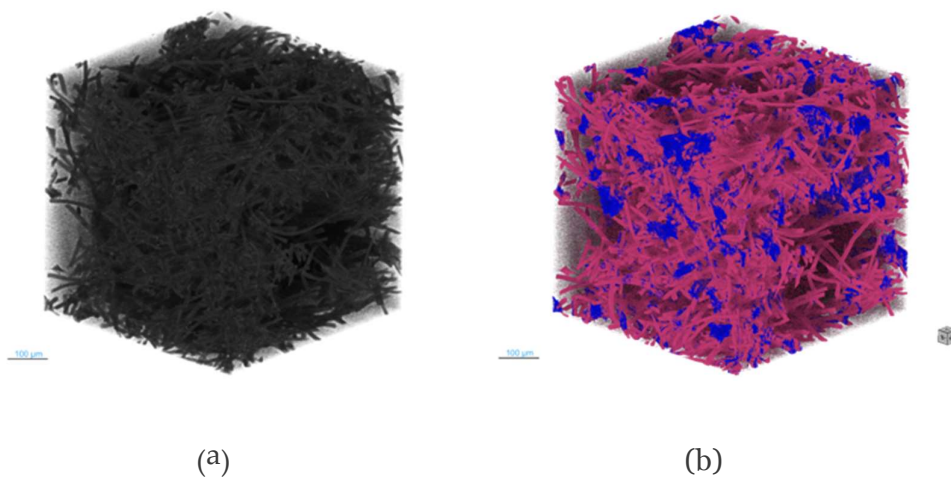
Figure 8: Synchrotron Scans Rendered in ORS Dragonfly, VDG Graphite/UHTR: (a) Original Render; (b) After Semantic Segmentation, Void Removed for Readability

3.4 Step 4: Scalar Properties Calculation

The densities of each material and the volume of the samples were used to calculate the weight percentage of each element from the microstructures [15-17]. Densities of each component and of the finished materials are listed in Table 1. The weights of each element and total weight of each sample are shown in Appendix A, Table A1. The weight is calculated using the voxel count, element density, and total volume of the 750-voxel cube, which is 1.03E-05 cm³. The weights of each class are calculated from the voxel count and the density of each class.

Table 1: Density of Each Element, Empirical Data for Virgin Materials

Material	Density (g/cc)
VDG Graphite Felt	0.090
WDF Graphite Felt	0.080
Quartz Felt	0.015
UHTR	1.200
VDG Graphite/UHTR	0.270
WDF Graphite/UHTR	0.300
Quartz/UHTR	0.310

Below, the percentage weight and volume of each element class are shown for all six LDFA samples. Figure 9a shows the weight percent. The resin is by far the largest weight contributor, which is reasonable as the density of resin is more than ten orders of magnitude larger than the fiber felts. Figure 9b shows the percent volume of each element class in the LDFA samples. The void represents an extremely small part of the weight of each sample due to the low density of air at standard temperature and pressure. However, the void makes up around 90% of the volume of the samples, which is expected with the lowdensity classification of these novel TPS materials.

<div style="writing-mode: vertical-lr;">London Journal of Engineering Research</div>

A Novel Approach to Analyzing the Microstructures of Thermal Protection Systems Materials for Hypersonic Applications

(e)

(b)
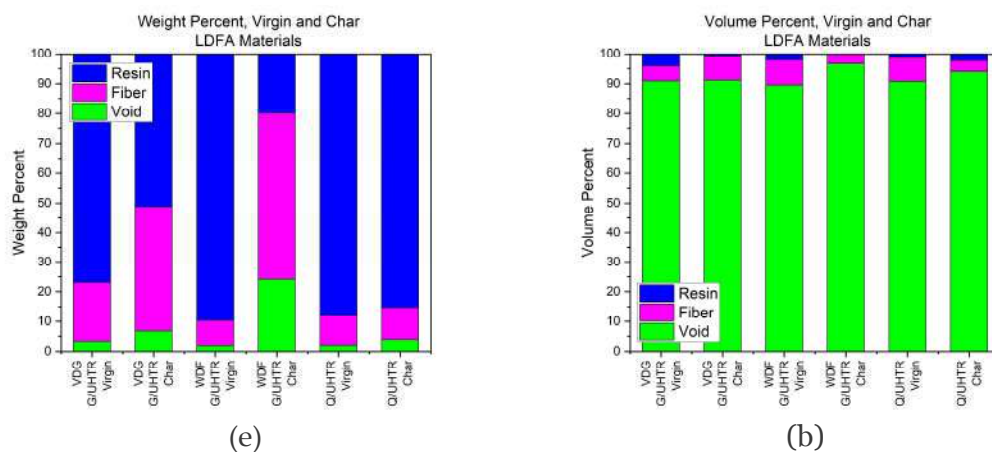
Figure 9: Segmentation Quantitative Comparison: (a) Weight Percent of Virgin Material; (b) Volume Percent of Virgin Material

3.5 Step 5: Virgin Material vs. Char Material Comparison

Virgin and char materials were compared both qualitatively and quantitatively to foster understanding of the changes to microstructures of TPS materials after aerothermal testing. The low-density preform material Polybenzimidazole (PBI) is shown in Figure 10 in virgin and char states. The density is very clearly lower for the char material and the fibers are less contiguous.

(f)

(b)
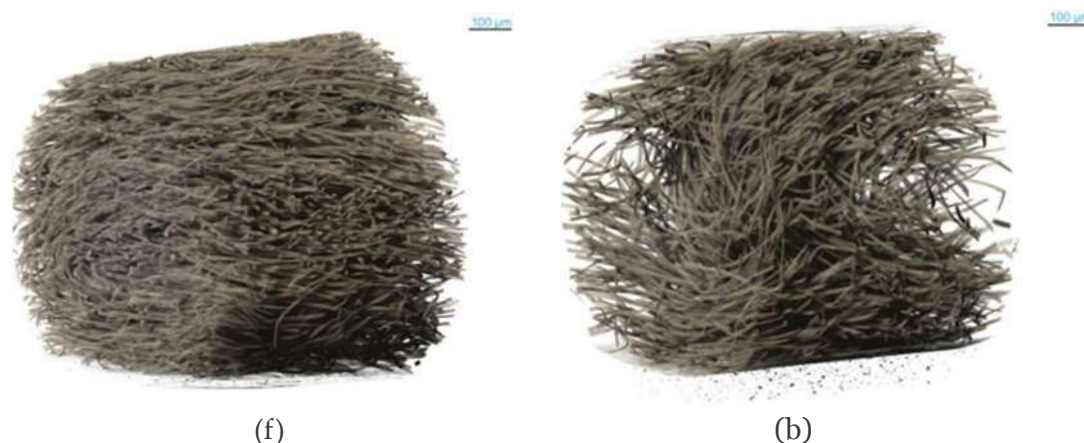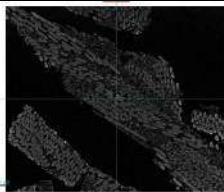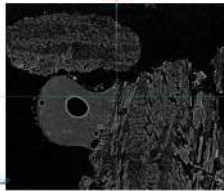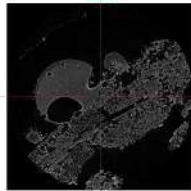
Figure 10: PBI Material 3D Rendering: (a) Virgin; (b) Char

The medium-density material MXB-360, which is a glass/phenolic material produced by Sioux Manufacturing, is shown before and after testing in Table 2 and Figure 11. From other analysis including TGA and EDX, it is known that MXB-360 decomposes into carbonaceous char and silica-oxide glass during testing [25]. The glass element is incredibly clear in the microstructural images in Table 2 and Figure 11 as the rounded bubble shapes in the char material. This visual element is completely missing from the virgin material. The charred sample was exposed to 1,000 W/cm² for 30s on the OTB.

A Novel Approach to Analyzing the Microstructures of Thermal Protection Systems Materials for Hypersonic Applications

Table 2: MXB-360 Virgin and Char Microstructures Comparison

Material	Method	XY-Face	XZ-Face	YZ-Face
MXB-360	Virgin			
	Char			

(**a**)   (**b**)
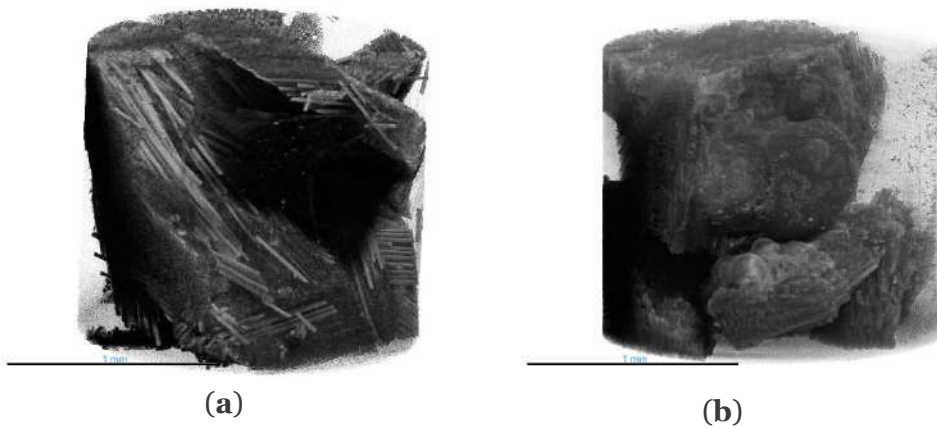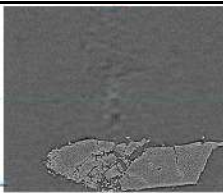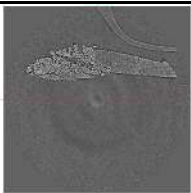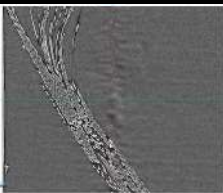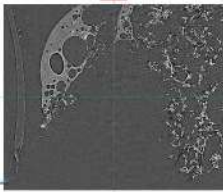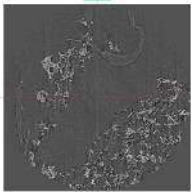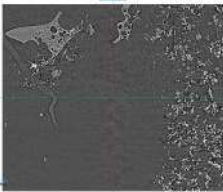
Figure 11: MXB-360 Glass/phenolic Virgin and Char Microstructures Comparison: (a) Virgin Material Isometric View; (b) Char Material Isometric View

The medium-density material carbon/UHTR, is shown before and after testing in Table 3 and Figure 12. The result of vibrations can be seen in the slight ripples in the background of the virgin material images. The contiguous material seen in the background of Figure 12b is actually the sample holder and should be ignored. The charred sample was tested on the Inductively Coupled Plasma torch (ICP) [33]. The char material looks completely different structurally from the virgin material and includes several large bubbles. Additional analysis is in progress.

Table 3: C/UHTR Virgin and Char Microstructures Comparison

Material	Method	XY-Face	XZ-Face	YZ-Face
C/UHTR	Virgin			
	Char (ICP)			

(a)

(b)
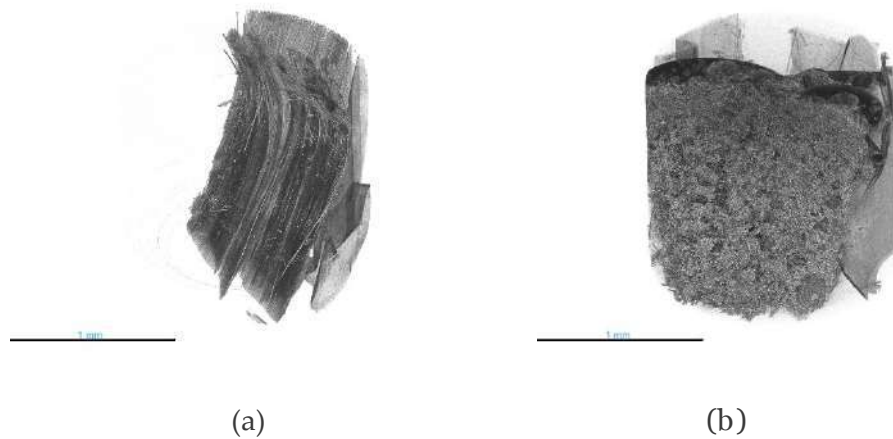
Figure 12: C/UHTR Virgin and Char Microstructures Comparison: (a) Virgin Material Isometric View; (b) Char (ICP) Material Isometric View

The medium-density material MX-4926 MC Carbon/Phenolic, is shown before and after testing in Table 4 and Figure 13. Sample 1-45 and 1-46. The virgin material is much more uniform than the char material. No individual fibers or frayed edges of material are visible in Figure 13a, but they are in Figure 13b. Additionally, the char material takes up more volume within the cylinder than the virgin material. From the 2D slices, it is clear that the denser the material is, the harder it is to visualize without extensive image ma- nipulation. Additional analysis is in progress.

Table 4: MX-4926N MC C/Ph Virgin and Char Microstructures Comparison

Material	Method	XY-Face	XZ-Face	YZ-Face
MX-4926N MC	Virgin			
	Char (ICP)			

(a)

(b)
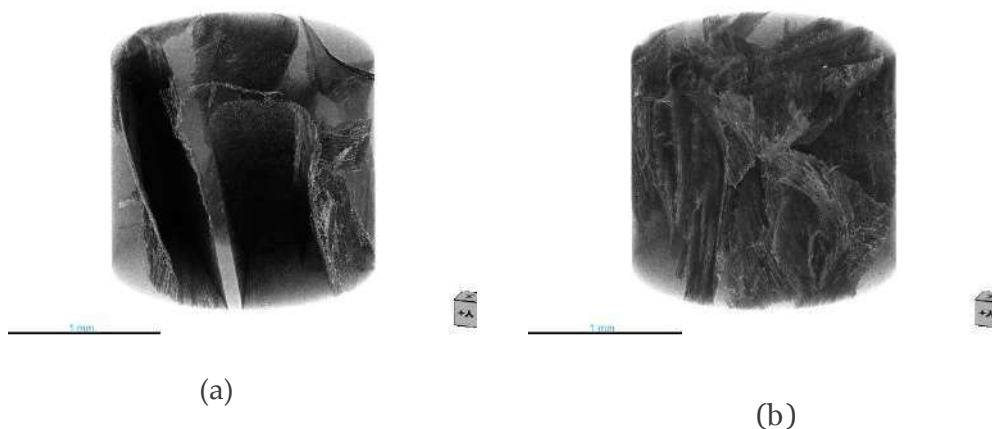
Figure 13: MX-4926N MC C/Ph Virgin and Char Microstructures Comparison: (a) Virgin Material Isometric View; (b) Char Material Isometric View

After segmentation of the LDFAs, the virgin and char materials were compared to see if there was a consistently higher volume percentage of void in the charred materials, Figure 14. The three felt/UHTR ablators show a clear decrease in density after testing. The percentage volume of void is higher for the char than the virgin material in each case. This is also confirmation that the segmentation method has the capability to compare virgin and char materials. The table of values for each segmentation method are shown in Appendix A, Table A2.
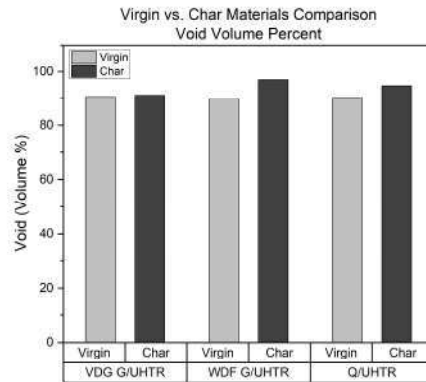
Figure 14: Virgin vs. Char Materials Comparison, Void Volume Percent

3.6 Step 6: Thermal Conductivity Calculation

NASA's PuMA software was used to calculate the thermal conductivity of each of the samples [34, 35]. These samples were cropped to 500 voxels to fit within computational requirements. The calculation was conducted within PuMA for ORS Dragonfly. For a sanity check, PuMA was first used to confirm anisotropy of quartz preform that was visually apparent. In Figure 15a, the original render of the quartz preform is shown. Figure 15b shows the output of the PuMA thermal conductivity calculation. The results are also shown in Table 5, and confirm an anisotropic thermal conductivity that is maximized in the z- z direction, which is parallel to the fibers in Figure 15.

(a)

(b)
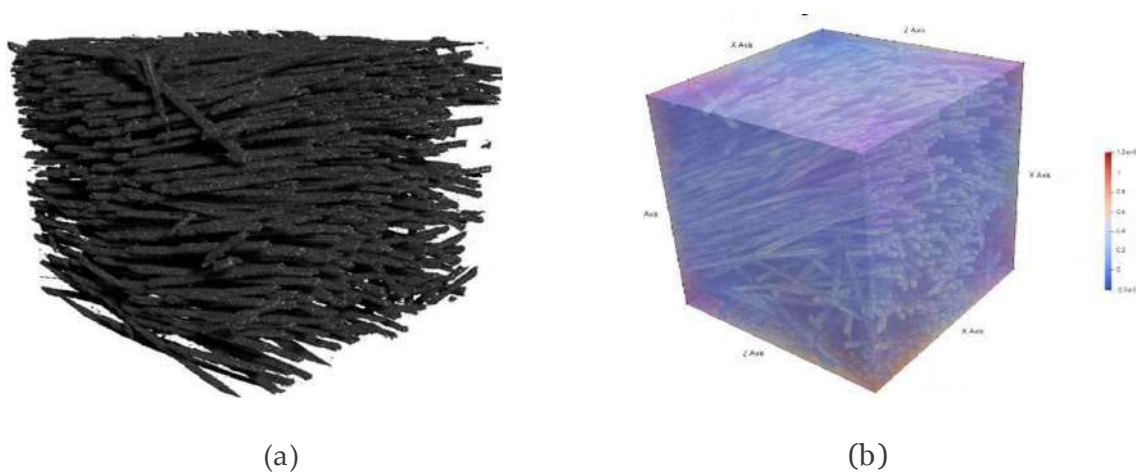
Figure 15: Quartz Preform: (a) Virgin Material Isometric View With Void Removed; (b) PuMA Thermal Conductivity Output

Table 5: Thermal Conductivity of Quartz Preform, Calculated With PuMA

Thermal Conductivity (W/mK)	x	y	z
x	**0.35**	0.02	0.07
y	0.02	**0.52**	0.38
z	0.67	0.38	**1.27**

To use PuMA, a thermal conductivity value was assigned to each material in the segmented model. These values were mostly taken from manufacturer's data sheets and are shown in Appendix A, Table A3. Since PuMA only accepts one thermal conductivity value for each material, materials with anisotropic thermal conductivity may result in inaccurate calculations. Additionally, this calculation is performed at standard temperature and pressure, which is currently the only option available with PuMA. Finally, PuMA is only for low-density materials. The calculation shown below is therefore for the virgin and char LDFA VDG Graphite/UHTR in Table 6 and Table 7, respectively.

Table 6: Thermal Conductivity of Virgin VDG Graphite/UHTR, Calculated With PuMA

Thermal Conductivity (W/mK)	x	y	z
x	**0.14**	0.00	0.03
y	0.00	**0.53**	0.02
z	0.02	0.13	**0.52**

Table 7: Thermal Conductivity of Char VDG Graphite/UHTR, Calculated With PuMA

Thermal Conductivity (W/mK)	x	y	z
x	**0.17**	0.01	0.26
y	0.02	**0.41**	0.01
z	0.04	0.04	**0.09**

The results of PuMA are also shown in pictorial form in Table 8. The thermal conductivity in each direction is more uniform for the virgin material than the char material. This is a very logical and promising result combined with the reasonable thermal conductivity values. In future, these values will be compared to experimentally measured thermal conductivity for the LDFAs.

Table 8: VDG Graphite/UHTR Thermal Conductivity

Material	Method	X-Applied Heat	Y-Applied Heat	Z-Applied Heat
VDG Graphite/UHTR	Virgin			
	Char			
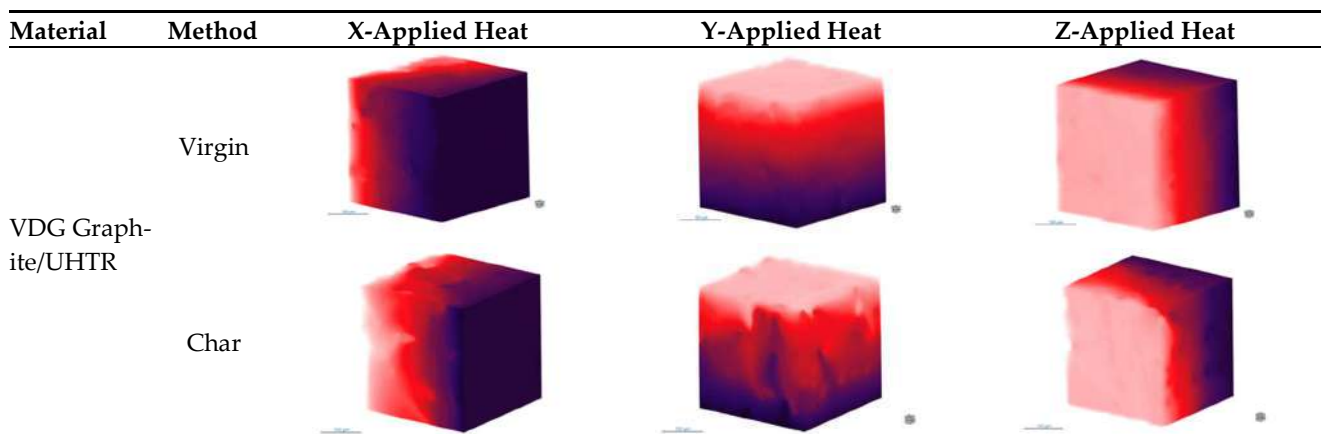
3.7 Step 7: In-Situ Experiments

In the future, in-situ micro-CT scans will be taken while performing thermal and mechanical properties testing at the LBNL/ALS facility [34, 35]. Three sets of in-situ tests are planned. Pyrolysis in air or inert gas (argon) of neat resins and low-density flexible ablators (LDFAs) at elevated temperature around 1,000°C will be conducted to examine phase change reactions of these materials. This will provide invaluable information about the performance of TPS materials under thermal testing. Mechanical properties such as compression strength, tensile strength, and three-point bend will be examined and quantified using in-situ synchrotron scans at room temperature first using specially designed test chambers at LBNL/ALS [36-39]. These mechanical properties tests will later be performed at elevated temperatures up to 1,500°C.

The above three micro-CT experiments will combine a novel experimental and modeling approach to study LDFAs. Development of this methodology will enable the design, fabrication, and characterization of the next generation of high-performance TPS materials including high-density TPS materials, such as carbon/carbon composites and ceramic matrix composites.

V. CONCLUSIONS

The goal of this novel methodology is to discover and quantify connections between the microstructures and the ablation performance of these TPS materials. Following these systematic steps allows for the full characterization of a material's microstructures. In the future, each of these parameters will be linked back to and validated by an experimental measurement. Comparing similar ablative materials to each other allows for better understanding of how microstructures can contribute to differences in ablation performance. This allows researchers to link *processing-properties-performance* relationships of TPS materials. In the future, this methodology will be utilized for generative design of novel TPS materials.

VI. FUTURE WORK

Mechanical properties of the ablative materials will be investigated as a part of this methodology. For example, char strength is an important factor in ablative performance. A mechanical char strength tester has been created and used on several materials [40, 41]. These results will be compared to a calculated char strength from material microstructures transferred into an FEA program. Material response (MR) modeling is also another important part of this integrated research, MR modeling will enable our research group to predict the heat transfer and ablation performance of these novel TPS materials [23].

Selected ablators will be tested and evaluated using an inductively coupled plasma (ICP), LHMEL, and HYMETS arc jet test facilities [33, 42]. The experimental data obtained from these test facilities will be used to validate our microstructures-based model and material response simulation.

High-density TPS materials will also be investigated using this approach including Ceramic Matrix Composites (CMCs) and Carbon/Carbon Composites (CCCs) for hyper-sonic TPS applications.

Other methods of preserving sample integrity when creating synchrotron samples will also be explored. This could include epoxy to encapsulate samples before cutting, and coring full length samples [15].

Data Availability Statement: The data presented in this study are available on request from the corresponding author. The data are not publicly available due to some scanned materials being pro- prietary.

ACKNOWLEDGMENTS

Source and used the Beamline 8.3.2 Synchrotron Micro-Computed Tomography.

Appendix A

Table A1: Weight of Each Element and Total for the Virgin Materials, Calculated and Experimental

Material	Method	Void Weight (µg)	Fiber Weight (µg)	Resin Weight (µg)	Total Weight (µg)
Sample 1-12 Virgin VDG Graphite / UHTR	Experimental Value	-	-	-	135.00
	Segmented with Semantic Segmentation	0.58	3.45	13.46	17.50
Sample 2-24 Virgin WDF Graphite / UHTR	Experimental Value	-	-	-	150.00
	Segmented with Semantic Segmentation	0.58	2.48	26.56	29.62
Sample 1-16 Virgin Quartz / UHTR	Experimental Value	-	-	-	155.00
	Segmented with Semantic Segmentation	0.58	2.89	25.00	28.47

Table A2: Void Percent Volume for All Six Samples, Both Segmentation Methods

Material	Method	Void Volume (%)
Sample 1-12 Virgin VDG Graphite / UHTR	Segmented with Semantic Segmentation	90.09
Sample 1-23 Char VDG Graphite / UHTR	Segmented with Semantic Segmentation	91.24
Sample 2-24 Virgin WDF Graphite / UHTR	Segmented with Semantic Segmentation	90.05
Sample 1-25 Char WDF Graphite / UHTR	Segmented with Semantic Segmentation	96.69
Sample 1-16 Virgin Quartz / UHTR	Segmented with Semantic Segmentation	89.42
Sample 1-27 Char Quartz / UHTR	Segmented with Semantic Segmentation	94.04

Table A3: Density of Each Element in the LDFA Materials

Material	Thermal Conductivity at 20°C (W/mK)
VDG Graphite Felt	0.090 [16]
WDF Graphite Felt	0.080 [16]
Quartz Felt	0.035 [17]
UHTR	0.344*
Air / Void	0.028 [43]

* UHTR thermal conductivity is currently being investigated. The number used is for a carbon/polysiloxane composite, not pure resin.

REFERENCES

1. Rabinovitch, J., *Advancing EDL Technologies for Future Space Missions: From Ground Testing Facilities to Ablative Heatshields.* 2014, California Institute of Technology: Ann Arbor. p. 198. DOI: 10.7907/XKM7-7368.

2. Natali, M., J.M. Kenny, and L. Torre, *Science and technology of polymeric ablative materials for thermal protection systems and propulsion devices: A review.* Progress in Materials Science, 2016. *84*: p. 192-275. DOI: https://doi.org/10.1016/j.pmatsci.2016.08.003.

3. Uyanna, O. and H. Najafi, *Thermal protection systems for space vehicles: A review on technology development, current challenges and uture ros ects.* Acta Astronautica

3. Uyanna, O. and H. Najafi, *Thermal protection systems for space vehicles: A review on technology development, current challenges and future prospects*. Acta Astronautica 2020. *176*: p. 341-356. DOI: https://doi.org/10.1016/j.actaastro.2020.06.047.

4. Coindreau, O., C. Mulat, C. Germain, J Lachaud, and G.L. Vignoles, *Benefits of X-Ray CMT for the Modeling of C/C Composites*.

5. Advanced Engineering Materials, 2011. *13*(3): p. 178-185. DOI: https://doi.org/10.1002/adem.201000233.

6. Salvo, L., P. Cloetens, E. Maire, S. Zabler, J.J. Blandin, J.Y. Buffière, W. Ludwig, E. Boller, D. Bellet, and C. Josserond, *X-ray micro-tomography an attractive charac-terisation technique in materials science*. Nuclear Instruments and Methods in Physics Research Section B: Beam Interactions with Materials and Atoms, 2003. *200*: p. 273-286. DOI: https://doi.org/10.10 16/S0168-583X(02)01689-0.

7. Landis, E.N. and D.T. Keane, *X-ray microtomography*. Materials Characteriza-tion, 2010. *61*(12): p. 1305-1316. DOI: https://doi.org/10.1016/j.matchar.2010.09.012.

8. Maire, E., *X-Ray Tomography Applied to the Characterization of Highly Porous Materials*. Annual Review of Materials Research, 2012. *42*(1): p. 163-178. DOI: 10.1146/annurev-matsci-070511-155106.

9. MacDowell, A., D. Parkinson, A. Haboub, E. Schaible, J. Nasiatka, C. Yee, J. Jameson, J. Ajo-Franklin, C. Brodersen, and A. McElrone, *X-ray micro-tomography at the Advanced Light Source*. SPIE Optical Engineering + Applications. Vol. 8506. 2012: SPIE.

10. Laboratory, L.B. *MicroCT Home*. [cited 2022; Available from: https://microct.lbl.gov/.

11. Makovetsky, R., N. Piche, and M. Marsh, *Dragonfly as a Platform for Easy Image-based Deep Learning Applications*. Microscopy and Microanalysis, 2018. *24*(S1): p. 532-533. DOI: 10.1017/S14319276180031 5X.

12. Lateef, F. and Y. Ruichek, *Survey on semantic segmentation using deep learning techniques*. Neurocomputing, 2019. *338*: p. 321- 348. DOI: https://doi.org/10.1016/j.neucom.2019.02.003.

13. Garcia-Garcia, A., S. Orts-Escolano, S. Oprea, V. Villena-Martinez, P. Martinez-Gonzalez, and J. Garcia-Rodriguez, *A survey on deep learning techniques for image and video semantic segmentation*. Applied Soft Computing, 2018. *70*: p. 41-65. DOI: https://doi.org/10.1016/j.asoc.2018.05.018.

14. Garcia-Garcia, A., S. Orts-Escolano, S. Oprea, V. Villena-Martinez, and J. Garcia-Rodriguez, *A review on deep learning techniques applied to semantic segmentation*. arXiv preprint arXiv:1704.06857, 2017.

15. Ferguson, J.C., F. Panerai, A. Borner, and N.N. Mansour, *PuMA: the Porous Microstructure Analysis software*. SoftwareX, 2018. *7*: p. 81-87. DOI: https://doi.org/10.1016/j.softx.2018.03.001.

16. Hou, Y., C. Yee, W. Li, J. Koo, L. Li, B. Rech, W. Fahy, H. Wu, and J. Buffy, *A novel ablative material for thermal protection system: Carbon fiber/polysiloxane composites*. Aerospace Science and Technology, 2022. *129*: p. 107822. DOI: 10.1016/j.ast.2022.107822.

17. *Technical Data Sheet, Graphitic Felt*. [cited 2023.

18. *Technical Data Sheet, Quartzel Felts*. Advanced Ceramic Composites 2023 [cited 2023; Available from: https://www.quartz.saint-gobain.com/products/quartzel/felts.

19. Christopher Fish, J.B., *High performance compositions and composites*. 2017, Burning Bush Technologies LLC, Techneglas LLC: United States.

20. Fish, C., *High performance compositions and composites*. 2017, Techneglas LLC: United States.

21. Schellhase, K., J. Koo, H. Wu, and J. Buffy, *Experimental Characterization of Material Properties of Novel Silica/Polysiloxane Ablative*. Journal of Spacecraft and Rockets, 2018. *55*: p. 1-13. DOI: 10.2514/1.A34044.

22. Solvay. *MX 4926N MOLDING COMPOUND Technical Data Sheet*. 2023 [cited 2023; Available from: https://www.solvay.com/en/product/mx-4926n-mx-4926n-mc#product-documents.

23. Koo, J.H., M. Natali, B. Lisco, E. Yao, and K. Schellhase, *In Situ Ablation Recession and Thermal Sensor for Thermal Protection Systems*. Journal of Spacecraft and Rockets, 2014. *55*(4). DOI: 10.2514/1.A33925.

24. Bernstein, S., C.M. Yee, W. Li, M.E. Ewing, and J.H. Koo, *Comparison of Material Response Models for Low-Density Ablative Materials*, in *AIAA SciTech 2023 Forum*. 2023, American Institute of Aeronautics and Astronautics. DOI: 10.2514/6.2023-2023.

25. Wu, H., A. Kafi, C. Yee, O. Atak, J.H. Langston, R. Reber, J. Misasi, S. Kim, W.P. Fahy, S. Bateman, and J.H. Koo, *Ablation Performances of Additively Manufactured High-Temperature Thermoplastic Polymers*, in *AIAA Scitech 2020 Forum*. 2020. DOI: 10.2514/6.2020-1125.

26. Yee, C.M.K., *Development and validation of an ablative material response model for MXB-360 and MXBE-350*. 2021, University of Texas: Austin, TX, MS Thesis.

27. Fu, T., A. Zong, J. Tian, and C. Xin, *Gardon gauge measurements of fast heat flux transients*. Applied Thermal Engineering, 2016. *100*: p. 501-507. DOI: https://doi.org/10.1016/j.applthermaleng.2016.02.043.

28. *Dragonfly Pro*. 2022, Object Research Systems (ORS) Inc.

29. Provencher, B., N. Piché, and M. Marsh, *Simplifying and Streamlining Large-Scale Materials Image Processing with Wizard-Driven and Scalable Deep Learning*. Microscopy and Microanalysis, 2019. *25*(S2): p. 402-403. DOI: 10.1017/S1431927619002745.

30. Otsu, N., *A Threshold Selection Method from Gray-Level Histograms*. IEEE Transactions on Systems, Man, and Cybernetics, 1979. **9**(1): p. 62-66. DOI: 10.1109/TSMC.1979.4310076.

31. Sinchuk, Y., P. Kibleur, J. Aelterman, M.N. Boone, and W. Van Paepegem, *Variational and Deep Learning Segmentation of Very-Low-Contrast X-ray Computed Tomography Images of Carbon/Epoxy Woven Composites*. Materials, 2020. *13*(4): p. 936.

32. Jadon, S. *A survey of loss functions for semantic segmentation*. in *2020 IEEE Conference on Computational Intelligence in Bioinformatics and Computational Biology (CIBCB)*. 2020. DOI: 10.1109/CIBCB48159.2020.9277638.

33. Zeiler, M.D., *ADADELTA: An Adaptive Learning Rate Method*. Cornell University, 2012. DOI: https://doi.org/10.48550/arXiv.1212.5701.

34. Greene, B.R., N.T. Clemens, P.L. Varghese, S. Bouslog, and S.V.D. Papa, *Characterization of a 50kW Inductively Coupled Plasma Torch for Testing of Ablative Thermal Protection Materials*, in *55th AIAA Aerospace Sciences Meeting*. DOI: 10.2514/6.2017-0394.

35. Ferguson, J.C., F. Panerai, J. Lachaud, A. Martin, S.C.C. Bailey, and N.N. Mansour, *Modeling the oxidation of low-density carbon fiber material based on micro-tomography*. Carbon, 2016. *96*: p. 57-65. DOI: https://doi.org/10.1016/j.carbon.2015.08.113.

36. Francesco Panerai, B.B., Justin Haskins, Collin Foster, Harold Barnard, Eric Stern and Jay Feldman, *Morphological Evolution of Ordinary Chondrite Microstructure during Heating: Implications for Atmospheric Entry*. The Planetary Science Journal, 2021. *2*. DOI: 10.3847/PSJ/ac1749.

37. Schöberl, E., C. Breite, A. Melnikov, Y. Swolfs, M.N. Mavrogordato, I. Sinclair, and S.M. Spearing, *Fibre-direction strain measurement in a composite ply under quasi-static tensile loading using Digital Volume Correlation and in situ Synchrotron Radiation Computed Tomography*. Composites Part A: Applied Science and Manufacturing, 2020. *137*: p. 105935. DOI: https://doi.org/10.1016/j.compositesa.2020.105935.

38. Schöberl, E., M. Mavrogordato, I. Sinclair, and S. Spearing, *Fibre direction strain measurement in a composite ply under pure bending using Digital Volume Correlation and Micro-focus Computed Tomography*. Journal of Composite Materials, 2020. *54*(14): p. 1889-1912. DOI: 10.1177/0021998320918648.

39. Schöberl, E., C. Breite, S. Rosini, Y. Swolfs, M. Mavrogordato, I. Sinclair, and S. Spearing, *A novel particle-filled carbon-fibre reinforced polymer model composite tailored for the*

application of digital volume correlation and computed tomography. Journal of Composite Materials, 2021. *55*(14): p. 1907-1934. DOI: 10.1177/0021998320966388.

40. Rosini, S., M.N. Mavrogordato, O. Egorova, E.S. Matthews, S.E. Jackson, S. Mark Spearing, and I. Sinclair, *In situ statistical measurement of local morphology in carbon-epoxy composites using synchrotron X-ray computed tomography.* Composites Part A: Applied Science and Manufacturing, 2019. *125*: p. 105543. DOI: https://doi.org/10.1016/j.compositesa.2019.105543.

41. Rech, B.M., *Char Strength of Low-Density Thermal Protection Systems Materials*, in *AIAA SCITECH 2023 Forum*. DOI: 10.2514/6.2023-2022.

42. Lewis, J.A., M.H. Jaramillo, and J.H. Koo, *Development of a shear char strength sensing technique to study thermoplastic polyurethane elastomer nanocomposites.* Polymers for Advanced Technologies, 2017. *28*(12): p. 1707-1718. DOI: https://doi.org/10.1002/pat.4044.

43. Zhao, Y., B. Chen, and J.H. Koo, *Aerothermal Testing of Ablatives for Material Performance*, in *AIAA Scitech 2020 Forum*. DOI: 10.2514/6.2020-1855.

44. Kadoya, K., N. Matsunaga, and A. Nagashima, *Viscosity and Thermal Conductivity of Dry Air in the Gaseous Phase.* Journal of Physical and Chemical Reference Data, 1985. *14*(4): p. 947-970. DOI: 10.1063/1.555744.

Assessment of Cybersecurity Deployment to Power System Smart Grid

Adeloye A.A, Abood S.I, Annamalai A, Butler-Purry K & Chouikha M.F

A&M University, Texas

ABSTRACT

This comprehensive study delves into the multifaceted landscape of modern power systems, encompassing their intricate infrastructure, the integration of smart grid technology for optimized energy management, the critical significance of cybersecurity in safeguarding against a plethora of cyber threats, and the identification of gaps in the deployment of effective cybersecurity measures. The investigation delves into three primary deployment clusters, focusing on system operation continuity protection, network security, and data protection, each pivotal in ensuring smart grids' secure and seamless operation. Moreover, the study underscores the importance of frequency bias tie line control in maintaining stability within interconnected grids and addresses the evolving tactics of cyber attackers in exploiting vulnerabilities in power systems.

By assessing recent cyber-physical compromise incidents and their cascading consequences, the research highlights the urgency of robust defense strategies and the need for international collaboration in strengthening the resilience of power system smart grids.

Index terms: cybersecurity, cyber-threats, cyber- physical compromise, power system stability, critical infrastructure, smart grid.

Classification: LCC: QA76.9.A25

Language: English

Assessment of Cybersecurity Deployment to Power System Smart Grid

Adeloye A.Aᵅ, Abood S.Iᵟ, Annamalai Aᵖ, Butler-Purry K,ꟺ & Chouikha M.F¥

ABSTRACT

This comprehensive study delves into the multifaceted landscape of modern power systems, encompassing their intricate infrastructure, the integration of smart grid technology for optimized energy management, the critical significance of cybersecurity in safeguarding against a plethora of cyber threats, and the identification of gaps in the deployment of effective cybersecurity measures. The investigation delves into three primary deployment clusters, focusing on system operation continuity protection, network security, and data protection, each pivotal in ensuring smart grids' secure and seamless operation. Moreover, the study underscores the importance of frequency bias tie line control in maintaining stability within interconnected grids and addresses the evolving tactics of cyber attackers in exploiting vulnerabilities in power systems.

By assessing recent cyber-physical compromise incidents and their cascading consequences, the research highlights the urgency of robust defense strategies and the need for international collaboration in strengthening the resilience of power system smart grids. This comprehensive analysis culminates in a resounding call for fortified cybersecurity frameworks to safeguard the reliability of power supply in the face of evolving cyber threats.

Index terms: cybersecurity, cyber-threats, cyber-physical compromise, power system stability, critical infrastructure, smart grid.

Author α σ ρ ꟺ ¥*:* Department of Electrical and Computer Engineering, Prairie View A & M University, Texas.

ꟺ*:* Department of Electrical and Computer Engineering, Texas A & M University, Texas.

I. INTRODUCTION

1.1 Power Systems Architecture

The power system forms the electricity infrastructure backbone, enabling a reliable electricity supply to homes, businesses, and industries [1] [2].
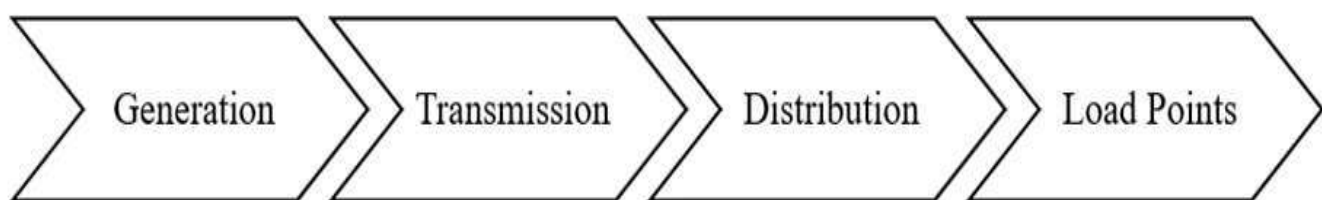
Figure 1: Block Diagram of a Basic Power System

The block diagram described in Figure 1 represents a complex power system network that delivers electricity from power plants to end-users. It comprises generation, transmission, and distribution infrastructure, which requires careful planning, operation, and maintenance for a reliable and resilient power supply [3].

High-voltage transmission lines interconnect different regions, efficiently transferring electricity. Substations step down the voltage for distribution through lower-voltage power lines to individual consumers [4].

System operators manage and coordinate power system operations to maintain stability and address imbalances [5]. Increased demand for electricity, the integration of renewable energy sources, and the need for grid modernization are some of the complexities that have impacted the conventional power system architecture. and the need for real time operational monitoring and control. Consequently, there is a heightened need for real-time operational monitoring and control to address these challenges.

1.2 Smart Grid Overview

The smart grid integrates digital technologies into energy management, enabling real-time monitoring and control of electricity flows [6]. It facilitates two-way communication between power providers and consumers, optimizing energy demand and supply. The Advanced Metering Infrastructure (AMI) provides real-time energy usage data to consumers for informed decisions. Distribution automation enhances grid reliability by deploying sensors and intelligent switches [7] [8]. The smart grid prioritizes grid resilience and security through redundancy and cybersecurity measures. Demand-side management strategies encourage consumers to adjust energy consumption behaviors, reducing peak demand [9].
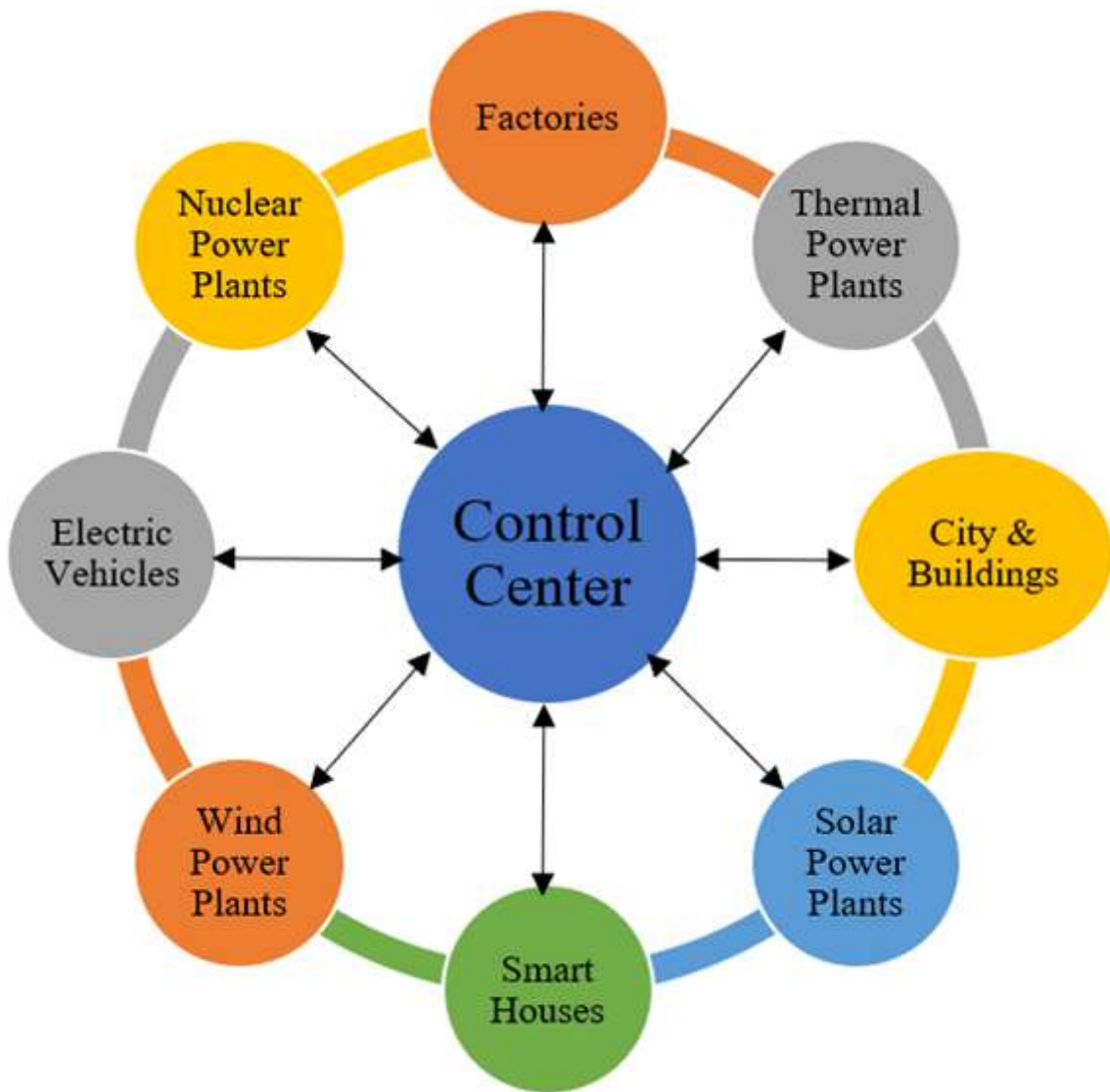
Figure 2: A Block Diagram of the Smart Grid Process Flow

Figure 2 illustrates a block diagram of a smart grid process flow. Electric vehicle (EV) integration employs smart charging infrastructure based on grid conditions and user preferences [10]. Smart grid analytics analyze sensor data, aiding optimization and predictive maintenance. Interoperability is maintained through common standards for seamless integration of devices and systems [11]. The smart grid supports renewable energy integration, microgrids, and storage, promoting sustainability, efficiency, and energy independence [4].

1.3 Significance of Cybersecurity to Smart Grid

Cybersecurity in power system smart grids encompasses various measures and technologies designed to protect critical infrastructure from cyber threats while ensuring a sustained grid operation [12]. One type of cybersecurity measure is network security, which involves securing communication networks and data transmission channels within the smart grid, and includes implementing firewalls, secure gateways, and virtual private networks (VPNs) to prevent unauthorized access and protect against network-based attacks [13]. Another important type is application security, which focuses on securing the software applications and control systems used in power system smart grids [14].

Application security involves implementing secure coding practices, conducting regular vulnerability assessments, and ensuring the integrity and authenticity of software updates [15]. The primary objective of this publication is to explore three primary deployment clusters of cybersecurity that directly impacts smart grids. The ultimate purpose for this is to identify successful technological measures for addressing vulnerabilities arising from specific types of cyberattacks on the smart grid.

II. LITERATURE REVIEW

2.1 Cybersecurity Deployment Clusters that are Smart Grid Focused

The deployment of cybersecurity measures spans various spheres to ensure comprehensive protection against cyber threats [16]. Three primary deployment categories directly impacting the smart grid's smooth operation were identified and briefly examined from twenty-three general cybersecurity protection measures examined. This was after the long list of measures was categorized into groups with primary focus areas as identified in Table 1:

Table 1: Cybersecurity Deployment Clusters

1	Target System Operation Assurance
2	Risk Management and Policy
3	Network Security
4	Software Application & Management
5	Data Protection
6	Human Capital Security Awareness & Collaboration

The first is the system operation continuity protection which upholds uninterrupted smart grid operation, safeguarding against cyber threats that could disrupt power delivery. Measures include redundancy in critical components, real-time monitoring, and incident response plans to ensure uninterrupted power supply [17] [5]. Network security which is the second, involves securing communication pathways between grid components to prevent unauthorized access and data maniPulation.

Techniques such as firewall deployment, intrusion detection systems, and encrypted communication protocols are used to shield against cyberattacks [15]. Data protection which is the third, ensures the confidentiality and integrity of sensitive information exchanged within smart grid systems [18]. Encryption mechanisms, access controls, and data loss prevention techniques are implemented to prevent unauthorized access and ensure critical data's safe transmission and storage [8]. Based on which of the three clusters might likely result in system fatality, a research decision was taken to focus on the impact of the system operation continuity protection.

2.2 Specific Aspects of Cybersecurity Protection in Smart Grid

A few cybersecurity protection aspects were closely studied regarding system operation continuity protection. A major factor that

London Journal of Engineering Research

informed this cluster selection from the three closely studied is the importance of an uninterrupted smart grid operation in the event of a cybersecurity threat. Afterward, three specific cybersecurity protection aspects against system operation discontinuity were selected and closely examined.

The first was anomaly detection and behavioral analytics, which involves utilizing advanced technologies like machine learning to identify unusual behavioral patterns within the smart grid system that might indicate a cyber threat [14] [16]. Security measures to physically protect critical infrastructure components from unauthorized access or tampering, such as secured access points and surveillance systems, were studied [19]. The third was business continuity planning which entails developing strategies and plans to ensure the continued operation of the smart grid in the face of cyber incidents, aiming to minimize downtime and maintain power supply reliability [9].

III. METHODOLOGY

This study utilized a comprehensive approach to analyze each study section. Relevant sources [15] [17] were carefully identified, and important research events were closely observed, including recent publications relating to cybersecurity deployment to the smart grid [20] [10] [17]. This survey identified and closely studied three primary deployment clusters of cybersecurity crucial to the smart grid.

The publication then focused specifically on one within the examined group of clusters. Afterward, it delved into specific aspects of cybersecurity deployment to the smart grid, emphasizing the top three that may directly impact the power supply. The significance of frequency as a key power system stability parameter is emphasized, particularly regarding smart grid stability and protection. The content also involves analyzing recent cyber-physical compromise incidents in power systems' smart grids and addressing vulnerabilities in the deployment of cybersecurity for smart grids.

3.1 Criticality of Frequency Bias Tie Line Control to Smart Grid Stability

Among the vital power system stability parameters, a frequency common to the three closely examined aspects holds the utmost significance, aside from voltage magnitude and rotor angle [5]. Frequency bias tie line control is used in power systems to maintain stable frequency across interconnected grids by adjusting power flow between them in response to frequency deviations caused by load changes or disturbances [3]. Generators in one grid increase or decrease power output based on the frequency difference between interconnected grids, with adjustments proportional to a predetermined frequency bias coefficient [17].

This control mechanism helps restore frequency balance and stability, preventing cascading failures and blackouts. By coordinating power flow adjustments, frequency bias tie line control contributes to grid reliability and effective load management [5] [2]. This technique is essential to power systems operation, especially in interconnected smart grids where maintaining frequency stability is crucial for preventing widespread grid failures [17]. For a network of interconnected tie lines within a smart grid, active power P (W) varies linearly with frequency $f (Hz)$. The $P - f$ relationship is described by the expression in equation (1) [20].

$$\frac{\Delta P}{\Delta f} = - k \qquad (1)$$

Where k is a constant (frequency bias factor) dependent upon the system's load and governing characteristics in $\frac{MW}{Hz}$.

ΔP is the change in active power, Δf is the change in frequency and ΔP_{total} is the total active power change within an interconnected system [5]. For an isolated system, equation (2) holds true

$$\Delta P + k\Delta f = 0 \qquad (2)$$

However, for N interconnected system elements, equation (1) is expanded to equation (3)

$$\Delta P_{total} = \Delta P_1 + \Delta P_2 + ...\Delta P_N$$

$$=- \; k_1 \Delta f - k_2 \Delta f - \ldots k_N \Delta f$$

$$= \; -\left(k_N\right)\Delta f \qquad (3)$$

Equation (3) represents the system stiffness. This is the relationship between power change and frequency change in an interconnected system, with a stiffer system exhibiting smaller frequency changes for a given load change [20].

VI.   DISCUSSION

4.1   Analysis of Recent Cyber-physical Compromise Incidents in Power Systems Smart Grid

Analysis of recent cyber-attacks on power system smart grids sheds light on the evolving landscape of cyber threats and their impact on critical infrastructure [20] [9]. Several high-profile cyber-attacks on power system smart grids, such as the Ukraine power grid attack in 2015 and the Not Petya malware attack in 2017, have demonstrated the potential consequences of successful cyber intrusions [17]. These attacks targeted the control systems and communication networks of power grids, causing widespread power outages, disruptions to critical services, and financial losses [21]. The methods employed in recent cyber-attacks on power system smart grids include phishing attacks, malware infections, exploitation of vulnerabilities in software and hardware, and supply chain attacks.

Sophisticated threat actors, including state-sponsored groups and cybercriminal organizations, are responsible for orchestrating these cyber-attacks, highlighting the need for robust defense measures [22]. Cyber-attacks' impact on power system smart grids goes beyond financial losses, as they can have severe implications for public safety, national security, and economic stability [19]. These impacts on power grids can disrupt essential services, such as healthcare, transportation, and communication, leading to social and economic upheaval. The analysis of recent cyber-attacks highlights attackers' growing sophistication and persistence as they continually adapt their tactics to exploit vulnerabilities in power system smart grids [16]. The consequences of cyber-attacks on power grids

extend to reputational damage for the affected organizations and erode public trust in the reliability of the power supply.

4.2   Existing Vulnerabilities in the Deployment of Cybersecurity for Smart Grid Protection

Incident response and recovery efforts in the aftermath of cyber-attacks on power system smart grids involve extensive forensic investigations, system restoration, and strengthening of security measures [23]. The recent cyber-attack analysis pinpoints current deficiencies in the deployment of cybersecurity for smart grid protection – beginning from the control and communication systems which were the identified targets [24].

Other gaps include the need for proactive defense strategies, continuous monitoring, threat intelligence sharing concerns, vulnerability assessments, differing priorities, regulatory complexities, limited resources, technological and cultural differences

Collaboration between government agencies, power utilities, and cybersecurity experts is also crucial in mitigating the effect of cyber-attacks and strengthening the resilience of power system smart grids [25]. Lessons from recent cyber-attacks inform the development of robust cybersecurity frameworks, regulations, and industry standards for power system smart grids.

The event also highlights the importance of educating personnel and end-users about cyber threats, promoting a security culture, and fostering resilience against potential attacks [26]. Technological advancements, such as integrating artificial intelligence and machine learning, can aid in early detection and response to cyber threats targeting power system smart grids. International cooperation and information-sharing platforms facilitate a coordinated response to cyber-attacks on power grids, enabling the exchange of best practices and threat intelligence [27].

V.   CONCLUSION

The foundation of a robust electricity supply lies in a well-structured power system that caters to

the energy needs of homes, businesses, and industries. As depicted in Figure 1, this intricate network involves multiple components working in tandem to ensure a seamless flow of electricity.

Integrating smart grid technology further optimizes this operation, allowing real-time monitoring, communication, and efficient energy management. Ensuring cybersecurity protection in smart grids is paramount, as demonstrated by the critical significance of frequency, voltage magnitude, and rotor angle in maintaining system stability. Completing comprehensive cybersecurity measures, focusing on system operation continuity protection, network security, and data protection, is a crucial defense against cyber threats in this modern energy landscape.

REFERENCES

1. I. Irene, "Cybersecurity Concerns on Real-time Monitoring in Electrical Transmission and Distribution Systems (SMART GRIDS)," 2020.

2. A. Michael, V. Venkatesh, and M. Richard, "A Survey of Cyber-Physical Power System Modeling Methods for Future Energy Systems," IEEE Access, Vol. 10, pp. 99875-99896, 2022.

3. S. Dhaou, "A Survey on Information Communication Technologies in Modern Demand-Side Management for Smart Grids: Challenges, Solutions and Opportunities.," IEEE Engineering Management Review, Vol. 51, No 1, pp. 76-107, 2023.

4. K. Tim, E. Raphael, K. Benedikt, H. Immanuel, and H. Martin, "Cybersecurity in Power Grids: Challenges and Opportunities," MDPI Sensors, pp. 2-19, 2021.

5. N. A. Ahmad, A.-K. Saif, and M. Qaraqe, "Anomaly Detection in Smart Grids: A Survey From Cybersecurity Perspective," International Conference on Smart Grid and Renewable Energy (SGRE), 2022.

6. M. Amira and G. Gibin, "Smart Grid - Evaluation and Review," International Conference on Smart Grid and Renewable Energy (SGRE), vol. 3, 2022.

7. E. M. C. Balduino, I. Loretta and P. Dan, "Cyber Security of Smart Grid Infrastructure," pp. 303-308, 2018.

8. H. Burhan and G. Manimaran, "A Novel Methodology for Cybersecurity Investment Optimization in Smart Grids Using Attack-Defense Trees and Game Theory," IEEE Power & Energy Society Innovative Smart Grid Technologies Conference (ISGT), pp. 1-5, 2022.

9. P. Dimitrios, S. Panagiotis, L. Thomas and G. S. Antonios, "A Survey on SCADA Systems: Secure Protocols, Incidents, Threats and Tactics," IEEE Communications Surveys & Tutorials, Vol. 22, No. 3, pp. 1942-1976, 2020.

10. M. Fazel, S. Mehrdad, A. Majid, and S. Bahram, "A Review of Cyber-Resilient Smart Grid," World Automation Congress (WAC), IEEE Xplore, pp. 11-15, 2022.

11. I. K. Asif and P. Deepak, "A Review of Cyber Securities in Smart Grid Technology," 2nd International Conference on Computation, Automation and Knowledge Management (ICCAKM), vol. 2, pp. 151-156, 2021.

12. S. Salsabeel, Q. Fatma, A. Raafat, A. Fadi Aloul, and A. Ali, "Smart Grid Cyber Security: Challenges and Solutions," International Conference on Smart Grid and Clean Energy Technologies, pp. 170-175, 2015.

13. Z. Peng, Z. Talha, and L. Hao, "Blockchain for Cybersecurity in Smart Grid: A Comprehensive Survey," IEEE Transactions on Industrial Informatics, Vol. 17, No. 1, pp. 3-19, 2021.

14. Z. Zhiheng and C. Guo, "An Overview of Cyber Security for Smart Grid," pp. 1128-1131, 2018.

15. D.-G. Vasco, F. M. Joao, L. Celson and N. B. Paul, "Smart Grid Security Issues," pp. 534-538, 2015.

16. R. V. Taylor and V. Andrew, "Cybersecurity in the Blockchain Era," A Survey on Examining Critical Infrastructure Protection with Blockchain-Based Technology, pp. 107-112, 2020.

17. D. T. Nguyen, S. Q. Nguyen, B. L. Vo, V. T. Vu, and F. Goro, "A Comprehensive Review of Cybersecurity in Inverter-Based Smart Power System Amid the Boom of Renewable Energy," IEEE Access (IEEE Power & Energy Society Section), pp. 35846-35875, 2022.

18. Y. Ye, Q. Yi, S. Hamid, and T. David, "A Survey on Cyber Security for Smart Grid Communication," IEEE Communications Surveys & Tutorials, vol. 14, no. 4, pp. 998-1010, 2012.

19. U. R. Poojith, S. Balwinder and S. Ranjana, "Cyber Security Enhancement of Smart Grids Via Machine Learning - A Review," 21st National Power Systems Conference (NPSC), no. 21, 2020.

20. R. Syed, S. Mark, M. Jimmy, and S. John, "Application of Artificial Intelligence to Network Forensics: SUrvey, Challenges, and Future Directions," IEEE Access, Vol 10, pp. 110362-110384, 2022.

21. D. Sourav and S. Ranjana, "A Simple Cyber Attack Detection Scheme for Smart Grid Cyber Security Enhancement," National Power System Conference (NPSC), vol. 21, 2020.

22. K. Vatan and C. P. Gupta, "Cyber Security Issue in Smart Grid," IEEE 4th International Conference on Computing, Power and Communication Technologies (GUCON), pp. 1-9, 2021.

23. S. Shahriar, B. Sahba, A. Thnwa and M. Samantha, "Smart Grid and Cybersecurity Challenges," IEEE, vol. 5, pp. 1-8, 2020.

24. N. N. Tu, L. Bing-Hong, N. Nam P and C. Jung-Te, "Cyber Security of Smart Grid: Attacks and Defenses," 2020.

25. S. I. Abood, Power System Generation, Stability and Control, Australia: Central West Publishing, 2021.

26. F. John, P. Obiomon and S. I. Abood, Power System Operation, Utilization and Control, Florida: CRC Press, 2023.

27. S. I. Abood and M. H. Fayyadh, Philosophy of Power System Protection and Security, New York: Nova Science, 2021.

London Journal of Engineering Research

Assessment of Cybersecurity Deployment to Power System Smart Grid

This page is intentionally left blank

Big Data in Construction Perspective: Exploration of Google Cloud based Technologies and Offerings

Rajesh Saxena & S.K.Soni

Rabindranath Tagore University

ABSTRACT

This paper critically explores and reviews the literature to identify the data trends and how the construction industry can benefit from big data. The big data has brought the revolutionary changes in all the industries and construction industry is also not remaining untouched. Big data engineering (BDE) and statistics are among the most crucial steps for integrating big data technology in construction. We have reviewed related papers published in the various research and education institute across the world. The current application of Big Data in construction industry is already wide spread and future opportunities like big data research into construction safety, site management, heritage conservation, and project waste minimization and quality improvements are giving it totally new dimensions. Construction industry generates large amount of data every day but this data which has huge potential but not gets utilized effectively mainly due to lack of technology adoption. This paper will try to give different perspective of Big Data with the appropriate use of Big Data Engineering, Tools and Technologies.

Keywords: big data; big data engineering; big data analytics; big data storage; big data processing; machine learning; artificial intelligence; google cloud platform.

Classification: LCC: T58.64

Language: English

Big Data in Construction Perspective: Exploration of Google Cloud based Technologies and Offerings

Rajesh Saxena[α] & S. K. Soni[σ]

ABSTRACT

This paper critically explores and reviews the literature to identify the data trends and how the construction industry can benefit from big data. The big data has brought the revolutionary changes in all the industries and construction industry is also not remaining untouched. Big data engineering (BDE) and statistics are among the most crucial steps for integrating big data technology in construction. We have reviewed related papers published in the various research and education institute across the world. The current application of Big Data in construction industry is already wide spread and future opportunities like big data research into construction safety, site management, heritage conservation, and project waste minimization and quality improvements are giving it totally new dimensions. Construction industry generates large amount of data every day but this data which has huge potential but not gets utilized effectively mainly due to lack of technology adoption. This paper will try to give different perspective of Big Data with the appropriate use of Big Data Engineering, Tools and Technologies. We will also discuss the currently available tools such as computer-aided drawing (CAD) and building information modeling (BIM) and how they are providing tremendous opportunities to researcher in construction industry. We will also discuss how the rise of interest in big data is making it more effective due to the adoption of technology such as robotics, smartphones, computers and other gadgets. These gadgets helps in model development gathering data which gets used in the development of varioustechnique for Algorithm development, machine learning (ML), statistical analysis, and computational.

Author α: Department of Civil Engineering Rabindranath Tagore University Bhopal, Madhya Pradesh.
σ: Department of Civil Engineering Rabindranath Tagore University Bhopal, Madhya Pradesh.

I. INTRODUCTION

Construction is a data-intensive sector where the bulk of data is generated and not capitalized on adequately due to slow technology adoption. Big data, a relatively new technology, are not properly adopted by construction. There are various steps involved in using big data, including data acquisition, storage, classification, and refining. These steps are handled through various software programs to refine the associated big data and make it usable for research and practical purposes In the case of construction, some barriers to big data adoption include latency, data privacy, data availability, data governance, poor broadband connectivity at construction sites, and cost implication for long-term use. For instance, big data adoption in construction may have latency issues with lower transfer rate and response time required due to software issues or network problems which may be a hurdle for some time-sensitive construction applications.

The construction industry is also benefiting from big data in a way that has revolutionized its traditional operational methods to a more automated process. The presence of digital tools and technologies for designing and executing construction projects has made the construction

London Journal of Engineering Research

industry take enormous leaps in the last two decades.

The possibility of modeling building structures and identifying the functionality of those structures before they are built has led to industrial investments in big data and related technologies. Computer-aided design (CAD), such as building information modelling (BIM), is a term now synonymous with the construction industry.

The three-dimensional modeling of buildings and other construction infrastructures leads to the generation of digital files which can be stored in various formats, leading to a bulk of data generation. Other digital innovations such as digital twins, 3D laser scanning, and advanced wearable gadgets incorporated in hats, shoes, gloves, and other sensor-based tools have revolutionized the construction industry and helped generate useful big data.

Big data in the construction industry can accumulate quickly and become storage heavy due to the large size of the 3D modeling files and a huge amount of daily data generated by wearable gadgets. Management of such big data is a hectic but essential task as the usefulness of the models lies in ensuring that they are available for viewing and leveraging as and when needed. Apart from providing the ease of modeling infrastructure, big data also provide the opportunity to develop sustainable structures by using test models before actual constructions. These are made possible by using digital twins, geographical information systems (GIS)-based 3D point cloud structures, and other cloud-based scanning systems.

Furthermore, the software that enables CAD and BIM further feeds into the databases and contributes to big data.

The applications of big data in the construction industry are immense. Identifying how big data can be applied to the construction industry remains the real challenge.

Since each construction project leads to more data generation, it is crucial to analyze and sort the data accordingly. Some of the key features within the construction industry that can benefit from big data

- Construction safety
- Efficiency
- Waste minimization
- Productivity
- Competitive Advantage
- Pollution Management
- Project Management
- Claims Management
- Procurement

II. METHODOLOGY

The purpose of this study is to explore other nonconventional ways to control the cost and achieve the cost effectiveness in construction.

In order the achieve above stated purpose, following methodologies are outline:

- Step-1
  - Aim

- Step-2
  - Objectives

- Step-3
  - Literature Review

- Step-4
  - Google Clound Platform -Technology Exploration

- Step-5
  - Conclusion

III. AIM

- The core aim of using different technologies is to simplify how datasets can be used to guide future construction projects.
- The guiding principle here is to use modern technology to upgrade and update the ways in which information could be streamlined for the benefit of different projects.
- Identifying the materials that best suit a particular structure, developing project timelines, and streamlining the resources can become much more straightforward if the construction projects are developed with the help of big data technologies
- The overall purpose of this paper is to explore various tools and techniques for the effective use to Big Data in construction.

IV. OBJECTIVES

- The overall objective of this paper is to explore Tools and Technique which can be used to use Big Data for construction and its management based on the review of existing literature.
- The existing literature on big data does not provide Technology focus approach to use Big data for construction management and this is the very reason construction industry is lagging behind in the use of big data in the construction industry.
- The paper research work focus on following aspects

- o How can we use Technologies for big data for research in construction engineering and management?
- o How can we use Big Data Engineering to process and Store Big Data
- o How can we use Big Data Analytics to use Big data in construction
- o How can we use Machine Learning to effective use Big Data in construction
- o How can we use Cloud Offerings (GCP) in construction?
- o How to use 10 Vs of Big Data
- o How can big data be used for planning construction projects in a futuristic way?

V. LITERATURE REVIEW

5.1 Big Data Trends

Following are sequence of trends Big Data have gone through since 2016

- **2016**
  - Cloud computing and Big Data for construction

- **2017**
  - Development of Big data modes for construction

- **2018**
  - Implementing Big Data in construction engineering

- **2019**
  - Construction Management through Big Data

- **2020**
  - Public awareness of construction using Big Data

- **2021**
  - Harnessing ML and Big Data for futuristic construction Project

- **2022**
  - Artificial Intelligence (AI),Deep learning

- **2023**
  - Block chain, Chat GPT

5.2 Big Data Research Techniques

Following are the various research techniques getting used in Big Data

- **Big Data Analysis**
- **Block Chain**
- **Data Bases ,Data Mining & Statistics**
- **KDD & Pattern Recognition**
- **3D & Computational Neuroscience**
- **Artificial Intelligence**
- **Chat Bots & Chat GPT**

5.3 Big Data Domains

☐ Big Data is classified in to Major Domain BDE & BDA. These two main domains are further divided in to many classes and subclasses. The third domain that comes under the canopy of Big Data is ML.

- Big Data Domains
- Bata Data Engineering
- Big Data Analytics
- Machin Learning

5.4 Big Data Engineering

1. Big data analytics (BDA) is supported by BDE that provides a framework to conduct it. BDE has tremendous applications in construction.
2. It has been used for BIM to improve project management.
3. It has also been used to improve building design and for effective performance monitoring, project management, safety, energy management, decision-making design framework, resource management, quality management, waste management and others.
4. To understand BDE, it is important to discuss big data platforms. These platforms are divided into two groups based on variations in their inherent characteristics.

   4.1 Horizontal Scaling Platforms (HSP)
   HSP utilizes multiple servers by distributing processing across them and bringing new machines into the cluster. In construction, HSPs have been used for waste management, profitability performance, smart road construction, and others.
   4.2 Vertical Scaling Platforms (VSP) VSPs are single-server-based configura- tions that achieve the scaling by upgrading the hardware of the related server. VSPs have been reported in one-off construction projects, transportation and others.
5. BDAS (Berkeley Data Analytics Stack)has been in the limelight since it has greater performance gains over Hadoop.
6. Hadoop has been widely utilized in big data applications. The tools offered by these platforms are useful in the storage and processing of big data.

7. Classification of Big Data in to its key domains
   I.   Big Data Engineering
   i.   Big Data Processing
       a.   Map Reduce
       b.   DAG
   ii. Big Data Storage
       a.   NoSQL
       b.   Distributed File System
           a) HDFS
           b) Tachyon
8. Big Data Processing-Distributed and parallel computation is present in the core of BDE. In construction, big data processing has been utilized for waste management, prefabricated construction project management, profitability analyses, and other construction management applications.

   8.1. MapReduce (MR)
   - MapReduce was developed for the handling of big data. It utilizes a distributed processing model in which two functions, as indicated by the name itself, map and reduce, are employed to write analytical tasks. Mappers and reducers are the processes that collect Big Data from these functions for further processing. Initially, mappers collect and read the input information to process it for subsequent results generation. The output of mappers is used by reducers which give the results that are ultimately stored in the file system
   - MR has been used by Jiao et al. to develop an augmented framework for BIM. Similarly, it has also been used in construction knowledge maps and other big data applications.
   - The overall features and application of MapReduce is the reduction of data into

manageable chunks. The use of MapReduce not only distributes data into smaller chunks but also helps develop datasets that present a more analytic view of big data.

- Having organized datasets within the construction industry is of key importance as it can greatly increase the efficiency of data management and decision making based on data analysis.

- Hadoop was the popular and first big data platform that introduced and made it easy for people to work on MR by executing its programs successfully. For tasks requiring batch processing, MR proved itself to be an effective tool as a typical cluster contains interlinked mappers and reducers that assist by running MR programs side by side at the same time

- Yet another resource negotiator (YARN) has also been introduced, which functions by providing resource management and scheduling related functions of MR and has made it easy to implement innovative applications by Hadoop.

- Hadoop models have been used in construction for smart buildings and disaster management , failure prediction of construction firms [56], workers' safe behaviors in a metro construction project and other relevant applications.

8.2. Directed Acyclic Graph

- Big data platforms also use Directed Acyclic Graph (DAG) which is an alternative processing model. In comparison with MR, DAG works by relaxing map-then-reduce, the style of MR, which is supported by Spark.

- Spark is widely accepted for reactive and iterative applications due to its supremacy over MR in high expressiveness and in-memory computation

- Disk-resident and memory-resident tasks are conducted ten and one hundred times faster using Spark than MR.

- DAGs provide major advantages that enable experts and researchers to construct complex causal relationships in which nodes represent stochastic variables, and directed edges (arrows) indicate direct probabilistic dependencies among the relevant variables.

- DAGs are also able to encode deterministic as well as probabilistic relationships among the variables.

- The usage of Spark and associated DAGs has been reported for construction profitability analysis, waste management, energy monitoring service on smart campuses , and others.

- Spark and Hadoop are among the ML tools with enormous potential in cons- truction engineering and management.

- The speed of both these systems is better than other algorithms and ML tools currently in use in the construction industry.

- Fault tolerance in both these systems is also high and has greater scalability than existing models.

- The data storage in these systems is slightly different in that Spark uses a memory system while Hadoop utilizes a disk for data storage.

- The language for both these tools is also different since Spark is written in Scala while Hadoop has been developed using JavaScript.

- Despite the slight differences, both these tools provide the opportunity to process data in the form of batches and at a higher speed than previously existing models, making them potential tools for futuristic model developments in construction engineering and management.

- JavaScript has been used in construction to anticipate building material reuse, automated progress control coupled with laser scanning, shared virtual reality for design and management, construction information mining

- Scala has been used for the process information modeling concept for on-site construction management.

8.3. Big Data Processing in Construction

- Big data processing has been effectively utilized in the construction industry for failure prediction data, construction waste analytics, profitability data, modular and prefabricated construction, fire incident management, smart campus energy monitoring, healthier cities management, smart road management, and others.

- Though MR and Spark have their own significance, these are less frequently employed in the construction industry to process big data such as BIM-associated data. Partial BIM models' retrieval was optimized by MR by Bilal, et al. and Chang and Tsai The authors found a loop in the Hadoop MR logic of data distribution.
- Another research group worked for naive and expert BIM users by developing a system for BIM data storage and retrieval. The authors developed a system for cloud BIM to retrieve and represent big data intelligently. This system helped develop an interactive interface to maximize the usability and utility of construction big data. Complex BIM data are retrieved by processing proposed natural languages after reformulating user queries. This data are then visualized by mapping on various visualizations. Before query evaluation, two BIM collections are merged to optimize the process of query execution. Using this technology, a 40% reduction in response time has been witnessed compared to other traditional technologies.
- Currently, the utilization of BIM is limited across the construction and facilities management stages. The real intent of BIM could only be achieved once applied at each stage of the building lifecycle.

9. Big Data Storage-
- Big data storage is also an important aspect of BDE. In construction, big data storage has been explored for forecasting the success of construction projects, smart buildings data storage, tender price evaluation, and others.
- Despite the availability of BIM data storage, the current applications in construction still require successful implementation. Social BIM, proposed by Das et al., captures building models and the social interactions among the users. The authors developed BIM Cloud based on the distributed BIM framework.
- Similarly, a two-tiered hybrid data infrastructure was proposed by Jeong et al. for data management and monitoring of bridges. In this model, the client tier efficiently completes some analytical tasks by storing structured data momentarily using MongoDB,

while the central tier stores sensor data permanently using Apache Cassandra. Lin et al. also used MongoDB to store BIM data obtained through building models.
- Overall big data storage is provided by either emerging NoSQL databases or distributed file systems, as explained subsequently

9.1. Distributed File Systems

- The distributed file systems consist of Hadoop Distributed File System (HDFS) and Tachyon.
- HDFS is designed to deal with large and complex databases such as those related to BIM, waste, and other construction big data sources.
- It operates with the commodity servers grouped together in a cluster.
- As it utilizes several servers, the probability of hardware failure also increases. To overcome this problem, HDFS introduces fault tolerance achieved through the distribution of data and their replication. However, in situations where low-latency data access is required, HDFS is not a suitable option as it shows inferior performance.
- HDFS has been utilized by construction researchers for observing construction workers' behavior, improving road performance, and investigating profita- bility performance.
- Furthermore, based on the distributed input from HDFS, it facilitates building predictive models for conducting building simulations that give output in a predictive model markup language.
- Tachyon is a distributed file system designed to extend HDFS benefits by providing access to the distributed data across the cluster at memory speed.
- Tachyon has been utilized in construction for handling unstructured documents and file storage.
- The Tachyon performs better than HDFS, is backward compatible and can handle the MapReduce jobs without any further modifications.

9.2. NoSQL Databases

- Relational databases have been common for data management in past decades. However,

new applications were designed for better performance, scalability, and flexibility as the technology emerged. Relational databases lag because of their special processing and storage needs.

- As a result, new systems were devised to fill this technology gap. One such system is the "Not only SQL" system that has optimized data management in several ways.
- NoSQL has been widely used in different industries, including construction, dueto its fragmented nature. Some examples of NoSQL in construction include integration of lessons learned knowledge in BIM], web service framework for construction supply chain collaboration and management, and Social BIM Cloud implementation .
- NoSQL systems store schema less data in a non-relational model. It does not set too many restrictions on value and allows easy product determination. Generally, when NoSQL databases are set to key values, they carry out only specific tasks without evaluating specific values. The key-value database is mainly tailored to the business accessed through the primary key. These systems have four data models that are briefly discussed below.

i. Key-value: This is the simplest data model used for unstructured data storage. However, the data lack self-description. It has been used for knowledge management in construction and integration of lessons learned knowledge in BIM. Big data utilization in BIM can be beneficial to discover root causes of poor building performance, perform real-time data queries, improve the decision-making process, improve productivity, and reveal new designs and services in the construction industry, as is the case in every industry.

ii. Document: This model can store self-describing data. However, this model can lag in terms of efficiency. It has been used for unified lifecycle data management in architecture, engineering, construction, and facilities management through BIM integration.

iii. Columnar: Aggregated columns, grouped sub-columns, and sparse data can be stored by using this model. It has been used for integrating digital construction through the internet of things and smart archiving of energy and petroleum construction projects.

iv. Graph: This model works well for property-graph-based huge datasets in relationship traversal. It has been used for the 4D construction management information model of prefabricated buildings and the development of a BIM-enabled software tool for facility management.

1. *Big Data Analytics:*
   a. Big Data Analytics
      i. Statistics
         1. Bayesian Analysis
         2. Resampling
         3. Shrinkage
         4. Tree-based Analysis
      ii. Data Mining

- BDA gathers information from a variety of disciplines. All these disciplines have one thing in common: to find out data patterns. Some of these related disciplines are data mining, statistics, business analytics, predictive analytics, data analytics, knowledge discovery from data, and the most recent one, big data.
- Big data use the previous techniques to broaden the field of data analytics. For BDA, some of the ML-based tools are developed.
- In construction projects, BDA has been used for improving building design and effective performance monitoring, project safety, energy, resource, overall management and decision-making frameworks, and quality and waste management.
- Big data analytics has been taken a step further by developing predictive analysis techniques.
- Ngo et al. used a factor-based big data predictive analytic tool for analyzing the capacity of construction industries to deal with big data. This tool was tested and validated on four different construction organizations to ensure that the predictive analytic method could improve how the construction industry can use big data.

- The integration of big data in the construction industry remains an avenue that requires further research in terms of big data analytics.
- Overall, data analytics is conducted through statistical, data mining, and regression techniques, as explained below

1.1. Statistics

- Statistics has wide applications in the construction industry.
- Statistical techniques including Monte Carlo simulation, Gaussian distribution, non-Bayesian methods, correlation analysis, factor analysis, decision trees, Naïve Bayes, and others have been reported by various studies in construction.
- Some of the areas that benefitted from statistics include learning from post-project reviews, identifying causes of construction delays, analyzing buildings for structural damages, construction litigation, and identifying and recognizing heavy machinery and workers.
- Other examples of statistics in construction are those of bidding statistics to predict completed construction cost, accidents statistics, quality control, and six sigma for project success]. From measuring the bid-to-win ratio to how much a project is over budget or schedule, and KPIs, the more numbers you can put behind your work, the better. Data not only allow for more visibility into the state of a particular project, but relevant industry statistics and facts can provide valuable information needed to make important future decisions regarding preconstruction and planning, productivity tools, risk assessment, and workforce and operational efficiency.

1.2. Data Mining

- Data mining is used to extract meaningful patterns in the data. It has been an integral part of all big data management systems. It employs the techniques used in pattern recognition, ML, and statistics. Several models are assessed, and the ones with the best tolerance and high accuracy are selected and used for obtaining predictive results.

- In construction, data mining has been reported in waste management, BIM-based construction engineering quality management, and other relevant areas.
- Data mining detects useful regularities and information necessary for decision making for construction management projects.
- A data mining method such as cluster analysis is important for the construction industry, as it combines different construction objects into homogeneous groups and investigates them.
- Data mining is supported through data warehousing. Specially structured data is stored in data warehousing for querying and analysis. Extract, transform and load (ETL) is a program that allows the collation of transactional data and operational data.
- Warehouse Data analysis is conducted using Online Analytical Processing (OLAP), which performs better than SQL in computing breakdown and data summaries. OLAP has been used for cost data management in construction cost estimates by Moon et al. OLAP technology deals with the operational data and data obtained using big data technology. OLAP is presented as a multidimensional cube that rapidly processes datasets.
- Similarly, different data mining techniques have been used to identify construction delays. For analyzing construction datasets, Kim et al. presented a framework of knowledge discovery in databases (KDD).
- In the KDD, the most time-consuming and challenging step is data preprocessing. Nevertheless, KDD is a powerful tool for identifying casual relationships in construction projects and reducing construction variability by identifying and eliminating causes for possible deviations. With the application of KDD, randomness of construction projects and novel patterns can be determined. Other techniques include dimensional matrix analysis, link analysis, and text analysis . Other datasets with information related to delay causes, BIM-based knowledge discovery, intelligent learning, and the prevention of occupational injuries can be easily extended in the domain of data mining.

Big Data in Construction Perspective: Exploration of Google Cloud based Technologies and Offerings

1.3. Regression Techniques

- Based on an input variable, regression predicts the value of the target variable. It is a supervised ML method.
- Regression is categorized into simple linear and multiple linear regression based on explanatory variables.
- In simple linear regression, the relationship between two variables (an explanatory variable x and a dependent variable y) is modeled using ML.
- While in multiple linear regression, two or more explanatory variables are used and their relationship with the dependent variable is modeled. The more common regression technique is multiple linear regressions.
- Regression has been extensively used in construction research. For example, it has been used to predict properties of concrete cured under hot weather , predicting final cost for competitive bids on construction projects , determining contingency in international construction projects, estimating performance time for construction projects and others.
- Moreover, regression has been used for cost estimation, which is a difficult task in the early stages of the project. Adoption of parametric methods such as regression and multiple regressions can be applied as both analytical and predictive techniques to estimate the overall reliability of the cost estimation.

2. The 10 vs. of Big Data-

- The most crucial properties of big data include their value, volume, velocity, variety, veracity, volatility, validity, variability, vulnerability, and visualization, also known as the 10 vs. of big data
- In terms of the use of big data in the field of construction, analyzing the vs. can help explore how big data can be used for developing better construction models in the future.
- Overall, multiple construction-related studies have reported the usage of vs. of big data. For example, velocity has been reported for high-speed construction data processing. Value has been reported for smarter universities and campuses. Volume has been

reported for mass level offsite construction material and component production. Variety has been reported for investigating the profitability performance of construction projects. Veracity has been reported for forecasting the success of construction projects. Similarly, variability has been reported for modeling occupational accidents in construction projects.

2. *Machine Learning:*

  a. Machine Learning
   i. Regression
     1. Linear Regression
     2. Ridge Regression
     3. Neutral Network Regression
     4. Lasoo Regression
     5. Decision Tree Regression
     6. Random Forest
     7. KNN Model
     8. Support Vector Machines
   ii. Classification
   iii. Clustering
     1. Centroid Based Clustering
     2. Density Based Clustering
     3. Distribution Based Clustering
     4. Hierarchical Clustering
   iv. Natural Language Processing
   v. Information Retrieved(IR)

- One AI subdomain is ML which can be used to learn from the data using computational systems.
- ML is further categorized into:

  (i) supervised learning;
  (ii) unsupervised learning;
  (iii) association
  (iv) numeric prediction.

- ML has several applications in the construction industry. It uses different approaches, including rule-based learning approaches, case-based reasoning techniques, artificial neural networks, and hybrid methodologies.
- ML has immense potential as a tool in the field of construction. Over the last two decades, several ML algorithms have been proposed to aid and improve the overall process of construction. For example, ML has been used to predict properties of concrete,

contract management, site safety and injury prediction, delay risks management, BIM integrated on-demand site monitoring, and other areas of construction engineering and management.

- Various ML tools are integrated at different steps along with the construction management processes. Different ML interfaces such as PyTorch and Keras.io help develop computational models based on existing data for building futuristic construction models.

- BIM can also be improved by using big data and ML tools, as these technologies allow the opportunity to explore how technology could be applied to the construction industry .

- Over the last few years, different algorithms have been explored to predict various project phases and guide construction projects from inception to closure.

- Firstly, decision trees and similar tools are used for developing an overall project timeline to predict or determine construction project performance in various phases.

- Secondly, statistical analysis tools are used for analyzing previous projects and choosing guiding principles for future projects .

- Finally, design tools are integrated with ML algorithms to build 3D construction models and graphics for building models.

- These computational models enable analyzing construction projects by planning through look-up schedules and looking for ways to improve buildings and other structures. The combined use of big data, ML, and AI holds the potential to develop seamless construction projects and enable the development of structures that can withhold severe weather conditions and disasters.

- For example, one of the key uses of ML tools in futuristic construction projects can be the development of structures that can stand through natural disasters and provide safety nets to communities during floods and other disasters.

- Similarly, post-disaster evacuation and rescue of individuals can also be carried out more easily if the area contains structures such as roads and buildings built through the use of

statistical modeling, thus providing safe routes for people.

- Although the automation of construction projects remains a future goal, the integration of different ML algorithms is already underway. Managing costs, timelines, and human resources on a construction project are areas guided by various algorithms and computational models.

- The ML approach can also be applied to develop leading indicators to classify sites according to their safety risk in construction projects

Future Opportunities of Big Data in Construction-

- There is immense potential for the use of big data in the construction industry. The use of big data and ML can enable construction automation.

- The construction industry is quite dynamic and demanding, with the need for labor strength and human resources to ensure the smooth running of projects. The constant challenge of keeping projects on track and ensuring that new buildings and structures are made up to modern standards puts much strain on the project management teams. These roadblocks can greatly be reduced with the use of big data and ML.

- The core aim of using big data in the construction industry is to enhance the project planning phases and speed up the overall construction process by predicting the possible timelinesfor particular projects and identifying what factors can be worked on to improve the overall process

- The automation of the construction projects will require the combined use of big data, deep learning, and ML tools.

- The use of big data and related tools can ensure that existing data and information can be used for drafting guiding principles and then building computational models accordingly. For example, using sensor-based wearable personal protective equipment, the big data of near misses, onsite accidents, hazards, and other issues can be generated for

Big Data in Construction Perspective: Exploration of Google Cloud based Technologies and Offerings

developing safety plans and management techniques.

- Big data, BIM, and cloud-powered simulations can help minimize project waste and help produce superior quality constructed facilities.
- Big data artifacts generated by 3D scanners for as-built drawing development are another key advantage whereby the rehabilitation plans of ancient heritage sites can be developed.
- The future holds great potential for the construction industry through big data integration. Some of the key opportunities for the construction industries lie in using big data for business and environmental sustainability. The current roadblocks faced by the construction industry can be overcome in the future through the integration of information extracted through big data.
- The use of information gathered from past and present projects can help develop sustainable infrastructure in the long term. It is possible to avoid past mistakes and use better quality products guided by the information found through big data in construction.
- Future research directions in the field of construction rely heavily on big data as the presence of information sources can help in building better infrastructure and greatly improve building designs and the overall construction business. The construction industry must move towards automation and build upon the integration of technology to make the future use of big data seamless and hassle-free.
- The use of big data tools, BIM, and CAD can only be possible if the relevant support and integration systems are present. Hence, the future of the construction industry depends on upgrading the present environment gradually.
- Overall, the role of big data in enabling the entire process of futuristic construction projects is undeniable.
- Data play a crucial role in developing training models and smoothly enabling the process of construction.
- Future developments in this field will also include the generation and use of more algorithms and models that rely on big data, owing to the need to train the models reliably.

- All above highlighted benefit of Big Data can be taken to the next level by utilizing Cloud Offering in the Market.
- Now a days Cloud provider like Google, Amazon and Microsoft are offering various platforms and services for the effective utilization of Big Data.
- Following are some benefit of using cloud services in conduction industry:
o Data generated by Construction industry is huge and storing and processing data can be very expensive.
o Cloud provides data storage in cheap rate which can be accessed from anywhere easily. No need to physically score data on your premises.
o Cloud Storage is scalable so can be optimized based construction site requirement.
o Cloud provides various tools and technique for effectively managing construction data.
o Cloud Big Data offering helps in effectively storing and managing huge volume of construction data.
o Wide range of data analytical tools available on Cloud platforms can be used to process and effectively utilize the huge volume of Construction data.
o Cloud providers various Machine Learning and Artificial Intelligence capability which can be ,if effectively used , can be game changer to address following concerns associated with construction industry
▪ Effective planning specifically when construction industry has to deal with lot of unknowns
▪ Effectively managing day to day construction activities by giving due consideration of dependent tasks and activities
▪ AI can be helpful with forecast and planning the construction activities accordingly.
▪ Safety and Security concern of construction industry can also be effectively address by using various Cloud offering
▪ One construction project experience and data can be used effectively planning for future projects.

Google Cloud Platform(GCP) -Technology Exploration

- **Google Cloud Platform Domains**
  - **GCP Platform Services**

- **GCP Data Analytics**

- **GCP AI/ML Services**

6.1 GCP Platform Services

Compute:

App Engine: App Engine enables you to build and host applications on the same systems that power Google applications. App Engine offers fast development and deployment; simple administration, with no need to worry about hardware, patches or backups; and effortless scalability.

Compute Engine: Compute Engine offers scalable and flexible virtual machine computing capabilities in the cloud, with options to utilize certain CPUs, GPUs, or Cloud TPUs. You can use Compute Engine to solve large-scale processing and analytic problems on Google's computing, storage, and networking infrastructure.

App Engine & Compute Engine offerings can be very useful for processing the big data in construction industry where data demand in dynamic in nature require flexibility in terms of processing power and scalability.

Workload Manager: Workload Manager is a rule-based validation service for evaluating workloads running on Google Cloud. If enabled, Workload Manager scans application workloads to detect deviations from standards, rules, and best practices that improve system quality, reliability, and performance.
Work load Manager can provide great amount of help to manage the dynamic workload of construction industry which required to effective management the demand deviations.

Storage

Cloud Storage: Cloud Storage is a RESTful service for storing and accessing your data on Google's infrastructure. The service combines the performance and scalability of Google's cloud with advanced security and sharing capabilities.

Persistent Disk: Persistent Disk is a durable and high performance block storage service for Google Cloud Platform. Persistent Disk provides SSD and HDD storage that can be attached to instances running in either Compute Engine or Google Kubernetes Engine.

Cloud Filestore: Cloud Filestore is a scalable and highly available shared file service fully-managed by Google. Cloud Filestore provides persistent storage ideal for shared workloads. Above mentioned Google Storage options should be explored to establish best suited storage mechanism to Store Big Data in construction industry which is normally very huge in volume.

Databases

AlloyDB: AlloyDB is a fully-managed, Postgre SQL-compatible database for demanding transactional and analytical workloads. It is designed to provide enterprise-grade performance and availability while maintaining compatibility with open-source PostgreSQL.

Cloud Bigtable: Cloud Bigtable is a fast, fully-managed, highly-scalable NoSQL database service. It is designed for the collection and retention of data from 1TB to hundreds of PB.

Datastore: Datastore is a fully-managed, schemaless, non-relational datastore. It provides a rich set of query capabilities, supports atomic transactions, and automatically scales up and down in response to load. It can scale to support an application with 1,000 users or 10 million users with no code changes.

Firestore: Firestore is a NoSQL document database for storing, syncing, and querying data for mobile and web apps. Its client libraries

London Journal of Engineering Research

provide live synchronization and offline support, while its security features and integrations with Firebase and Google Cloud Platform accelerate building serverless apps.

Memorystore: Memorystore, which includes Memorystore for Redis and Memorystore for Memcached, provides a fully-managed in-memory data store service that allows customers to deploy distributed caches that provide sub-millisecond data access.

Cloud Spanner: Cloud Spanner is a fully-managed, mission-critical relational database service. It is designed to provide a scalable online transaction processing (OLTP) database with high availability and strong consistency at global scale.

Cloud SQL: Cloud SQL is a web service that allows you to create, configure, and use relational databases that live in Google's cloud. It is a fully-managed service that maintains, manages, and administers your databases, allowing you to focus on your applications and services.

Construction Industry generate huge amount of data which is very diverse in terms of all 10 V's which include variety, value, volume, velocity, variety, veracity, volatility, validity, variability, vulnerability, and visualization. Above available Data bases those are available on GCP can be effectively use to store the construction data based on the data demand.

6.2 GCP Data Analytics

BigQuery: BigQuery is a fully-managed data analysis service that enables businesses to analyze Big Data. It features highly scalable data storage that accommodates up to hundreds of terabytes, the ability to perform ad hoc queries on multi-terabyte datasets, and the ability to share data insights via the web.

Cloud Composer: Cloud Composer is a managed workflow orchestration service that can be used to author, schedule, and monitor pipelines that span across clouds and on-premises data centers. Cloud Composer allows you to use Apache Airflow without the hassle of creating and managing complex Airflow infrastructure.

Cloud DataFusion: Cloud Data Fusion is a fully-managed, cloud native, enterprise data integration service for quickly building and managing data pipelines. Cloud Data Fusion provides a graphical interface to help increase time efficiency and reduce complexity and allows business users, developers, and data scientists to easily and reliably build scalable data integration solutions to cleanse, prepare, blend, transfer, and transform data without having to wrestle with infrastructure.

Cloud Life Sciences (formerly Google Genomics): Cloud Life Sciences provides services and tools for managing, processing, and transforming life sciences data.

Data Catalog: Data Catalog is a fully-managed and scalable metadata management service that empowers organizations to quickly discover, manage, and understand their data in Google Cloud. It offers a central data catalog across certain Google Cloud Services that allows organizations to have a unified view of their data assets.

Dataform: Dataform provides an end-to-end experience for data analysts to develop, test, version control, and schedule complex SQL workflows.

Dataplex: Dataplex is an intelligent data fabric that helps customers unify distributed data and automate management and governance across that data to power analytics at scale.

Dataflow: Dataflow is a fully-managed service for strongly consistent, parallel data-processing pipelines. It provides an SDK for Java with composable primitives for building data-processing pipelines for batch or continuous processing. This service manages the life cycle of Compute Engine resources of the processing pipeline(s). It also provides a monitoring user interface for understanding pipeline health.

Datalab: Datalab is an interactive tool for exploration, transformation, analysis and visualization of your data on Google Cloud Platform. It runs in your cloud project and enables you to write code to use other Big Data

and storage services using a rich set of Google-authored and third party libraries.

Dataproc: Dataproc is a fast, easy to use, managed Spark and Hadoop service for distributed data processing. It provides management, integration, and development tools for unlocking the power of rich open source data processing tools. With Dataproc, you can create Spark/Hadoop clusters sized for your workloads precisely when you need them.

DataprocMetastore: DataprocMetastore provides a fully-managed metastore service that simplifies technical metadata management and is based on a fully-featured Apache Hive metastore. DataprocMetastore can be used as a metadata storage service component for data lakes built on open source processing frameworks like Apache Hadoop, Apache Spark, Apache Hive, Presto, and others.

Datastream: Datastream is a serverless change data capture (CDC) and replication service that enables data synchronization across heterogeneous databases, storage systems, and applications with minimal latency.

Google Earth Engine: Google Earth Engine is a platform for global-scale analysis and visualization of geospatial datasets. Google Earth Engine can be used with custom datasets, or with any of the publicly available satellite imagery hosted (and ingested on a regular basis) by Earth Engine Data Catalog.

*Looker (Google Cloud core): Looker (Google Cloud core) is a business intelligence and embedded analytics solution hosted on Google infrastructure. With Looker (Google Cloud core), customers can build semantic models using various data sources, develop customized insights from the models, and share those insights for collaboration via dashboards and other services.

*Looker Studio: Looker Studio is a data visualization and business intelligence product. It enables customers to connect to their data stored in other systems, create reports and dashboards using that data, and share them throughout their organization.

- Looker Studio Pro: Looker Studio Pro is a paid edition of Looker Studio that adds enterprise governance, team management features, and other features listed at https://cloud.google.com/looker-studio/ or a successor URL. Unlike Looker Studio, Looker Studio Pro is eligible for partner resale.

Pub/Sub: Pub/Sub is designed to provide reliable, many-to-many, asynchronous messaging between applications. Publisher applications can send messages to a "topic" and other applications can subscribe to that topic to receive the messages. By decoupling senders and receivers, Pub/Sub allows developers to communicate between independently written applications.

Data Analysis is one of important aspect which is required to effectively use the Big Data in construction industry.It is required for effective planning and managing the construction activities. Above mentioned Data Analytics tools available on GCP can be proved very effective mechanism to explore the various dimensions of construction data.

6.3 GCP AL/ML Services

AI Solutions

Anti Money Laundering AI (AML AI): AML AI enhances financial institutions' legacy transaction monitoring systems with an AI-powered risk score to improve financial crime risk detection.

Contact Center AI (CCAI): CCAI uses AI to improve the customer experience in contact centers. It includes Agent Assist, Dialogflow Essentials, Dialogflow Customer Experience Edition (CX), Insights, Speech-to-Text, Text-to-Speech, and Speaker ID.

Contact Center AI Insights: Contact Center AI Insights helps customers extract value from their contact center data by identifying sentiment and topics and highlighting key insights in the data.

Contact Center AI (CCAI) Platform: CCAI Platform is a contact-center-as-a-service (CCaaS) platform leveraging CCAI. It integrates directly with CRMs and queues and routes customer

interactions across voice and digital channels to resource pools, including human agents.

DialogflowEssentials(ES): Dialog flow ES is a development suite for voice and text conversational apps that can connect to customer applications and telephony and digital platforms.

Dialogflow Customer Experience Edition (CX): Dialogflow CX is a development suite for creating conversational AI applications including chatbots and voicebots. It includes a visual bot building platform, collaboration and versioning tools, bot modularization tools, and advanced IVR feature support.

Discovery Solutions: Discovery Solutions enable customers in retail, media, and other verticals to deliver Google-quality search results and recommendations.

- *Recommendations AI: Recommendations AI enables customers to build a personalized recommendation system using ML models.
- *Recommendation Engine API: Recommendation engine API is the Version 1 API of Recommendations AI.
- *Retail Search: Retail Search, powered by Google's Retail API, allows retailers to leverage Google's search capabilities on their retail websites and applications.

Document AI: Document AI is a unified console for document processing that lets you quickly access all document processing models and tools. Customers can use Document AI's pre-trained models for document extraction, including OCR, Form Parser and specialized models.

- Document Workbench: Document Workbench allows you to build a custom classification, extraction or splitting model.
- *Human-in-the-Loop AI: Human-in-the-Loop AI uses Document AI to provide workflow tools for human verification of data extracted from documents.
- Document AI Warehouse: Document AI Warehouse is a highly-scalable, fully managed data management and governance platform that integrates with enterprise document workflows to store, search, and organize documents and their metadata.

Talent Solution: Talent Solution offers access to Google's machine learning, enabling company career sites, job boards, ATS, staffing agencies, and other recruitment technology platforms to improve the talent acquisition experience.
Pre-Trained APIs

Cloud Natural Language API: Cloud Natural Language API analyzes text to identify entities, sentiment, languages, and syntax.
Cloud Translation API: Cloud Translation API automatically translates text from one language to another language.

Cloud Vision: Cloud Vision classifies images into categories, detects individual objects and faces, and finds and reads printed words.

Media Translation API: Media Translation API is a gRPC API that automatically translates audio from one language to another language (e.g., French to English) and supports streaming real time.

Speaker ID: Speaker ID allows customers to enroll user voice prints and later verify users against a previously enrolled voice print.

Speech On Device: Speech On Device deploys speech-to-text and text-to-speech services locally on embedded hardware and operating systems.

Speech-to-Text: Speech-to-Text converts audio to text by applying neural network models.

Text-to-Speech: Text-to-Speech synthesizes human-like speech based on input text in a variety of voices and languages.

Timeseries Insights API: Timeseries Insights API enables large-scale time series forecasting and anomaly detection in real time.

Video Intelligence API: Video Intelligence API analyzes videos to extract metadata, add annotations, and identify entities in a video.

Visual Inspection AI: Visual Inspection AI automatically detects, classifies, and localizes abnormalities foundin images to improve production quality and develop analytics.
AI Platform/Vertex AI

AI Platform Data Labeling: AI Platform Data Labeling helps developers label data and centrally

manage labels for training and evaluating machine learning models.

AI Platform Training and Prediction: AI Platform Training and Prediction enables customers to easily train and deploy machine learning models.

AutoML: AutoML enables customers to leverage Google's transfer learning and Neural Architecture Search to build custom models using a variety of data types. AutoML Services include AutoML Natural Language, AutoML Tables, AutoML Translation, AutoML Video, and AutoML Vision.

Deep Learning VM and Container: Deep Learning VM and Container provides virtual machine and Docker images with AI frameworks that can be customized and used with Google Kubernetes Engine (GKE), Vertex AI, Cloud Run, Compute Engine, Kubernetes, and Docker Swarm.

Vertex AI Platform: Vertex AI Platform is a service for managing the AI and machine learning development lifecycle. Customers can (i) manage datasets and associated labels; (ii) build pipelines to train and evaluate models using Google Cloud algorithms or custom training code; (iii) deploy models for online or batch use cases; (iv) manage data science workflow using Vertex AI Workbench (also known as Notebooks); and (v) create business optimization plans with Optimization AI.

Vertex AI Neural Architecture Search (NAS): Vertex AI NAS leverages Google's neural architecture search technology to generate, evaluate, and train model architectures for a customer's application.

Vertex AI Vision: Vertex AI Vision is a service that allows you to easily build, deploy, and manage computer vision applications with a fully managed, end-to-end application development environment.

Generative AI Services

Generative AI Services include: (i) Services listed in this subsection, (ii) any Service identified as a "Generative AI Service" or similar designation in the Documentation, and (iii) any feature of a Service identified as a "Generative AI Feature" or similar designation in the Documentation.

Generative AI App Builder: Generative AI App Builder allows customers to leverage foundational models, conversational AI, and search technologies to create multimodal chatbots and search experiences.

Generative AI Supporton Vertex AI: Generative AI Support on Vertex AI includes features for generative AI use cases, including large language, text-to-image, and image-to-text models that are available in Model Garden and Generative AI Studio.

AI/ML like any other industry has immense potential as a tool in the field of construction. Various AI and ML services available on GCP, as mentioned above, offers tremendous opportunities to process Big Data in construction industry.

These can be to predict properties of concrete, contract management, site safety and injury prediction, delay risks management, BIM integrated on-demand site monitoring, and other areas of construction engineering and management.

VII. CONCLUSIONS

- The construction industry is yet to reap the true benefits of using big data aptly. Over the last two decades, the rapid growth of big data technologies has caused a spike in the number of models and platforms that have been developed for increasing digitalization across different fields. However, the same level of digitalization has not truly been harnessed or integrated by the construction industry.
- However, the state of implantation of adoption in construction is below par. Therefore, the utilization and commercialization of big data to benefit the construction industry are crucial. An extensive literature review enabled us to identify the potential of big data in construction as the industry generates huge amounts of data daily and can greatly improve using the latest technologies.
- The development of online tools and software which enable infrastructure modeling and CAD is a crucial step in the right direction for futuristic constructions.

London Journal of Engineering Research

- Having explored the existing ML tools, we found that these tools, coupled with big data, can be applied in the construction industry.
- There are currently various gaps and pitfalls that act as barriers to using big data to its full potential.
- Firstly, data generation is much faster than the tools available for processing it. Moreover, big data integration into the construction industry is quite an uphill task even with the existing data processing tools.
- After going through this paper along with other papers which I reviewed, I want to further work on following areas which I still think that need more focus and research .
  - o Big Data use to Improvement the Productivity and Performance Improvement
  - o Big Date use for effective construction management
- In order to meet the above 2 objectives , my approach would be to develop some processes and protocol by using various analytical tool, storage mechanism and ML/AI processes available on Google Cloud Platform (GCP)
- Various Capability like Compute, Storage, Data bases, Data Analytics and AI/ML services available on GCP can be proved as game changer for the effective utilization of Big Data in construction Industry.

REFERENCES

1. Big Data in Construction: Current Applications and Future Opportunities https://www.mdpi.com/2504-2289/6/1/18 By Hafiz SulimanMunawar; Fahim Ullah; Siddra Qayyum;DanishShahzad
2. Application of Big Data Technology in Construction Organization and Management of Engineering Projects https://iopscience.iop.org/article/10.1088/1742-6596/1616/1/012002 Lijian Pei[1]Published under licence by IOP Publishing Ltd. Journal of Physics: Conference Series, Volume 1616, 3rd International Symposium on Big Data and Applied Statistics 10-12 July 2020, Kunming, ChinaCitation Lijian Pei 2020 J. Phys.: Conf. Ser. 1616 012002 DOI10.1088/1742-6596/1616/1/012002.
3. Review of Big Data Integration in Construction Industry Digitalization https://www.frontiersin.org/articles/10.3389/fbuil.2021.770496/full Omar Sedeeq Yousif1* RozanaBinti Zakaria1 Eeydzah Aminudin1 Khairulzan Yahya1 Abdul RahmanMohd Sam1 Loganathan Singaram1 Vikneswaran Munikanan2 MuhamadAzani Yahya2 Noraziah Wahi3 SitiMazzuana Shamsuddin3.
4. Big Data in the construction industry: A review of present status, opportunities, and future trends https://pure.coventry.ac.uk/ws/portalfiles/portal/13749152/Big_Data_in_construction_Industry.pdf Bilal, M, Oyedele, LO, Qadir, J, Munir, K, Ajayi, SO, Akinade, OO, Owolabi, HA, Alaka, HA & Pasha, M.
5. Big data technology in construction https://www.e3s-conferences.org/articles/e3sconf/pdf/2019/23/e3sconf_form2018_01032.pdf Nikolay Garyaev* and VeneraGaryaeva.
6. Building Information Modeling (BIM) and BIG Data Analytics for Construction Industry https://www.academia.edu/70816308/Building_Information_Modeling_BIM_and_BIG_Data_Analytics_for_Construction_Industry Profile image of Yusuf ArayiciYusufArayici 2019.
7. Investigating profitability performance of construction projects using big data: A project analytics approach July 2019. https://www.researchgate.net/publication/334201799_Investigating_profitability_performance_of_construction_projects_using_big_data_A_project_analytics_approach Journal of Building Engineering 26:100850, DOI:10.1016/j.jobe.2019.100850 License;CC BY 4.0 Authors: Muhammad Bilal; Lukumon O. Oyedele; Habeeb O. Kusimo; Hakeem A. Owolabi;; Anuoluwapo O. Ajayi; Olúgbénga O Akinadé; Manuel Davila Delgado
8. Cloud computing in construction industry: Use cases, benefits and challenges https://www.researchgate.net/publication/347679916_Cloud_computing_in_construction_industry_Use_cases_benefits_and_challenges December 2020; Automation in Construction 122(1):103441 DOI:10.1016/j.autcon.2020.10

3441 ; License CC BY-NC-ND 4.0 Authors: Sururah Apinke Bello; Lukumon O. Oyedele; Olúgbénga O Akinadé; Muhammad Bilal;Manuel Davila Delgado; Lukman Akanbi; Anuoluwapo O. Ajayi; Hakeem A. Owolabi

9. Transformative role of big data through enabling capability recognition in construction https://www.tandfonline.com/doi/full/10.1080/01446193.2022.2132523. Bernard Tuffour Atuahene; Sittimont Kanjanabootra & Thayaparan Gajendran Pages 208-231 | Received 01 Aug 2021, Accepted 30 Sep 2022, Published online: 19 Oct 2022.

10. Big Data and Management https://journals.aom.org/doi/abs/10.5465/amj.2014.4002?journalCode=amj Gerard George; Martine R. Haas and Alex Pentland Published Online: 4 Apr 2014 https://doi.org/10.5465/amj.2014.4002.

11. An Appraisal into the Potential Application of Big Data in the Construction Industry https://www.researchgate.net/publication/325993944_An_Appraisal_into_the_Potential_Application_of_Big_Data_in_the_Construction_Industry/fulltext/5b323ea74585150d23d55f01/An-Appraisal-into-the-Potential-Application-of-Big-Data-in-the-Construction-Industry.pdf SitiAisyah Ismail; ShamsulhadiBandi and Zafira Nadia Maaz Department of Quantity Surveying, Faculty of Built Environment, Universiti Teknologi Malaysia Email: aisyaaahismail@gmail.com

12. Big Data Technology in Construction Safety Management: Application Status, Trend and Challenge https://www.mdpi.com/2075-5309/12/5/533 by QingfengMeng; QiyuanPeng; Zhen Li;andXin Hu. School of Management, Jiangsu University, 301 Xuefu Road, Zhenjiang 212013, China. School of Architecture and Built Environment, Deakin University, 1 Gheringhap Street, Geelong, VIC 3220, Australi.

13. Readiness of Applying Big Data Technology for Construction Management in Thai Public Sector http://www.jait.us/uploadfile/2020/1216/20201216030941159.pdf
Korb Srinavin1, Wuttipong Kusonkhum1, Boonyarit Chonpitakwong1, Tanayut Chaitongrat2, Narong Leungbootnak1, and Phatsaphan Charnwasununth3 1 Department of Civil Engineering, KhonKaen University, Khon Kaen, Thailand 2 Faculty of Architecture, Urban Design and Creative Arts, Mahasarakham University, Mahasarakham, Thailand 3 Department of Housing, Faculty of Architecture, Chulalongkorn University, Bangkok, Thailand Email: korbsri@kku.ac.th, w.kusonkhum@gmail.com, boonyarit_por@kkumail.com, Tanayut.c@msu.ac.th, Narongl.fec@gmail.com, Phatsaphan.C@chula.ac.th

14. Big Data is a powerful tool for environmental improvements in the construction business https://iopscience.iop.org/article/10.1088/1755-1315/90/1/012184/pdf To cite this article: AleksandrKonikov and Gregory Konikov 2017 IOP Conf. Ser.: Earth Environ. Sci. 90 012184

15. Research on Construction Methods of Big Data Semantic Model https://www.iaeng.org/publication/WCE2014/WCE2014_pp213-218.pdf Li Kang, Li Yi, LIU Dong.

16. Big data in building energy efficiency: understanding of big data and main challenges https://cyberleninka.org/article/n/722385.pdf NatalijaKoseleva*, Guoda Ropaite Faculty of Civil Engineering, Department of Construction Technology and Management, Vilnius Gediminas Technical University, Sauletekio al. 11, 10223, Vilnius

London Journal of Engineering Research

This page is intentionally left blank

Fuel Consumption at Signalized Intersection Due to Delay

Arun Kumar & Praveen Aggarwal

ABSTRACT

In INDIA population is the root of many problems and is also directly linked with fuel consumption. And with increase in affordability index due to economic growth has led to higher aspiration amongst people (especially a need for increased comfort). With high numbers of vehicle on signals, waiting time increases which leads to a situation of heavy traffic congestion at traffic signals and intersections resulting in a very slow traffic movement even when the traffic lights switch green.

An idling vehicle is not only using up valuable fuel and damaging vehicle's engine, but also causing danger to the environment and a risk to the health of many others. Fuel consumption at signalized intersections has increased, as the vehicles are unable to cross the intersection during one green phase of signal because of long queues at the intersection. Extra fuel loss is due to personal mode of transportation, enhanced trip length and congested intersections. Usually when the vehicles are waiting for their turn to cross the intersection at signals, drivers normally keep their vehicle's engine on, resulting in extra consumption of fuel. This small amount of fuel wasted, if aggregated over number of cycles per day, for number of days per year and for number of signalized intersections results in a huge quantity of fuel. The wastage of fuel at these intersections results in a huge loss of valuable fuel resources. The paper presents the results of fuel loss at signalized intersections due to delay of vehicle.

Keywords: fuel loss; congestion; intersection; journey time, long queues.

Classification: LCC: TL175- TL178

Language: English

Fuel Consumption at Signalized Intersection Due to Delay

Arun Kumar[α] & Praveen Aggarwal[σ]

ABSTRACT

In INDIA population is the root of many problems and is also directly linked with fuel consumption. And with increase in affordability index due to economic growth has led to higher aspiration amongst people (especially a need for increased comfort). With high numbers of vehicle on signals, waiting time increases which leads to a situation of heavy traffic congestion at traffic signals and intersections resulting in a very slow traffic movement even when the traffic lights switch green.

An idling vehicle is not only using up valuable fuel and damaging vehicle's engine, but also causing danger to the environment and a risk to the health of many others. Fuel consumption at signalized intersections has increased, as the vehicles are unable to cross the intersection during one green phase of signal because of long queues at the intersection. Extra fuel loss is due to personal mode of transportation, enhanced trip length and congested intersections. Usually when the vehicles are waiting for their turn to cross the intersection at signals, drivers normally keep their vehicle's engine on, resulting in extra consumption of fuel. This small amount of fuel wasted, if aggregated over number of cycles per day, for number of days per year and for number of signalized intersections results in a huge quantity of fuel. The wastage of fuel at these intersections results in a huge loss of valuable fuel resources. The paper presents the results of fuel loss at signalized intersections due to delay of vehicle.

Keywords: fuel loss; congestion; intersection; journey time, long queues.

Author α: M. Tech student, Dept. of Civil Engineering, National Institute of Technology Kurukshetra, Haryana-136119, India.

σ: Prof., Dept. of Civil Engineering, National Institute of Technology, Kurukshetra, Haryana-136119, India.

I. INTRODUCTION

In the last few years with the increase in population there has been a significant growth in vehicular traffic for travelling and carrying goods from one place to another. With increase in demand of mobility, more vehicles are owned and operated. Increase in no. of vehicles results in traffic and transportation problems in the form of increment in traffic congestion, air & noise pollution, accidents, delays and emission of greenhouse gases. The long queues of vehicles results in delay and during this interval vehicle is generally in idling condition, causes extra fuel consumption. Moreover within two decades, there is continuous increment in vehicle ownership and vehicle size preferences. The tracking of energy consumption in transportation over the years must consider both the changes in travel patterns and vehicle fleet characteristics. It is well known that the energy consumption in transportation has a very high proportion of a society's total energy consumption. Therefore, from the perspective of saving energy and reducing energy consumption, study of transportation system not only reduce the total energy consumption, but also has an important significance for the future sustainable development of transportation. Ever increasing vehicular flow causes heavy delays at intersections due to stoppage of vehicles during red phase resulting in wastage of fuel at intersections.

II. LITERATURE REVIEW

Parida and Gangopadhyay (2008) observed various intersections in Delhi to estimate the savings in fuel consumption during delays. And on the basis of the savings accrued at low, medium and high volume intersections, the

savings at the total signalized intersections was estimated, assuming similar kind of remedial measures. They observed total 67.78% of saving in fuel consumption and expected 71.12% of saving in the economic loss due to extra fuel consumption. It was observed that 135.86 million kilogram CNG; 47.35 million litres diesel and 147.84 million litres petrol worth Rs. 9945 million is extra consumed during idling condition of vehicles at the signalized intersections in Delhi.

Shipchandler et al. (2008) estimated the total quantity of emissions of greenhouse gases produced in idling condition of vehicles in Chicago metropolitan area using reasonable assumptions. It was done by developing an emission factor and multiplying total number of vehicles and total idling time with this factor. It was observed that fuel consumed during idling of vehicles for heavy duty trucks was 1gallon/hr. and for passenger vehicles it was .5 gallon/hr.

Li et al. (2012) observed an advanced driving alert system that provides traffic signal status information to help drivers for avoiding hard braking at intersections and defines a method for evaluating fuel consumption & emissions at intersections. This study shows the savings on fuel consumption up to 8% and the reduction of CO_2 emissions around 7% when traffic was in medium congestion.

Tiwari et al. (2013) also estimated fuel wastage due to idling of vehicles at road traffic signal in Indore Madhya Pradesh. The classified traffic volume study was conducted for 12 hours from 10:00 am to 10:00 pm at seven signalized intersection for complete week to estimate extra fuel consumption because of idling of vehicles. The study shows that about 5.9×10^5 liters of petrol and diesel are being wasted.

Pal et al. (2012) evaluated the fuel consumption of vehicles at signalized intersections using precise instruments. Five red light traffic signals of different traffic volume had been considered and estimated the fuel loss during idling and delay of vehicles. An average fuel cost Rs.19, 175.00 was wasted per day due to delay at signalized intersections. It was also observed that 85%

drivers did not switch off the engine of a vehicle at red light traffic signals that lead to extra fuel consumption. The results showed that the delay of vehicles at five red light traffic signals was greater than 60 seconds that lead to wastage of 389.68 litres of diesel and 810.38 litres of petrol. Total loss output work found were Rs. 61,072 per day and Rs. 2, 22, 91,198 per annum. The fuel consumption for petrol car was 573 ml/hr. and diesel car was 705 ml/hr.

Vlieger et al. (2000) effect of normal and aggressive driving on the tailpipe pollutants and fuel consumption of vehicles were studied. The fuel consumption was highest in city traffic conditions and in rural conditions. The exhaust tailpipe pollutants were increased by 8 times for aggressive driving as compared with normal driving behaviour. The fuel consumption was increased by 20-45% during intense traffic conditions.

Carrico et al. (2009) human activities and behaviour played a dominant role for increase in tailpipe pollutants and fuel consumption of vehicles. The survey was done on 1300 drivers in United States for calculation of vehicle exhaust pollutants and fuel consumption. An aggressive driving contributed more tailpipe pollutants and fuel consumption as compared with normal driving behaviour.

Lim (2012) studied exhaust emissions from idling Heavy-Duty Diesel Trucks and Commercially Available Idle-Reducing Devices. The emissions and fuel consumption data generated from this study shows that on an average, a class-8 truck could emit 144 gm./hr. of NO^x and 8224 gm./hr. of CO_2, and could consume about 0.82 gallon/hr. diesel and also shows that the use of idling reduction devices cuts the emissions and fuel consumption.

III. TYPES OF FUEL CONSUMPTION MODELS

(a) Instantaneous fuel consumption model: - This type of fuel consumption model requires second by second individual data comprising of speed acceleration, de-acceleration, vehicle engine

London Journal of Engineering Research

speed, time and location along road section for every individual vehicle. It includes basic model and micro level model. Basic model is an engine type model which constitutes of vehicle design and engine torque as model parameters. Micro level model is a non-engine type model which includes second by second individual vehicle data.

(b) Delay type fuel consumption model: - In this type of model relationship is established between fuel consumption and commonly used traffic measures such as delay and stop. As delay is very effective and popular measure in traffic analysis work, so its use in fuel consumption model is advantageous.

(c) Speed type aggregate fuel consumption model:- In this type of model generally regression analysis is used to establish relationship between fuel consumption and various network wide variables such as travel time, average speed, travel distance and number of stops, as these type of model do not consider second by second speed change in estimation of fuel consumption. Moreover they are insensitive to small traffic condition changes.

IV.   OBJECTIVES OF THE STUDY

This study deals with the twelve hours traffic composition of a normal day of an intersection of a city. Total traffic count of the duration is calculated and also the delay during the duration is obtained. Fuel consumption due to delay of vehicles is also estimated along with the monetary losses.

V.   STUDY AREA

For the present work, the clock tower intersection of Saharanpur, a city of Uttar Pradesh in Northern India is chosen as the study area. Saharanpur is located at 29.97° N and 77.55° E. It is about 140 kilometres south- southeast of Chandigarh, 170 kilometres north-northeast of Delhi,65 kilometres north-northeast of Shamli, and about 68 kilometres southwest of Dehradun. It is the main intersection of city for going to neighbouring states Uttrakhand, Haryana and Himachal Pradesh. It is the busiest intersection of city as railway station and bus stand are just at a distance of few minutes. Also Dehradun chowk and the court road intersection are among main intersections of city as they connect the city to the rest of the area. According to census 2011, city had around 7.5 lakh population.

Increase in Road Network (2013-17):24.12km.
Total Road Length in city: 1783.22 Km.
Vehicles Growth (new registration) 2016-17: 43486 vehicles,
2017-18: 50178 vehicles,
2018-19: 60615 vehicles.
E-rickshaw & auto based transit system.

Bus Services for Inter & Intra transit: 18 Routes, 437 permit buses including private & government. Number of authorized parking lots increased (2014-17): 3 to 5;

Fig. 1: West Approach of Clock Tower Intersection

Fig. 2: Approach Towards East of Clock Tower Intersection

VI. DATA COLLECTION

Video graphic technique was used for collection of traffic data. A twelve hours video was collected from traffic police of the desired intersection of the normal day. In total a twelve hours video was collected i.e. from 7:00 am to 7:00 pm. The data collected was divided into lean hour, average hour and peak hour as observed on the basis of vehicular traffic count. Also manually observation of traffic data was done to know the lean average and peak hours of the intersection.

VII. DATA EXTRACTION

From the collected data, hourly traffic data was extracted very effectively and precisely. Data was extracted into various categories of vehicles such as two wheelers, three wheelers, bus, car, trucks and tractor trailers etc. The collected data was as follows as represented in the below tables. Table 1 represents the traffic data of the normal day of three main intersections..

From the extracted data, it was concluded that within this twelve hour study there were three lean hours, six average hours and three peak hours.

Table 1: Traffic volume of 3 intersections

Intersection	Type of intersection	Traffic count	Duration of data
Dehradun chowk	3 legged	22754	12 hours
Court road	3 legged	28294	12 hours
Clock tower	4 legged	33260	12 hours

London Journal of Engineering Research
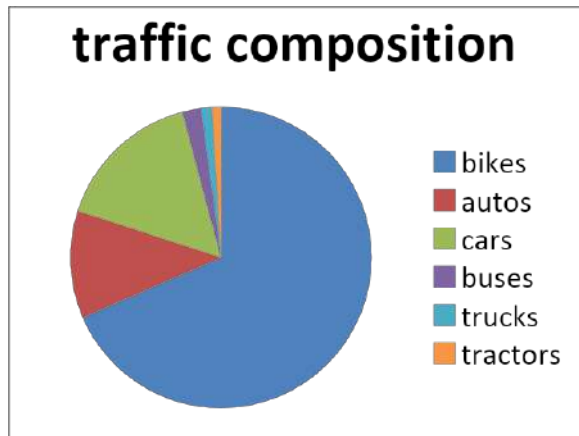
Figure 1: Traffic Composition of Clock Tower Intersection

VIII. CALCULATION OF DELAY

For calculation of delay Reilly's model is used. This model is the modified version of Akcelik's delay model. According to this model total delay is the combination of uniform delay and overflow delay. Now overflow delay is given as

OVERFLOW DELAY (OD) $=450[(X-1) + [(X-1)^2 +\sqrt{\{12*(X-X_o)/c*T\}}]$

UNIFORM DELAY (UD) $=0.25C(1-g/c)$

Where T is the analysis period in hours; X is volume to capacity ratio; c is the capacity in vehicles per hour; s is the saturation flow rate in vehicles per seconds green time; g is the effective green time in seconds

For Overflow Delay, $X>=X_o$, if $X<X_o$ then overflow delay is zero.

$X_o = 0.67+(s*g/600)$

Thus, total delay = uniform delay (UD) + overflow delay (OD).

In the present study the delay calculated is as follows:

Table 2: Calculated Delays

Hours	Delay calculated(sec/veh)
Lean hours	24
Average hours	38
Peak hours	90

Table 3: Total Delay Calculated (In Hours) for Different Vehicles

Vehicles	Delay for different hours			Total
	Lean hour	Average hours	Peak hours	
Bikes	25.49	130.43	164.95	320.87
Autos	3.64	20.58	33.45	57.37
Cars	5.39	28.90	43.10	77.39
Buses	0.349	3.8	5.17	9.32
Trucks	0.67	1.5	2.62	4.79
Tractors	0.54	1.65	2.12	4.31

IX. FUEL CONSUMPTION CALCULATION

Fuel consumption of vehicles is obtained using a CSIR-CRRI report of 2009 for fuel consumption of vehicles. The idling fuel consumption of vehicle is multiplied with the total delay of vehicle obtained in table 3. Table 4 gives different values for fuel consumption of different vehicles.

Table 4: Idling fuel consumption in ml/hr. (CSIR- CRRI 2009)

Serial no.	Vehicle type	Fuel consumption (ml/hr.)	Fuel type
1	Maruti gypsy	1045	Petrol
2	Maruti van	692	Petrol
3	Lml motor cycle	129	Petrol
4	Bajaj pulsar	166	Petrol
5	Honda active	118	Petrol
6	Ambassador car	952	Diesel
7	Mahindra jeep	1052	Diesel
8	Hyundai santro	563	Petrol
9	Taxi	1010	Petrol
10	Tata sumo	717	Petrol
11	Tata indica	547	Diesel
12	Esteem	740	Petrol
13	LCV	690	Diesel
14	HCV	1240	Diesel
15	Bus	3610	Diesel
16	Auto rickshaw	700	CNG

With using table 3 and table 4, total fuel consumption can be calculated by multiplying the idling fuel consumption of different vehicles to the total delay calculated in hours in table 3. Table 5 gives the total amount of fuel consumption of different vehicles.

Table 5: Total Fuel Consumption of Different Vehicles

Sr. No.	vehicle	Idling Fuel Consumption	Total delay	Total fuel consumption	Fuel type
1	Bikes	150 ml/hr.	320.87	48.13L/hr.	Petrol
2	Autos	700ml/hr.	57.37	40.11L/hr.	CNG
3	Cars	900ml/hr.	77.39	69.65L/hr.	Petrol
4	Buses	3610ml/hr.	9.32	33.64L/hr.	diesel
5	Trucks	1240ml/hr.	4.79	5.93L/hr.	diesel
6	Tractor trailer s	690	4.31	2.97L/hr.	diesel

From table 5 it is evident that a total of 117.78 litres of petrol, 42.54litres of diesel and 40.11litres of CNG is extra utilised during this 12 hours study. Table 6 shows the cost of extra fuel utilised during this 12 hours study.

Table 6: Total Cost of Extra Fuel Consumed

Sr. no.	Fuel type	Fuel consumed(L)	Present rate Rs/l	Total amount(Rs.)
1	Petrol	117.78	70.28	8227
2	Diesel	42.54	63.66	2708
3	CNG	40.11	51.95	2083

X. CONCLUSION

From this study it is concluded that a total of 117.78 litres of petrol is extra consumed Worthing of INR.8227, 63.67 litres diesel of INR.2708 and 40.11 litres CNG of INR.2083. Thus during this 12 hour study a total amount of 13018 INR is utilised on extra consumption of fuel. This study is limited to 12 hours and to one intersection only, if the

same study to be carried out annually and on all intersection of city then a huge amount of fuel wasted can be carried out.

XI. REMEDIAL MEASURES:

As it is well versed that petroleum products are non-renewable resources and cannot be replenished in short span. Also petroleum products are a major source of carbon emissions largely responsible for environment deterioration, they must be sustainably utilised.

- Switching off behaviour
- Encouraging public transport
- Encouraging non-motorised mode
- Imparting traffic education
- Removal and shifting of bus stand from centre of the city.
- Strict measure to remove encroachment from roadside.
- Route diversion of heavy vehicles.

REFERENCES

1. Carrico, Amanda R., Padgett Paul, Vandenbergh, Michael P., Gilligan Jonathan, Wallston, Kenneth A. (2009), Costly myths: Analysis of idling beliefs and behaviour in personal motor Vehicles, *Energy Policy*, Vol. 37, Issue 8, pp. 2881-2888.
2. CRRI Report (2009) Study on Losses of Petroleum Products at Traffic Intersections due to idling of vehicles at Delhi.
3. Li C. and Shimimoto S. (2012), ETC Assisted Traffic Light Control Scheme for Reducing Vehicles CO_2 Emissions, International Journal of Managing Information Technology (IJMIT) Vol.4, No.2
4. Lim H. (2012), Study of Exhaust Emissions from Idling Heavy-Duty Diesel Trucks and Commercially Available Idle-Reducing Devices submitted at U. S. Environmental Protection Agency.
5. Pal Manish, Sarkar Dipankar (2012), Delay fuel loss and noise pollution during idling of Vehicles at signalized intersection in Agartala city, India, *International institute for science Technology and institution,* Vol. 2, Issue 6, pp. 2222-1719.
6. Parida P. and Gangopadhyay S., "Estimation of fuel loss during idling of vehicles at signalized intersections of Delhi," Technical Report, Dept. Traffic and Transportation Planning., CRRI, New Delhi, 2008.
7. Shipchandler R. and Miller J., (2008), Estimating Smog Precursor Emissions From Idling Vehicles In The Chicago Metropolitan Area Illinois Sustainable Technology Centre Institute of Natural Resources Sustainability University of Illinois at Urbana-Champaign Submitted to the Metropolitan Mayors Caucus 177 North State Street, Suite 500 Chicago, Illinois
8. Tiwari K. P., Singh R. N and Balwanshi J.B.(2013)" Fuel Wastage and Emission due to idling of vehicles at road traffic signals", IJRET: International Journal of Research in Engineering and Technology, Volume:02 issue: 10, October -2013.
9. Vlieger, I. De., Keukeleere, D. De., Kretzschmar, J.G. (2000), Environmental effects of driving behaviour and congestion related to passenger cars, *Atmospheric Environment*, Vol. 34, Issue 27, pp. 4649-4655.

This page is intentionally left blank

Optimizing Texture Position for Improved Dynamic Stability and Operational Performance in Two-Lobe Journal Bearings

Niranjan Singh & R.K Awasthi

Sardar Beant Singh State University

ABSTRACT

This research paper presents a theoretical investigation into the optimization of texture position in two-lobe journal bearings using finite element method (FEM). Journal bearings play a vital role in various industrial applications by supporting rotating machinery and ensuring efficient operation. Surface texturing has emerged as a promising technique to enhance tribological performance by altering the hydrodynamic lubrication mechanisms. The present study is focussed on the influence of texture position on dynamic stability and operational efficiency. Through the development of a comprehensive FEM model, the dynamic behavior of the bearing system is analyzed under varying texture positions. The effects of different texture locations on the dynamic coefficients, including stiffness and damping, are evaluated to understand their impact on stability and performance. Subsequently, the operational performance metrics, such as friction reduction and load-carrying capacity, are quantified. The optimization process involves systematic exploration of texture positions using numerical algorithms to identify the optimal configuration that maximizes dynamic stability and operational efficiency.

Keywords: two-lobe textured journal bearing, load carrying capacity, dynamic stability, critical mass of journal, threshold speed, whirl frequency ratio.

Classification: LCC: TJ1075

Language: English

Optimizing Texture Position for Improved Dynamic Stability and Operational Performance in Two-Lobe Journal Bearings

Niranjan Singh[α] & R.K Awasthi[σ]

ABSTRACT

This research paper presents a theoretical investigation into the optimization of texture position in two-lobe journal bearings using finite element method (FEM). Journal bearings play a vital role in various industrial applications by supporting rotating machinery and ensuring efficient operation. Surface texturing has emerged as a promising technique to enhance tribological performance by altering the hydrodynamic lubrication mechanisms. The present study is focussed on the influence of texture position on dynamic stability and operational efficiency. Through the development of a comprehensive FEM model, the dynamic behavior of the bearing system is analyzed under varying texture positions. The effects of different texture locations on the dynamic coefficients, including stiffness and damping, are evaluated to understand their impact on stability and performance. Subsequently, the operational performance metrics, such as friction reduction and load-carrying capacity, are quantified. The optimization process involves systematic exploration of texture positions using numerical algorithms to identify the optimal configuration that maximizes dynamic stability and operational efficiency. The outcomes of this study provide insights into the intricate interplay between texture placement and the bearing's dynamic response, shedding light on the underlying mechanisms that lead to improved performance.

Author α: Model Institute of Engineering & Technology, Jammu, INDIA.

σ: Sardar Beant Singh State University, Gurdaspur, Punjab, INDIA.

I. INTRODUCTION

Two-lobe journal bearings find extensive use in various industries due to their capacity for high-speed, high-load support with minimal friction and wear. However, surface texture significantly impacts their performance. By enhancing lubrication and decreasing friction and wear, surface texturing improves these bearings. Such textures aid in generating hydrodynamic pressure and maintaining lubricating films. Texture attribute like location influence bearing performance. Optimal design parameters can be identified through numerical simulations and experiments.

Several studies have been undertaken to explore the effect of texture location on the performance parameters of two-lobe journal bearings. Hsu et al. [1] explored texture location's impact on performance of dynamic-loaded two-lobe journal bearings. Their study revealed that placing the texture at the leading edge enhanced load capacity and decreased friction, as opposed to mid-span or trailing edge placement. Kim et al. [2] investigated the impact of texture location and depth on two-lobe journal bearing performance under different conditions. They found that a 10 μm deep texture placed at the bearing's trailing edge improved stability and decreased friction. In contrast, placing the texture at the mid-span yielded opposite effects. Lee et al. [3] studied the effect of texture location on the performance of two-lobe journal bearings under various

London Journal of Engineering Research

lubrication regimes. They found that placing the texture at the mid-span of the bearing surface improved its load-carrying capacity and reduced its friction coefficient vis-a-vis placing the texture at the edges of the bearing surface.

Park et al. [4] studied the effect of texture location and depth on the performance characteristics of two-lobe journal bearings. They found that placing the texture at the edges of the bearing surface improved its stability and reduced its friction coefficient, while placing the texture at the mid-span of the bearing surface had the opposite effect. Experimental and numerical investigations were undertaken by Karthikeyan et al. [5] to explore the influence of texture location on the load-carrying capacity of two-lobe journal bearings. They found that the load-carrying capacity increased by 7.5% when the texture was located at 60° from the leading edge of the bearing. Using a combined experimental and numerical approach, Li et al. [6] conducted a study to examine the impact of texture location on the friction and wear characteristics of two-lobe journal bearings. Their findings revealed that the lowest friction coefficient and wear rate were achieved when the texture was located at 120° from the leading edge of the bearing.

Wu et al. [7] studied the effect of texture location on the stability of two-lobe journal bearings using a nonlinear dynamic analysis. They found that the stability threshold increased by 22.5% when the texture was located at 90° from the leading edge of the bearing. Zhang et al. [8] conducted a study to explore the influence of texture orientation and location on the performance characteristics of two-lobe journal bearings. The researchers discovered that placing the texture at the edges of the bearing surface with a 45° orientation resulted in enhanced load-carrying capacity and reduced friction coefficient, in contrast to placing the texture at the mid-span of the bearing surface with a 90° orientation. Zhou et al. [9] conducted an experimental study to explore the effect of different texture locations on the performance characteristics of two-lobe journal bearings. Their results revealed that the texture location had a significant impact on the friction coefficient and the bearing's stability. They concluded that the

optimal texture location was at the midpoint of the bearing's length.

Zhang et al. [10] studied the impact of texture location on the performance characteristics of two-lobe journal bearings under misalignment conditions using numerical simulations. They reported that the maximum oil film pressure was obtained when the texture was located at 180° from the leading edge of the bearing. In another study, Qiu et al. [11] conducted numerical simulations to investigate the impact of texture location on the lubrication performance parameters of journal bearings. The authors found that the optimal texture location depended on the load and the sliding velocity. Wang et al. [12] investigated the effect of texture location on the dynamic characteristics of a two-lobe journal bearing. The findings clearly indicated that the placement of textures had a notable impact on the dynamic stiffness and damping characteristics of the bearing. Based on these results, the authors reached the conclusion that by optimizing the location of textures, the dynamic performance of two-lobe journal bearings could be improved.

Li et al. [13] investigated the effect of texture location and texture size on the performance of a two-lobe journal bearing. The results showed that the texture location and size had a significant effect on the friction coefficient and load capacity of the bearing. The authors proposed an optimization method to determine the optimal texture location and size for improved bearing performance. Wang et al. [14] studied the impact of texture location and pattern on the performance parameters of two-lobe journal bearings. The authors found that placing the texture at the edges of the bearing surface with a sinusoidal pattern improved its load-carrying capacity and reduced its friction coefficient vis-a-vis placing the texture at the mid-span of the bearing surface with a rectangular pattern.

Li et al. [15] investigated texture positions' influence on two-lobe journal bearings using both experiments and simulations under varied loads. Their findings indicated the midpoint as the optimal texture location for all loads, impacting oil film thickness, pressure distribution, and

friction coefficient of the bearing. Zhao et al. [16] studied the effect of texture location on the load carrying capacity and friction coefficient of a two-lobe journal bearing. The study's findings revealed a substantial influence of texture location on both the load carrying capacity and friction coefficient of the two-lobe journal bearings. Consequently, the authors concluded that by optimizing the location of textures, the performance characteristics of these bearings could be enhanced. Another study by Liu et al. [17] examined the effect of texture location on the stability of a two-lobe journal bearing. The authors found that the texture location had a significant effect on the stability of the bearing.

They proposed an optimization method to determine the optimal texture location for improved bearing stability.

After an extensive review of the available literature, it has become evident that the understanding of the influence of texture location on the performance of two-lobe journal bearings is still insufficient. Consequently, this study aims to investigate the impact of texture location on the dynamic stability and performance parameters of two-lobe journal bearings operating under laminar flow conditions. Fig.1 depicts the schematic diagram of a smooth/textured two-lobe journal bearing for reference.
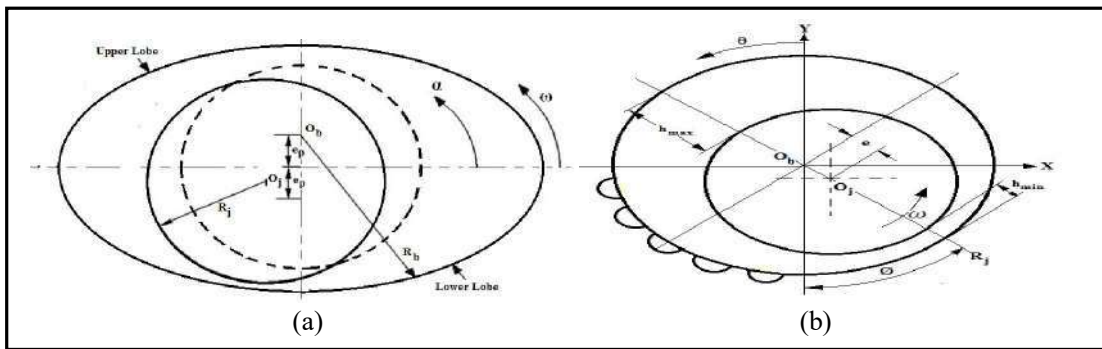
Fig. 1: (a) Depicts the Geometry of Smooth Two-Lobe Journal Bearing, (b) Textured Two-Lobe Journal Bearing

II. ANALYSIS AND MATHEMATICAL MODELING

The non-dimensional form of the governing Reynolds equation for a two-lobe journal bearing,

under the assumptions of Newtonian, isoviscous, and laminar fluid flow, can be mathematically represented as per previous studies [18, 19].

$$\frac{\partial}{\partial \alpha}\left(\bar{h}^3 \bar{F}_2 \frac{\partial \bar{p}}{\partial \alpha}\right) + \frac{\partial}{\partial \beta}\left(\bar{h}^3 \bar{F}_2 \frac{\partial \bar{p}}{\partial \beta}\right) = \bar{\Omega}\left[\frac{\partial}{\partial \alpha}\left\{\left(1 - \frac{\bar{F}_1}{\bar{F}_0}\right)\bar{h}\right\}\right] + \frac{d\bar{h}}{d\bar{t}} \tag{1}$$

Where $\bar{F}_0$, $\bar{F}_1$ and $\bar{F}_2$ are cross apparent viscosity integrals and can be calculated as

$$\bar{F}_0 = \int_0^1 \frac{1}{\bar{\mu}} d\bar{z}, \quad \bar{F}_1 = \int_0^1 \frac{\bar{z}}{\bar{\mu}} d\bar{z}, \quad \bar{F}_2 = \int_0^1 \frac{\bar{z}}{\bar{\mu}} d\bar{z}\left(\bar{z} - \frac{\bar{F}_1}{\bar{F}_0}\right) d\bar{z}$$

Fluid −Film Thickness (h̄)

The dimensionless expression for the fluid-film thickness $(\bar{h})$ of a two-lobe journal bearing system can be derived as per the findings from previous research [20].

$$\bar{h} = 1 - \left(\overline{X}_j - \overline{X}^i_L\right)\cos\alpha - \left(\overline{Z}_j \pm \bar{\delta} - \overline{Z}^i_L\right)\sin\alpha \tag{2}$$

Where $\overline{X}^i_L$ and $\overline{Z}^i_L$ represent the local coordinates of the lobe center for the ith lobe.

The fluid-film thickness $(\bar{h})$ for the upper-lobe of the two-lobe bearing system can be expressed as follows:

$$\bar{h} = 1 - \left(\overline{X}_j - \overline{X}^i_L\right)\cos\alpha - \left(\overline{Z}_j + \bar{\delta} - \overline{Z}^i_L\right)\sin\alpha + d_1 \tag{2a}$$

The fluid-film thickness $(\bar{h})$ for the lower-lobe of the two-lobe bearing system can be expressed as follows:

$$\bar{h} = 1 - \left(\overline{X}_j - \overline{X}^i_L\right)\cos\alpha - \left(\overline{Z}_j - \bar{\delta} - \overline{Z}^i_L\right)\sin\alpha + d_1 \tag{2b}$$

Where d_1 = dimple depth.

In the case of a bearing surface featuring spherical textures, the dimple depth (d_1) can be represented by the following expression, as indicated in earlier investigations [21, 22].

$$d_1 = \begin{cases} \left[\left(\dfrac{\bar{h}_p}{2} + \dfrac{\bar{r}_p^{\,2}}{2\bar{h}_p}\right)^2 - \bar{r}_p^{\,2}(\overline{X}_L^2 + \overline{Z}_L \qquad \dfrac{\bar{r}_p^{\,2}}{\bar{h}_p} - \dfrac{\bar{h}_p}{2}\right] \\ 0 \end{cases} \tag{2c}$$

2.1 FEM formulation

The fluid domain is discretized using four-noded quadrilateral iso-parametric elements. The pressure distribution within an element is assumed to be linear and can be mathematically expressed as [21]:

$$\overline{P} = \sum_{j=1}^{n_e} \overline{P}_j N_j \tag{3}$$

Where N_j represents the shape function of the element and n_e denotes the number of nodes per element. By employing Galerkin's Finite Element Method (FEM) approach, the global system of equations can be expressed in algebraic form as detailed in previous research [21].

$$[\overline{F}]^e \{\overline{P}\}^e = \{\overline{Q}\}^e + \overline{\Omega}\{\overline{R}_H\}^e + \overline{X}_j\{\overline{R}_{x_j}\}^e + \overline{Z}_j\{\overline{R}_{z_j}\}^e \tag{4}$$

$$\overline{F}_{ij}^{\,e} = \iint_{A^e} \bar{h}^3 \left[\frac{1}{12}\frac{\partial N_i \partial N_j}{\partial\alpha\partial\alpha} + \frac{1}{12}\frac{\partial N_i \partial N_j}{\partial\beta\partial\beta}\right] d\alpha\, d\beta \tag{4a}$$

$$\overline{Q_i}^e = \int_{\Gamma^e} \left\{ \left(\frac{\overline{h}^3}{12} \frac{\partial \overline{p}^e}{\partial \alpha} - \frac{\overline{\Omega h}}{2} \right) l_1 + \left(\frac{\overline{h}^3}{12} \frac{\partial \overline{p}^e}{\partial \beta} \right) l_2 \right\} N_i d\overline{\Gamma}^e \qquad (4b)$$

$$\overline{R_{H_i}}^e = \iint_{A^e} \frac{\overline{h}}{2} \frac{\partial N_i}{\partial \alpha} d\alpha d\beta \qquad (4c)$$

$$\overline{R_{xj_i}}^e = \iint_{A^e} N_i \cos \alpha \, d\alpha d\beta \qquad (4d)$$

$$\overline{R_{zj_i}}^e = \iint_{A^e} N_i \sin \alpha \, d\alpha d\beta \qquad (4e)$$

Where, l_1 & l_2 are the direction cosines and i, j =1,2..........n_e.

2.2 Boundary Conditions

The solution is obtained by applying the following boundary conditions:

a) The pressure at nodes located on the external boundary is set to zero.
b) The pressure of the fluid at the trailing edge of the positive region is assumed to be zero.
c) The pressure at the leading edge is considered to be atmospheric.

By simultaneously solving Equation (4), the pressure and fluid flow are determined. This approach is employed as, at each node, one of the two variables is already known.

2.3 Performance Characteristics

Static performance characteristics

Load carrying capacity ($\overline{F_0}$): The fluid-film reaction components along the X and Z directions can be expressed as per the findings from a previous study [23].

$$\overline{Fx_1} = \int_{-\lambda}^{\lambda} \int_0^{2\pi} \overline{p} \cos \alpha \, d\alpha d\beta \qquad (5)$$

$$\overline{Fz_1} = \int_{-\lambda}^{\lambda} \int_0^{2\pi} \overline{p} \sin \alpha \, d\alpha d\beta \qquad (6)$$

The resultant load carrying capacity is expressed as

$$\overline{F_0} = \left[\overline{Fx_1}^2 + \overline{Fz_1}^2 \right]^{\frac{1}{2}} \qquad (7)$$

Attitude angle (ϕ): The calculation of the attitude angle (ϕ) is performed using the following method:

$$\phi = \tan^{-1} \left(\frac{\overline{X_j}}{\overline{Z_j}} \right) \qquad (8)$$

Fluid-film Frictin force ($\overline{F_{j.}}$): The computation of the friction force in a journal bearing is accomplished using the equation provided in previous research [24].

$$\overline{F}_L = \sum_{e=1}^{n_e} \int_{A^e} \left(\frac{\overline{\Omega \tau_c}}{\overline{h}} + \frac{\overline{h}}{2} \frac{\partial \overline{p}}{\partial \alpha} \right) dA \tag{9}$$

The friction force in a journal bearing is determined based on the equation (9), wherein $\overline{\tau}_c$ represents

the normalized Couette shearing stress. In the case of laminar flow, $\overline{\tau}_c$ is set to zero.
The coefficient of fluid-film friction can be calculated using the following relation

$$\frac{\overline{F}_L}{\overline{F}_0} = f\left(\frac{R_j}{C} \right) \tag{10}$$

Dynamic performance characteristics

The dynamic performance characteristics refer to the behavior and performance of a system under varying dynamic conditions. By analyzing the dynamic performance characteristics, researchers can assess and optimize the system's response to dynamic forces and vibrations, ensuring its reliability, efficiency, and safety.

Fluid-Film Stiffness Coefficients: The dimensionless form of the fluid-film stiffness coefficients can be expressed as per the findings presented in previous research [25].

$$\overline{S}_{ij} = -\frac{\partial \overline{F}_i}{\partial \overline{q}_j}, (i = x, z) \tag{11}$$

The index 'i' corresponds to the force direction, while the index 'q' pertains to the displacement direction concerning the coordinates $\left(\overline{X}_j or \overline{Z}_j \right)$ of the journal center. The matrix of fluid-film stiffness coefficients can be represented as follows:

$$\begin{pmatrix} \overline{S}_{xx} & \overline{S}_{xz} \\ \overline{S}_{zx} & \overline{S}_{zz} \end{pmatrix} = - \begin{pmatrix} \frac{\partial \overline{F}_x}{\partial \overline{x}} & \frac{\partial \overline{F}_x}{\partial \overline{z}} \\ \frac{\partial \overline{F}_z}{\partial \overline{x}} & \frac{\partial \overline{F}_z}{\partial \overline{z}} \end{pmatrix} = - \begin{bmatrix} \frac{\partial}{\partial \overline{X}_j} \int_{-1}^{1} \int_{0}^{2\pi} \left(\overline{P} \cos\alpha \right) d\alpha d\beta & \frac{\partial}{\partial \overline{Z}_j} \int_{-1}^{1} \int_{0}^{2\pi} \left(\overline{P} \cos\alpha \right) d\alpha d\beta \\ \frac{\partial}{\partial \overline{X}_j} \int_{-1}^{1} \int_{0}^{2\pi} \left(\overline{P} \sin\alpha \right) d\alpha d\beta & \frac{\partial}{\partial \overline{Z}_j} \int_{-1}^{1} \int_{0}^{2\pi} \left(\overline{P} \cos\alpha \right) d\alpha d\beta \end{bmatrix} \tag{12}$$

Fluid-film Damping Coefficients: In non-dimesionalized form, the coefficients of fluid-film damping can be represented as [25].

$$\overline{C}_{ij} = -\frac{\partial \overline{F}_i}{\partial \dot{\overline{q}}_j}, (i = x, z) \tag{13}$$

Where $\dot{\overline{q}}$ represents the velocity components $\left(\dot{\overline{X}}_j or \dot{\overline{Z}}_j \right)$ at the center of the journal.
The matrix of fluid-film damping coefficients can be expressed as

$$\begin{pmatrix} \overline{C}_{xx} & \overline{C}_{xz} \\ \overline{C}_{zx} & \overline{C}_{zz} \end{pmatrix} = -\begin{pmatrix} \dfrac{\partial \overline{F}_x}{\partial \overline{x}} & \dfrac{\partial \overline{F}_x}{\partial \overline{z}} \\ \dfrac{\partial \overline{F}_z}{\partial \overline{x}} & \dfrac{\partial \overline{F}_z}{\partial \overline{z}} \end{pmatrix} = -\begin{bmatrix} \dfrac{\partial}{\partial \dot{\overline{X}}_j} \int\limits_{-1}^{1}\int\limits_{0}^{2\pi} \left(\overline{P}\cos\alpha\right) d\alpha d\beta & \dfrac{\partial}{\partial \dot{\overline{Z}}_j} \int\limits_{-1}^{1}\int\limits_{0}^{2\pi} \left(\overline{P}\cos\alpha\right) d\alpha d\beta \\ \dfrac{\partial}{\partial \dot{\overline{X}}_j} \int\limits_{-1}^{1}\int\limits_{0}^{2\pi} \left(\overline{P}\sin\alpha\right) d\alpha d\beta & \dfrac{\partial}{\partial \dot{\overline{Z}}_j} \int\limits_{-1}^{1}\int\limits_{0}^{2\pi} \left(\overline{P}\cos\alpha\right) d\alpha d\beta \end{bmatrix} \quad (14)$$

III. SOLUTION PROCEDURE

The study employed Finite Element Method (FEM) to analyze the effect of texture location on the performance of two-lobe journal bearings. The authors[25] detailed the selection of axial and circumferential elements and the overall methodology in their published work. To calculate static, dynamic, and stability characteristics, a systematic approach is developed considering texture location. A visual representation of the computation steps is given in Fig. 2, offering a clear and succinct depiction of the process.
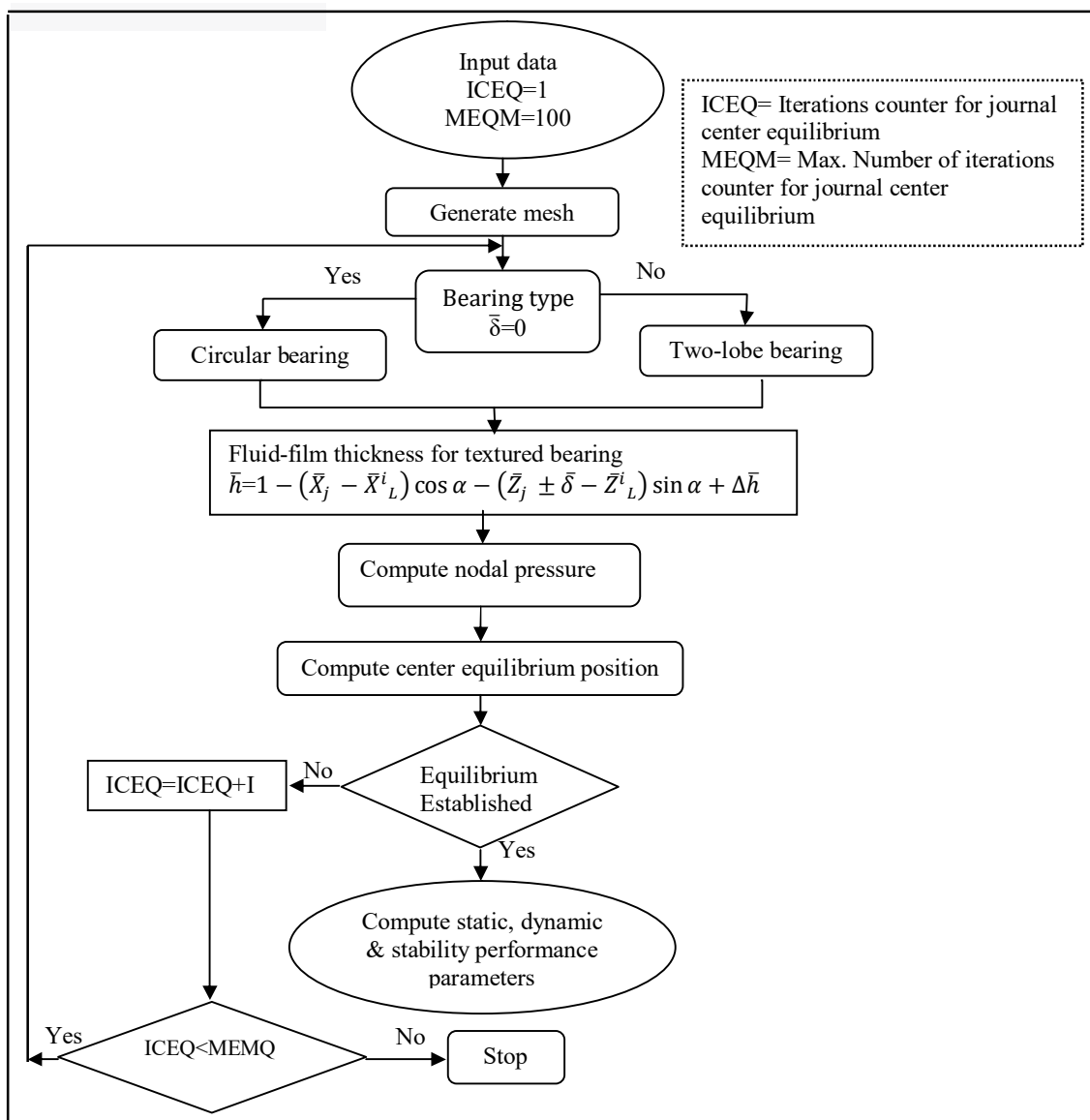

Fig. 2: Flow Chart of Solution Procedure

London Journal of Engineering Research

VI. RESULTS AND DISCUSSIONS

This study explores performance in smooth and textured two-lobe journal bearings through varied texture positions. A MATLAB code is developed and validated against prior research, ensuring computational accuracy. Static parameters align with Sinhasan and Goyal's [26] results, and dynamic parameters match Lund and Thomson's [27] findings, as shown in Tables 1 and 2. The study's operational and geometric parameters, outlined in Table 3, are derived from Singh and Awasthi's [25] work.

Table 1: Comparative Analysis of Static Performance Parameters of Two-Lobe Journal Bearing (Without Supply Groove) $[\lambda = 1.0, \overline{\Omega} = 1.0, \overline{\delta} = 0.5]$

Performance Characteristics	$\varepsilon = 0.25$		$\varepsilon = 0.35$	
	1	2	1	2
$\overline{W}_0$	3.2621	3.1388	5.5825	5.6887
ϕ	83.621	84.26	80.2180	78.83

1. Present work
2. Sinhasan & Goyal [26]

Table 2: Comparative Analysis Dynamic Performance Parameters of Two-Lobe Journal Bearing (With Supply Groove 20° Arc) $[\lambda = 1.0, \overline{\Omega} = 1.0, \overline{\delta} = 0.5]$

Performance Characteristics	$\varepsilon = 0.25$		$\varepsilon = 0.35$	
	1	2	1	2
$\overline{S}_{xx} / \overline{W}_0$	0.855	0.82	1.038	1.14
$\overline{S}_{xz} / \overline{W}_0$	3.3787	3.43	1.54	1.52
$\overline{S}_{zx} / \overline{W}_0$	-4.3815	-4.51	-3.46	- 3.54
$\overline{S}_{zz} / \overline{W}_0$	6.8685	6.95	5.16	4.99
$\overline{C}_{xx} / \overline{W}_0$	3.75	3.86	2.49	2.49
$-(\overline{C}_{xz} \approx \overline{C}_{zx}) / \overline{W}_0$	2.426	2.55	0.011	0.01
$\overline{C}_{zz} / \overline{W}_0$	13.457	13.74	8.90	9.04

1. Present work
2. Lund & Thomson [27]

Table 3: Geometric and Operating Values Used for Two-Lobe Textured Journal Bearing [25]

Operating and geometric parameters	Non-Dimensional Value
Speed parameter ($\overline{\Omega}$)	1.0
Eccentricity ratio (ε)	0.3
Clearance ratio (C_r)	0.001
Aspect ratio (L/D)	1.0
Shape of micro-dimple	Spherical
No. of dimples in circumferential direction ($N_{c\theta}$)	7
No. of dimples in axial direction ($N_{a\theta}$)	4
No. of nodes	63×21
Area density of dimple (S_p)	50%
Dimple radius ($\overline{r}_p$)	0.16
Dimple depth ($\overline{h}_p$)	0.16
Offset factor ($\overline{\delta}$)	0.4
a	0.2
b	0.2
L_x	2a
L_z	2b

The arrangement of textures on the bearing surface plays a crucial role in determining the performance characteristics of a two-lobe journal bearing. These textures are strategically placed depending on their location relative to the upstream and downstream regions of the bearing surface. In order to identify the most effective placement of textures on the bearing surface, nine different configurations of partially textured two-lobe journal bearings are considered, as illustrated in Fig. 4. Fig. 5 depicts the distribution of circumferential fluid-film pressure at the axial mid-plane of both smooth and textured two-lobe journal bearings.
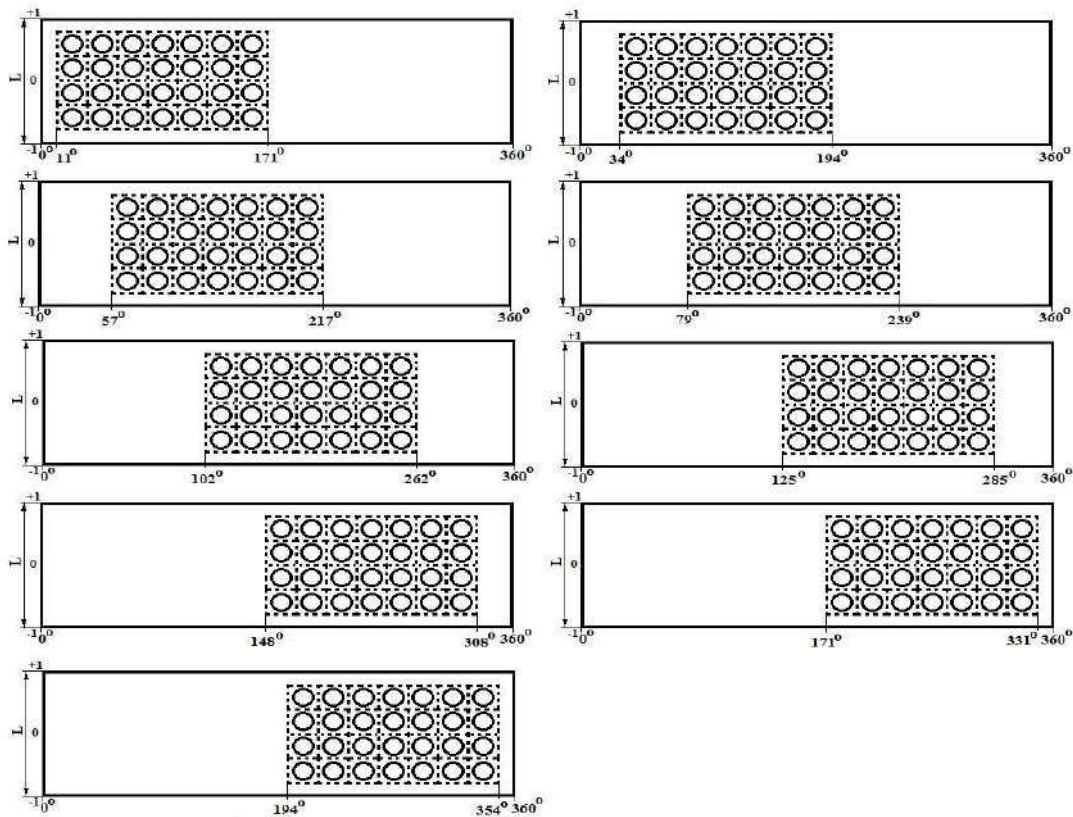

Fig. 4: Different Configurations of Partially Textured Two-Lobe Journal Bearing

Surface texturing introduces alterations in fluid-film pressure distribution, as depicted in Fig. 5. In the context of hydrodynamic lubrication, pressure is primarily generated near the region of minimum fluid-film thickness or clearance, while it reaches its lowest point at the area of maximum clearance or film thickness. In a two-lobe journal bearing, two pressure profiles form due to the dual fluid films—each for upper and lower lobes.
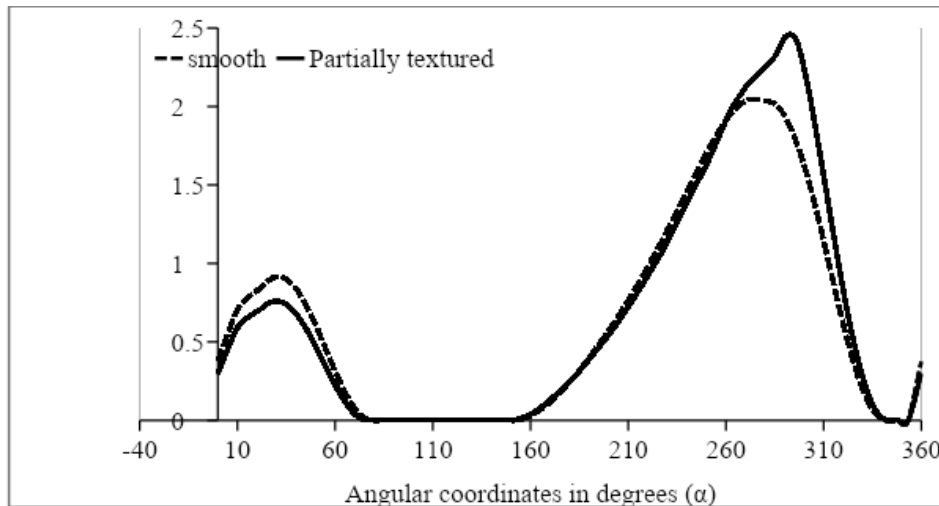
Fig. 5: Circumferential Fluid-Film Pressure at the Axial Mid Plane (β=0.0) for Bearing Configurations at ε=0.3

Load Carrying Capacity ($\overline{F}_0$)

Fig. 6 shows the variation in load carrying capacity ($\overline{F}_0$) for smooth and textured journal bearings, plotted against the location of textures on the bearing surface in the circumferential direction. Notably, the load carrying capacity of partially textured journal bearings reaches its maximum improvement when the textures are positioned within the pressure built-up region spanning from θ_1=148° to θ_2=308° in the circumferential direction, covering the entire axial direction. This improvement is in comparison to the load carrying capacity of smooth journal bearings. Similar findings have been reported by Singh & Awasthi [24]. For a specific dimple depth of 0.16, there is an 18.90% increase in the load carrying capacity as compared to a smooth journal bearing.

Maximum fluid-film pressure ($\overline{P}_{max}$)

Fig. 7 illustrates the variation in maximum fluid-film pressure ($\overline{P}_{max}$) for both smooth and textured journal bearings, plotted against the location of textures on the bearing surface in the circumferential direction. It is noted that the maximum fluid-film pressure of partially textured journal bearings exhibits an improvement when the textures are positioned within the pressure built-up region spanning from θ_1=125° to θ_2=285° in the circumferential direction, covering the

entire axial direction. This improvement is in comparison to the maximum fluid-film pressure of smooth journal bearings. Similar results have been reported by Singh & Awasthi [24]. For a specific dimple depth of 0.16, there is a remarkable 157.78% increase in the value of maximum fluid-film pressure ($\overline{P}_{max}$) when the textures are created in the region of 125°-285°, as compared to a smooth journal bearing.

Attitude angle (Φ)

Fig. 8 presents the variation in the attitude angle (Φ) for both smooth and textured journal bearings, plotted against the location of textures on the bearing surface in the circumferential direction. It is observed that the attitude angle (Φ) of partially textured journal bearings reaches its minimum value when the textures are positioned within the pressure built-up region ranging from θ_1=148° to θ_2=308° in the circumferential direction, covering the entire axial direction. This minimum value indicates that the partially textured journal bearing exhibits greater stability when the textures are created within the zone of 148°-308°, compared to a smooth journal bearing. For a specific dimple depth of 0.16, there is a 9.79% decrease in the value of attitude angle for the textured journal bearing, in comparison to the smooth journal bearing.

Lubricant end flow ($\overline{Q}$)

Fig. 9 depicts the variation in lubricant end flow ($\overline{Q}$) for both smooth and textured journal bearings,

plotted against the location of textures on the bearing surface in the circumferential direction. It is noted that the lubricant end flow of partially textured journal bearings achieves its maximum value when the textures are positioned within the pressure built-up region spanning from $\theta_1=125°$ to $\theta_2=285°$ in the circumferential direction, covering the entire axial direction. This maximum value indicates that the partially textured journal bearing exhibits a higher lubricant end flow compared to the smooth journal bearing. Similar results have been reported by Singh & Awasthi [90]. For a specific dimple depth of 0.16, there is a significant 28.50% increase in the value of lubricant end flow compared to the smooth journal bearing.

Fluid-film friction coefficient $(\bar{f})$

Fig. 10 illustrates the variation in the fluid-film friction coefficient $(\bar{f})$ for both smooth and textured journal bearings, plotted against the location of textures on the bearing surface in the circumferential direction. It is observed that the fluid-film friction coefficient $(\bar{f})$ of partially textured journal bearings reaches its minimum value when the textures are positioned within the pressure built-up region ranging from $\theta_1=148°$ to $\theta_2=308°$ in the circumferential direction, covering the entire axial direction. This minimum value indicates that the partially textured journal bearing experiences reduced fluid-film friction compared to the smooth journal bearing. It demonstrates that the flow of lubricant is more efficient in the case of a partially textured journal bearing when the textures are created within the zone of 148°-308°. For a specific dimple depth of 0.16, there is a remarkable 119.36% decrease in the value of the fluid-film friction coefficient $(\bar{f})$ for the textured journal bearing, compared to the smooth journal bearing.

4.1 Fluid-Film Stiffness Coefficients

In general, a higher stiffness coefficient indicates a bearing with greater stiffness capable of supporting heavy loads without excessive deflection. The presence of textures on the bearing surface can significantly influence the stiffness coefficients. When textures promote hydrodynamic lubrication, they contribute to increasing the stiffness coefficients. On the other hand, textures that hinder lubrication can lead to a decrease in stiffness. This is because hydrodynamic lubrication helps maintain a thin film of lubricant between the journal and bearing surfaces, reducing friction, wear, and increasing stiffness. Fig. 11 demonstrates the impact of texture location on the fluid-film stiffness coefficient in the horizontal direction of a two-lobe journal bearing. It is observed that the value of the fluid-film stiffness coefficient in the horizontal direction increases by 38.45% when the textures are created within the region of 148°-308° in the circumferential direction, covering the entire axial direction, compared to a smooth journal bearing.

Similarly, the texture on the bearing surface can be designed to achieve the desired stiffness coefficient in the vertical direction. This can be accomplished by optimizing the distribution of surface textures to enhance the contact area between the journal and the bearing surface. Fig. 12 illustrates the effect of texture location on the fluid-film stiffness coefficient in the vertical direction of a two-lobe journal bearing. It is noted that the value of the fluid-film stiffness coefficient in the vertical direction increases by 7.33% when the textures are created within the region of 125°-285° in the circumferential direction, covering the entire axial direction, compared to a smooth journal bearing. Surface textures tend to enhance the stiffness coefficient in the vertical direction because they provide additional contact area between the journal and the bearing surface. This increased contact area requires a higher force to move the journal vertically, resulting in a higher stiffness coefficient.

4.2 Fluid-Film Damping Coefficients

Surface textures can have a significant effect on the damping coefficients of a two-lobe journal bearing. In a journal bearing, the damping coefficients are affected by the flow of lubricant within the bearing. Fig. 13 illustrates the impact of texture location on the fluid-film damping coefficient in the horizontal direction of a

two-lobe journal bearing. It is observed that the value of the fluid-film damping coefficient in the horizontal direction increases by 1.81% when the textures are positioned within the region of 194°-354° in the circumferential direction, covering the entire axial direction, compared to a smooth journal bearing. The introduction of textures on the bearing surface can affect the flow of lubricant, thereby influencing the damping coefficient. These textures can enhance the flow of lubricant and promote the formation of hydrodynamic pressure, which is crucial for damping vibration.

In general, the vertical damping coefficient of a journal bearing is affected by the oil film thickness and the frictional losses in the bearing. Surface textures can affect the oil film thickness and distribution, and therefore the damping coefficient. Fig. 14 presents the impact of texture location on the fluid-film damping coefficient in the vertical direction of a two-lobe journal bearing. It is observed that the presence of textures on the bearing surface leads to a reduction in the value of the fluid-film damping coefficient in the vertical direction. The specific decrease in the damping coefficient would depend on the exact texture configuration and location. The presence of textures might reduce the ability of the bearing to retain and distribute oil effectively, and leading to increased friction and reduced damping.

4.3 Critical mass

Fig. 15 shows the effect of texture location versus critical mass of a two-lobe journal bearing. When a texture is added to the surface of a journal bearing, it creates a pattern of small grooves or ridges that can enhance the bearing's ability to retain lubrication and reduce friction. This can increase the load capacity of the bearing, allowing it to support a higher mass. It is noticed that the value of critical mass of a journal is increased by an amount of 29.288% when the surface textures are located in the zone of 125°-285° in the circumferential direction and over the entire axial direction in comparison to smooth bearing. A careful design and testing are necessary to ensure

optimal performance of the bearing with the texture in the desired location.

4.4 Threshold Speed

Fig. 16 shows the effect of texture location versus threshold speed of a smooth/textured two-lobe journal bearing. It is noted that the presence of textures on the bearing surface at proper location can increase the threshold speed of a journal bearing. The reason being that the addition of texture to the bearing surface can increase its load capacity, which may allow it to operate at higher speed without failing. For a specific eccentricity ratio 0.3 and dimple depth 0.16, the value of threshold speed of a journal bearing is increased by an amount of 3.19% when the surface textures are located in the zone of 125°-285° in the circumferential direction and over the entire axial direction in comparison to smooth bearing.

4.5 Whirl Frequency Ratio

Fig. shows 17 the effect of texture location versus whirl frequency ratio of a smooth/textured two-lobe journal bearings. The whirl frequency ratio of a two-lobe journal bearing is influenced by the location and geometry of the texture. The texture location can affect the whirl frequency ratio by altering the oil film flow, pressure distribution, and contact area between the journal and bearing. The simulation results indicate that the value the whirl frequency ratio is found minimum when the textures are created in the circumferential zone of 125°-285° and over the entire axial direction at eccentricity ratio 0.3 and dimple depth 0.16 as compared to smooth bearing. This is because of the reason that the texture located at 125°-285° on the bearing surface may reduce the stiffness of the bearing and increases the amplitude of the shaft motion, leading to a lower whirl frequency ratio. Therefore, it is essential to conduct a thorough analysis to determine the optimal texture location and geometry for a specific application.
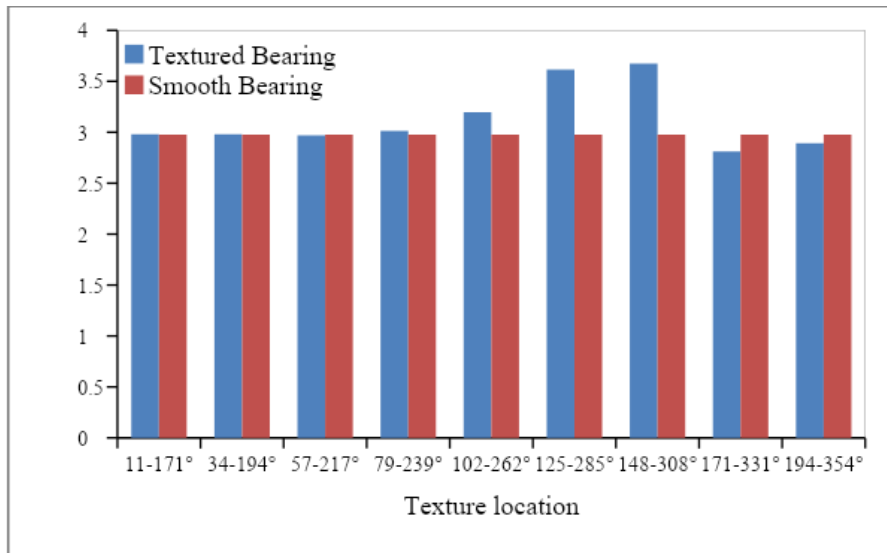
Fig. 6: Load Carrying Capacity Versus Texture Location in Circumferential Direction
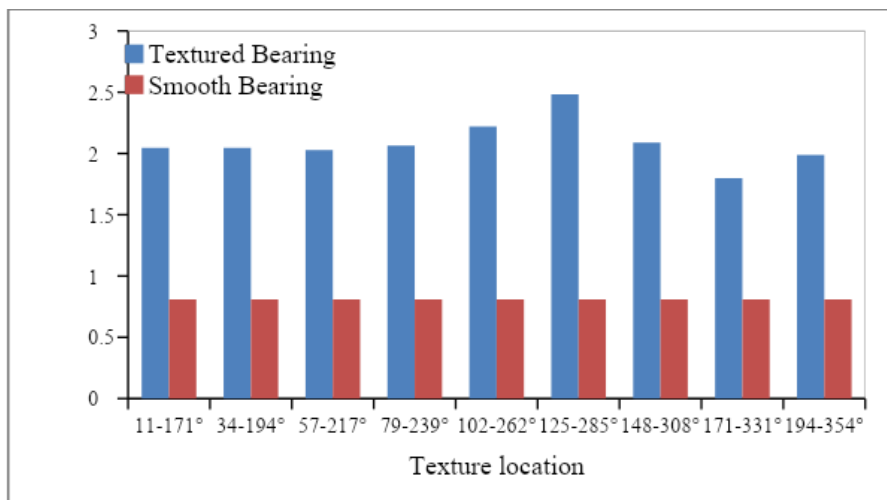

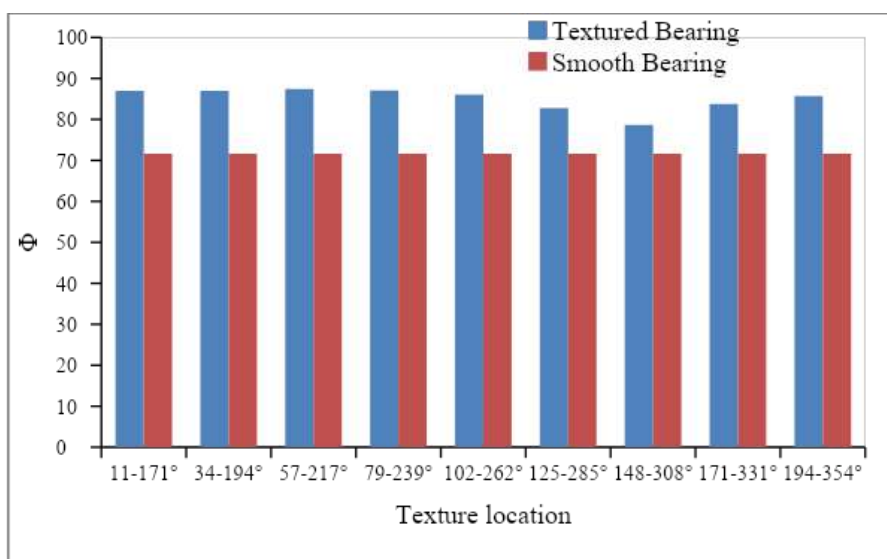Fig. 7: Maximum Fluid-Film Pressure Versus Texture Location in Circumferential Direction

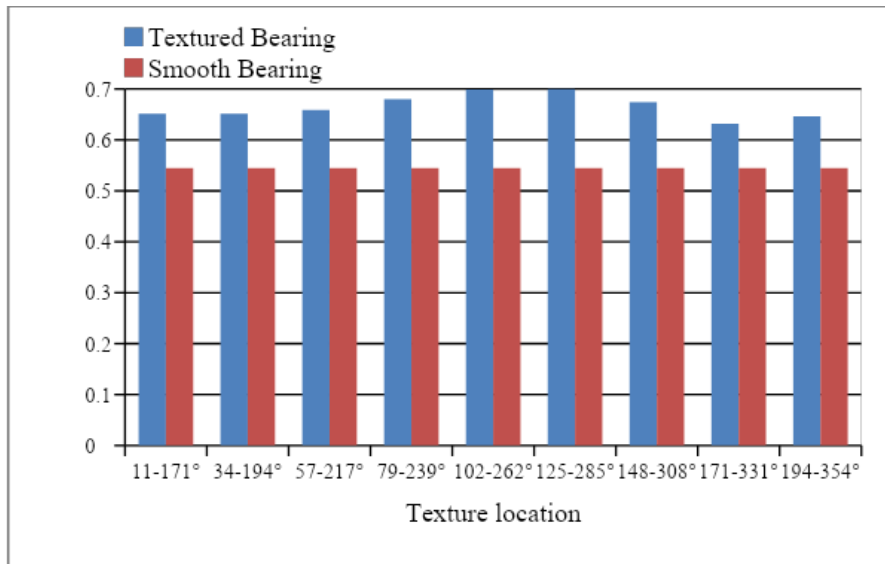Fig. 8: Attitude Angle Versus Texture Location in Circumferential Direction

Optimizing Texture Position for Improved Dynamic Stability and Operational Performance in Two-Lobe Journal Bearings

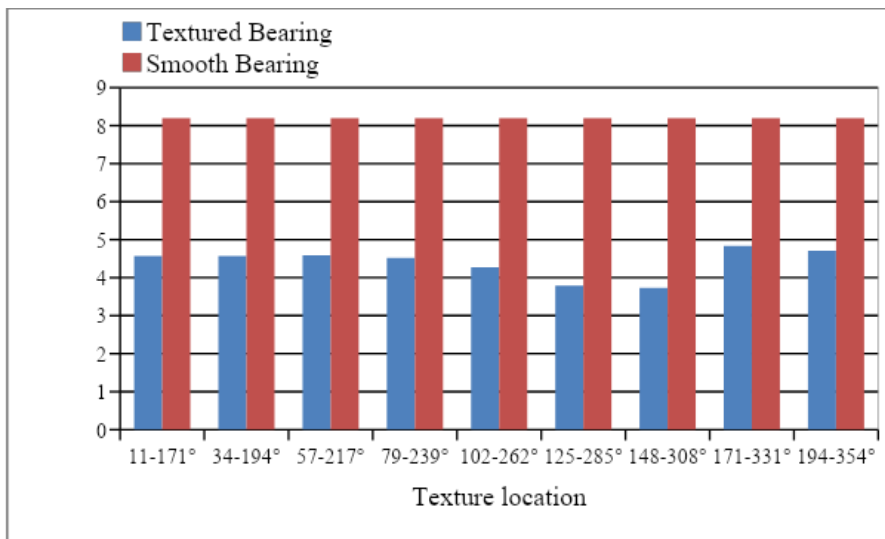Fig. 9: Lubricant End Flow Versus Texture Location in Circumferential Direction

Fig. 10: Fluid-Film Friction Coefficient Versus Texture Location in Circumferential Direction
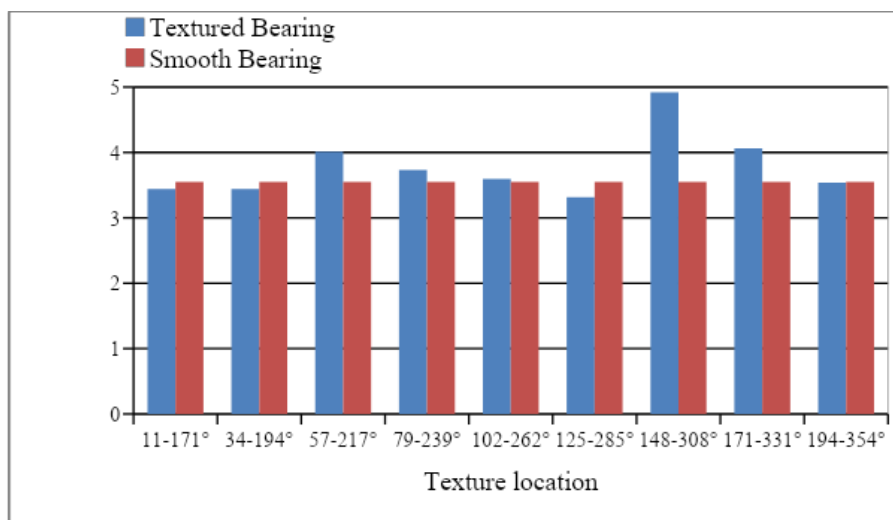

Fig. 11: Fluid-Film Stiffness Coefficient in Horizontal Versus Texture Location in Circumferential Direction
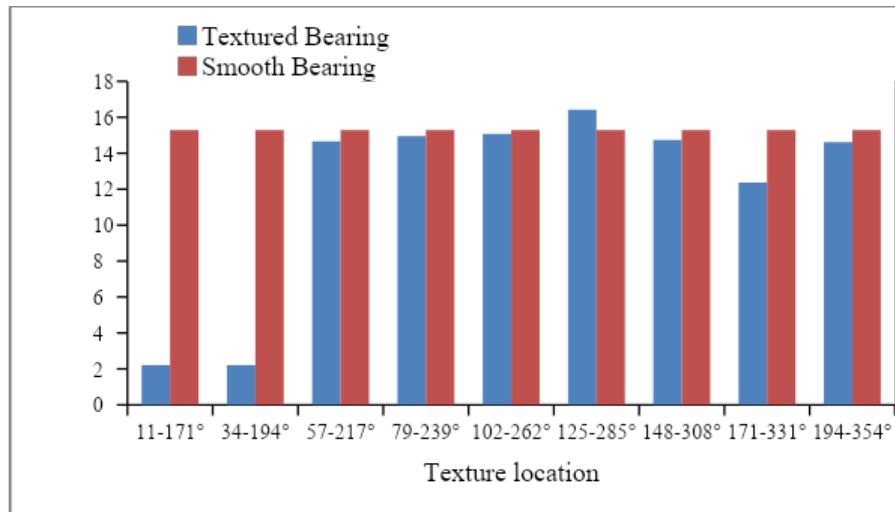
Fig. 12: Fluid-Film Stiffness Coefficient in Vertical Versus Texture Location in Circumferential Direction
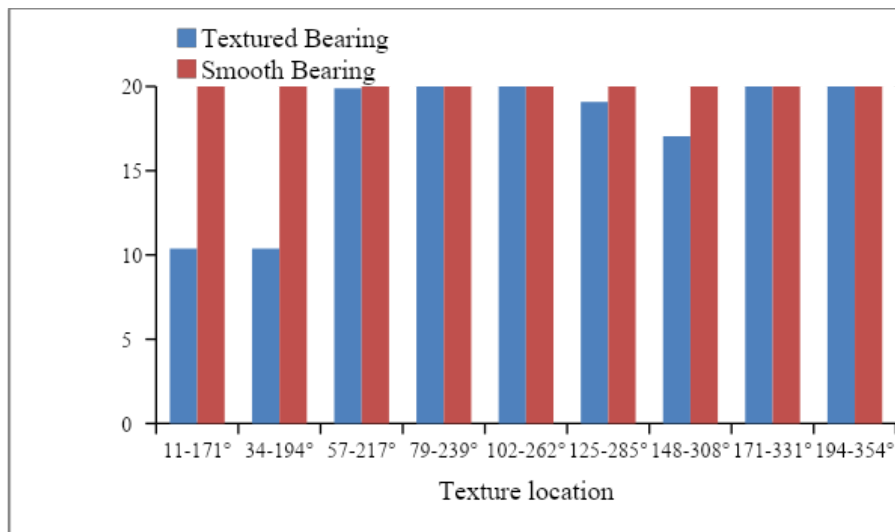

Fig. 13: Fluid-Film Damping Coefficient in Horizontal Versus Texture Location in Circumferential Direction
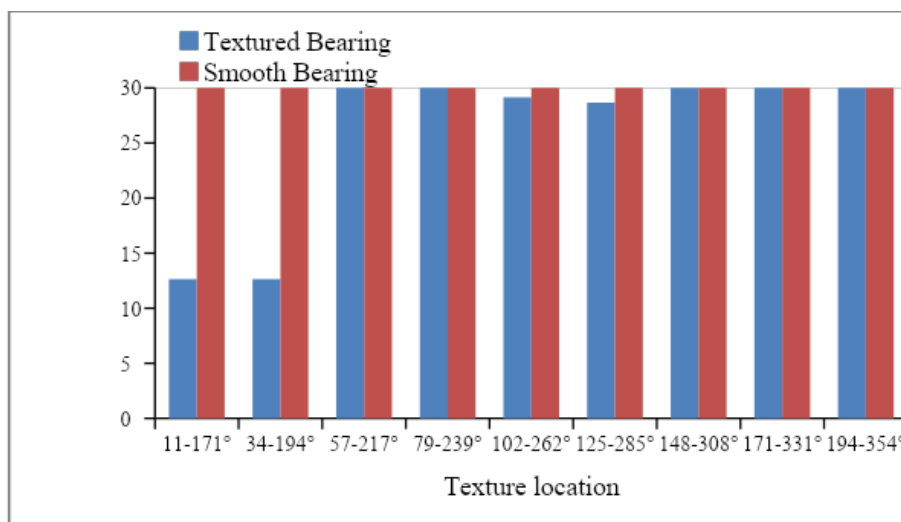

Fig. 14: Fluid-Film Damping Coefficient in Vertical Versus Texture Location in Circumferential Direction

Optimizing Texture Position for Improved Dynamic Stability and Operational Performance in Two-Lobe Journal Bearings
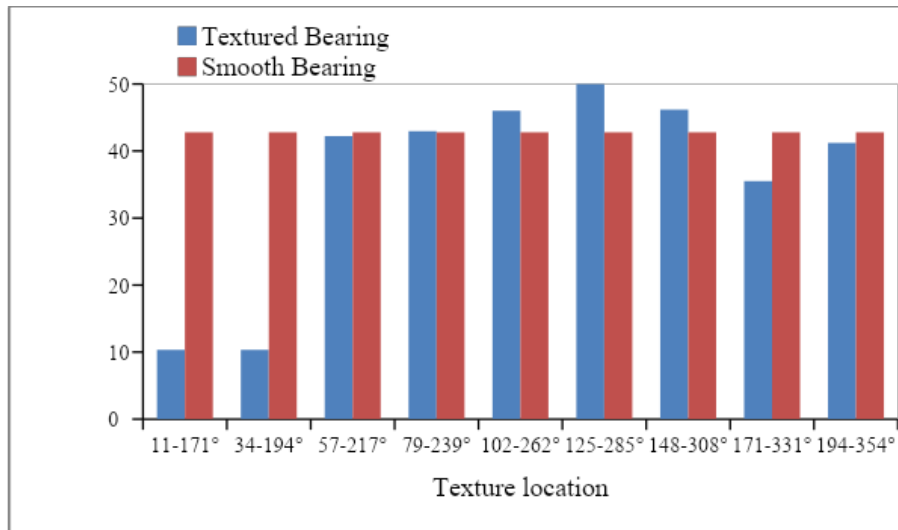
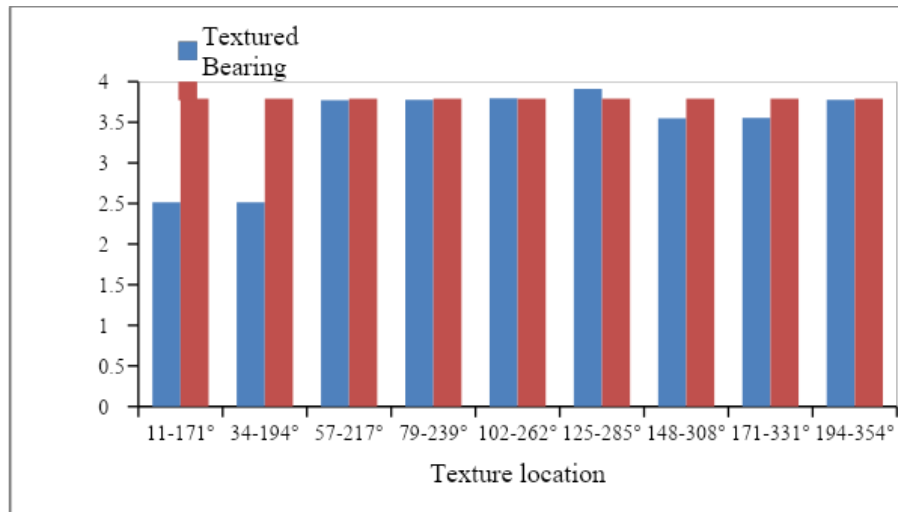*Fig. 15:* Critical Mass Versus Texture Location in Circumferential Direction

Fig. 16: Threshold Speed Versus Texture Location in Circumferential Direction
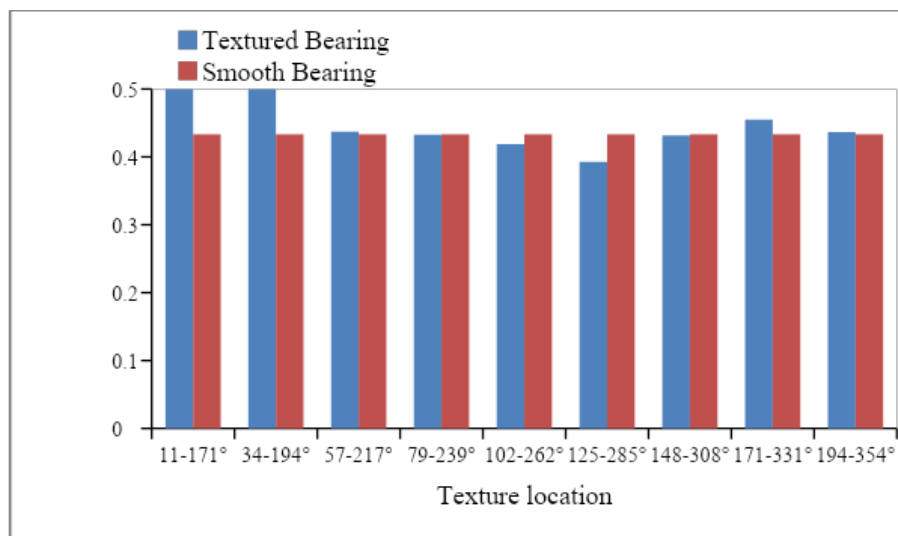

Fig. 17: Whirl Frequency Ratio Versus Texture Location in Circumferential Direction

V. CONCLUSIONS

This theoretical research paper delved into the critical aspects of optimizing texture position in two-lobe journal bearings to enhance both dynamic stability and operational performance. Through a comprehensive exploration of the underlying principles and governing equations, this study has contributed valuable insights to the field of tribology and mechanical engineering. Bases on the results presented, the following conclusions can be drawn:

1. The study underscores the importance of placing surface textures strategically within bearing clearance zones. Such placement significantly influences the dynamic behavior of the bearing system, reducing instabilities caused by operational variations like load shifts, speed fluctuations, and changes in lubrication.

2. Analyzing texture position's impact on stability charts and whirl frequency ratios reveals the link between surface patterns and bearing dynamics. Optimal texture placement significantly boosts dynamic bearing stability, reducing risks of vibrations and system failures.

3. The study delves into key benefits resulting from optimal texture positioning, including improved load carrying capacity and reduced friction. These advantages collectively contribute to extending bearing lifespan, reducing maintenance requirements, and increasing the operational efficiency of machinery and rotating equipment.

Nomenclature

NOMENCLATURE

Dimensional Parameters

c: Radial clearance, mm
D: Diameter of journal, mm
D_{ij} : Fluid-film damping coefficients (i, =1, 2) j
e: Eccentricity of journal, mm
F: Fluid-film reaction$\left(\frac{\partial h}{\partial t} \neq 0\right)$, N
Fx_1, Fz_1: Fluid-film reaction components in
X and Y direction$\left(\frac{\partial h}{\partial t} \neq 0\right)$, N
h: Nominal Fluid-film thickness, mm
h_p: Dimple depth, mm
L: Bearing length, mm
l1, l2: Direction cosines
N: Rotational speed, rpm
O_B : Bearing center
O_J : Journal center
p: Pressure, N/mm²
p_s : Reference pressure, N/mm²

$$\left(\frac{\mu \omega_j R_j^2}{c^2}\right)$$

$$r = \sqrt{\overline{x}_l^2 + \overline{z}_l^2}$$

R_j, R_b : Radius of journal and bearing, mm
S: Sommerfeld Number
S_{ij}: Fluid-film stiffness coefficients
(i, j=1, 2)
t: Time, sec
W: Load Capacity, N
W_0: External load, N
x: Circumferential coordinate
y: Axial coordinate

X_j, Z_j : Coordinates of journal center
X, Y, Z: Cartesian coordinate system
z: *Coordinate along film* thickness

Non-Dimensional Parameters

$$\overline{C}_{ij} = \left(\frac{c^3}{\mu R_j^4}\right) C_{ij}$$

$$\overline{D}_{ij} = D_{ij}\left(\frac{c}{p_s R_j^2}\right)$$

$$\overline{F}_x, \overline{F}_z = \left(\frac{F_x}{p_s R_j^2}, \frac{F_z}{p_s R_j^2}\right)$$

$$\overline{h}, \overline{h}_{\min}, \overline{h}_p = \left(\frac{h}{c}, \frac{h_{\min}}{c}, \frac{h_p}{c} \right)$$

$$\overline{M}_j = M_j \left(\frac{c^5 p}{\mu_r^2 R_j^6} \right)$$

$$\overline{p} = \frac{p}{p_s}$$

$$\overline{p}_{\max} = \frac{p}{p_s}$$

$$\overline{Q} = Q \left(\frac{\mu}{c_3 p_s} \right)$$

$$\overline{r} = \sqrt{\overline{X}_L^2 + \overline{Z}_L^2}$$

$$\overline{r}_p = \frac{r_p}{c} \text{ , dimple radius}$$

$$S_p = \frac{L_x \times L_z}{\pi \overline{r}_p^2}, \text{ area density of dimple}$$

$$\overline{S}_{ij} = S_{ij} \left(\frac{c}{p_s R_j^2} \right)$$

$$\overline{\tau}_c = t \left(\frac{c^2 p_s}{\mu_r R_j^2} \right)$$

$$\overline{W}_0 = \left(\frac{W}{p_s R_j^2} \right)$$

$$\overline{X}_j, \overline{Z}_j = \left(\frac{X_j}{c}, \frac{Z_j}{c} \right)$$

$$\overline{X}, \overline{Z} = \left(\frac{X}{c}, \frac{Z}{c} \right)$$

$$\alpha, \beta = \left(\frac{x}{R_j}, \frac{y}{R_j} \right)$$

$$\overline{\Omega} = \omega_j \left(\frac{\mu_r R_j^2}{c^2 p_s} \right)$$

$$\overline{S}_{th} = \frac{S_{th}}{\omega_I}$$

$$\overline{F}_{whirl} = \frac{F_{whirl}}{\omega_j}$$

Greek Letters

$\varepsilon = \dfrac{e}{c}$: eccentricity ratio

$\overline{\delta}$: Preload factor

θ: Textured zone

μ: Lubricant viscosity, Pa. sec

α: Angular coordinate, radian

ω_{rad} : Angular speed, radian/sec

∅ : Attitude angle, radian

Matrices

$\left[\overline{F} \right]$ = Assembled Fluidity Matrix

$\left\{ \overline{p} \right\}$ = Nodal pressure Vector

$\left\{ \overline{Q} \right\}$ = Nodal Flow Vector

$\left\{ \overline{R}_j \right\}$ = Column Vectors due to hydrodynamic terms

$\left\{ \overline{R}_{X_j} \right\}, \left\{ \overline{R}_{Z_j} \right\}$ = Global right hand side vectors due to journal center linear velocities.

Subscripts and Superscript
b: Bearing
j: Journal
max: Maximum value
 ˙: First derivative w.r.t. time

REFERENCES

1. Hsu C. H., Lin J. R and Wang C. C 2013 Effect of texture location on the performance of two-lobe journal bearings under dynamic loading. *Tribology Letters. 49(1): 63-72.*

2. Kim Y. J., Kim K. H and Lee S. Y 2015 Effect of texture location and depth on the performance of two-lobe journal bearings. *Proceedings of the Institution of Mechanical Engineers, Part J: Journal of Engineering Tribology.* 229(7): 742-750.

3. Lee S., Kim Y. J and Kim K. H 2015 Effect of texture location on the performance of two-lobe journal bearings. *Tribology International.* 90: 152-159.

4. Park J. H., Kim Y. J and Kim K. H 2016 Effect of texture location and depth on the

performance of two-lobe journal bearings. *Tribology International*. 103: 534-542.

5. Karthikeyan K., Kannan M and Vasudevan R 2016 Experimental and numerical investigation on the effect of texture location in a two-lobe journal bearing. *Tribology International*. 97: 308-318.

6. Li Y., Li H., Zhang X and Li S 2017 Effects of texture location on the tribological properties of a two-lobe journal bearing. *Tribology International*. 113: 346-357.

7. Wu Y., Wei X and Zhang Y 2018 Effect of texture location on the stability of a two-lobe journal bearing. *Tribology Letters*. 66(1): 1-12.

8. Zhang J., Li J and Li Y 2018 Effects of texture orientation and location on performance of two-lobe journal bearing. *Industrial Lubrication and Tribology*. 70(4): 707-715.

9. Zhou Z., Zhang W., Liu W and Yang D 2018 Experimental study on the effect of different texture locations on the performance of two-lobe journal bearings. *Tribology International*. 121: 224-233.

10. Zhang X., Li Y and Li H 2019 Effects of texture location on the performance of a misaligned two-lobe journal bearing. *Tribology International*. 136: 10-22.

11. Qiu S., Sun P., Zhang C and Wang J 2019 Numerical study on the effect of texture location on lubrication performance of journal bearings. *Industrial Lubrication and Tribology*. 71(4): 567-574.

12. Wang X., Liu Y., Zhou J and Liu Y 2019 Effects of texture location on the dynamic characteristics of two-lobe journal bearing. *Tribology International*. 131: 96-105.

13. Li Z., Li D., Zhang D and Shi Y 2020 Effects of texture location and size on the performance of two-lobe journal bearings. *Tribology International*. 142: 105993.

14. Wang Y., Zhang X and Zhou Z 2020 The effect of texture location and pattern on the performance of two-lobe journal bearing. *Proceedings of the Institution of Mechanical Engineers, Part J: Journal of Engineering Tribology*. 234(1): 17-30.

15. Li J., Li X., Zhang Y., & Yao B 2021 Effect of texture location on performance of two-lobe

16. journal bearings under different load conditions. *Tribology Transactions*, 1-13.

17. Zhao Z., Yu X., Wang Y and Gao D 2021 Effects of texture location on the performance of a two-lobe journal bearing. *Journal of Tribology*. 143(1): 011706.

18. Li Z., Li D., Zhang D., & Shi Y 2020 Effects of texture location and size on the performance of two-lobe journal bearings. *Tribology International*, 142, 105993.

19. Dowson D 1962 A generalized Reynolds equation for fluid film lubrication. *International Journal of Mechanical Sciences*. 4: 159-170.

20. Sinhasan R and Goyal K. C 1995 Transient response of a two-lobe journal bearing with non-newtonian fluid. *Tribology International*. 28: 233-239.

21. Sharma S. C and Yadav S. K 2014 Performance analysis of fully textured hybrid circular thrust pad bearing system operating with non-newtonian fluid. *Tribology International*. 77: 50-64.

22. Yadav S. K and Sharma S. C 2014 Performance of hydrostatic tilted thrust pad bearings of various recess shapes operating with non-newtonian fluid. *Finite Elements in Analysis and Design*. 87: 43-55.

23. Sharma S. C., Jain, S. C., Sinhasan, R., et al. 2001 Static and dynamic performance characteristics of orifice compensated hydrostatic flexible journal bearings with non-newtonian fluids. *Tribology Transactions*. 44: 242-248.

24. Shivank M and Pandey K. N 2019 Effect of surface texturing on the dynamic characteristics of hydrodynamic journal bearing comprising concepts of green tribology. *Proceedings of the Institution of Mechanical Engineers, Part J: Journal of Engineering Tribology*. 0: 1-11.

25. Singh N and Awasthi R. K 2020 Theoretical investigation of surface texture effects on the performance characteristics of hydrodynamic two-lobe journal bearing. *Proceedings of the Institution of Mechanical Engineers, Part J: Journal of Engineering Tribology*. 0: 1-14.

26. Singh N and Awasthi R. K 2021 Influence of surface textures on the dynamic stability and

performance parameters of hydrodynamic two-lobe journal bearings. *Proceedings of the Institution of Mechanical Engineers, Part J: Journal of Engineering Tribology*. 236(8)

26. Sinhasan R and Goyal K. C 1995 Transient response of a two-lobe journal bearing with non-newtonian fluid. *Tribology International*. 28: 233–239.

27. Lund J. J and Thomson K. K 1978 A calculation method and data for the dynamic coefficients of oil lubricated journal bearings system design and optimization. *Paper presented at ASME Design Engineering Conference,* Chicago, 1-2

Great Britain Journal Press Membership

For Authors, subscribers, Boards and organizations

Great Britain Journals Press membership is an elite community of scholars, researchers, scientists, profess-sionals and institutions associated with all the major disciplines. Great Britain memberships are for indivi - duals, research institutions, and universities. Authors, subscribers, Editorial Board members, Advisory Board members, and organizations are all part of member network.

Read more and apply for membership here:
https://journalspress.com/journals/membership

For Authors

For Institutions

For Subscribers

Author Membership provide access to scientific innovation, next generation tools, access to conferences/seminars/ symposiums/webinars, networking opportunities, and privileged benefits. Authors may submit research manuscript or paper without being an existing member of GBJP. Once a non-member author submits a research paper he/she becomes a part of "Provisional Author Membership".

Society flourish when two institutions Come together." Organizations, research institutes, and universities can join GBJP Subscription member-shipor privileged "Fellow Membership" membership facilitating researchers to publish their work with us, become peer reviewers and join us on Advisory Board.

Subscribe to distinguished STM (scientific, technical, and medical) publisher. Subscription member-ship is available for individuals universities and institutions (print & online). Subscribers can access journals from our libraries, published in different formats like Printed Hardcopy, Interactive PDFs, EPUBs, eBooks, indexable documents and the author managed dynamic live web page articles, LaTeX, PDFs etc.

GO GREEN AND HELP
SAVE THE ENVIRONMENT

JOURNAL AVAILABLE IN

PRINTED VERSION, INTERACTIVE PDFS, EPUBS, EBOOKS, INDEXABLE
DOCUMENTS AND THE AUTHOR MANAGED DYNAMIC LIVE WEB PAGE
ARTICLES, LATEX, PDFS, RESTRUCTURED TEXT, TEXTILE, HTML, DOCBOOK,
MEDIAWIKI MARKUP, TWIKI MARKUP, OPML, EMACS ORG-MODE & OTHER

support@journalspress.com
www.journalspress.com

*THIS JOURNAL SUPPORT AUGMENTED REALITY APPS AND SOFTWARES